بسم الله الرحمن الرحيم

Sudan University of Science and Technology
College of Graduate Studies

College of Petroleum Engineering and Technology

Department of Petroleum Exploration Engineering

Title of Thesis:

The Challenges of Shaly Sand Petrophysics and Formation Evaluations: Case Study Keyi Main Oil Field, Block 6, Sudan.

التغلب على التحديات المرتبطة بتفسيرات تسجيل الابار في المكامن النفطيه، ذات خاصيه الرمل الطيني،دراسه تطبيقيه في حقل (كي) النفطي في مربع 6 السودان.

Thesis started: April, 2014

Thesis submitted: December, 2016

Study program: MSc. Petroleum Exploration

Postgraduate Study by:

Eltayeb Adam Mohammed Bashar

This work has been carried out at the College of Petroleum Engineering and Technology, under the supervision of:

Dr. Abbas Musa Yagoub

March, 2017

ABSTRACT

The study area located in Keyi Main Oil Field of southern part of western escarpment trend of Fula sub-basin, Block-6, Muglad basin in Sudan.

Conventional logging data from wells, Keyi-4, Keyi-11, and dipole shear sonic data (XMAC) of Keyi-12, have been studied.

The ultimate goal of this research is to verify an accurate lithology, mineralogy, porosity, permeability and water saturation derived from Indonesian and dual water models of Ghazal and Zarga Formations.

Another aim is to overcome the challenges associated with gamma ray log (radioactive effect of potassium), thus identify reasonable shale content and clay type.

The methodology and workflow used for this work consists of three steps: logs analysis, core analysis and dynamic elastic rock properties techniques, moreover mineral base model or multi mineral analysis method used in this research for the logging interpretation, to describe the minerals components utilizing Elan Plus software.

A rock physics (Elastic constant) technique, based on wireline log data adopted, for dynamic elastic constant modeling identification, and constrain the logging interpretation results, by using log responses equations to calculate the density (synthetic) base on different mineral models assumptions and compare between original dynamic elastic modules and re-contracted elastic dynamic models.

In order to achieve all these results, a comprehensive analysis performed for logging interpretation, calibrated to core data and integrated with DST results.

The Studied reservoirs composed of dominant K-feldspar, Kaolinite, with considerable amount of quartz and traces of smectite and chlorite.

The rock type had been classified into three facies, based on capillary pressure curves and core porosity versus permeability.

The logging interpretation results and dynamic elastic models demonstrated an improvement in the reservoir characterization, obtained by integrating both logging interpretation and rock physics data.

Key Words: The Challenges for Shaly sand Petrophysics and Formation Evaluation, of Keyi oil-Field, Fula Sub basin, Sudan.

التجريد:

منطقة الدراسة في حقل (Keyi) ، وهو واحد من حقول النفط التي تقع في الجزء الجنوبي الغربي للجرف Structure belt،للحوض الفرعي للفولة (Fula sub basin) من حوض المجلد، في مربع الامتياز رقم 6،السودان. تم دراسة تسجيل بيانات الآبار التقليدية (Conventional well logging)،لكل من الابار Keyi-4 و-Keyi 11،وكذالك دراسه وتحليل البيانات الصوتية ثنائي القطب القصي Dipole Shear Sonic (XMAC) من البئر Keyi-12.

والهدف النهائي من هذا البحث هو التحقق من الخصائص الصخرية (Rock properties) بصوره دقيقة، و التعرف علي مكونات المعادن، و المسامية والنفاذية ودرجه تشبع المكامن بالسوائل المستمدة من طريقه المعادله الاندونيسية Indonesian Equation و معادلة ثنائيه التشبع المائي Dual Water Model،للطبقات قيد الدراسه (Ghazal and Zarga Formations). هدف آخر هو التغلب على التحديات المرتبطة بتسجل Gamma ray بسبب التأثير الإشعاعي للبوتاسيوم وبالتالي تحديد نسبة ونوع الطين.

المنهجية المستخدمة لهذا العمل تتكون من ثلاث خطوات:

اولا تحليل تسجلات الابارWell logging ونتائجها، ثانيا تحليل صخور اللباب core analysis وربطها بالنتائج الأساسية لتفسيرات الابار.وثالثا استخدام تقنيات الخواص الديناميكية للصخور المرنة Elastic rocks constant. من أجل تحقيق كل هذه النتائج،تم إجراء تحليل شامل لتفسيرات تسجيل الابار، ومقارنتها مع بيانات صخور اللباب (core) مع نتائج اختبار المكمن (DST)، بالاضافه لذلك استخدام نموذج الاساس المعدني(Mineral base model) ،او طريقة تحليل المعادن المتعدده Multi mineral analysis في هذه الدراسه لوصف الخصائص المعدنيه المكونه لصخور المكمن وذلك باستخدام برنامج حاسوبي متطور(Elan Plus software).

واستخدمت تقنية ثابت المرونة Elastic rock constant لصخور المكمن، على أساس بيانات تسجلات الابار لتحديد خواص المرونة للمكمن وربطها بنتائج تفسيرات تسجيلات الابار ، وذلك باستخدام معادلات(log responses equations) لإعادة حساب الكثافة على اساس النماذج المعدنية المختلفة Multi minerals Models ومقارنتها مع النسخة الأصلية لتقنية ثابت المرونة لصخور المكمن.

تم التعرف علي مكونات المعادن وهي تتكون بصوره واضحه من الفلسبار البوتاسي K-Feldspar، مع كمية كبيرة من والكولنيت Kaolinite ،الكوارتز Quartz و قليل من Smectite وChlorite

تم تصنيف انوع الصخور إلى ثلاث سحنات (Facies) علي اساس خواصها،من خلال خاصيه الضغط الشعريةCapillary pressure للصخور،وايضا بواسطة المسامية والنفاذية لصخور اللباب Core porosity and permeability.

أظهرت نتائج تسجيلات الابار Well logging interpretations results والنماذج الديناميكية المرنة Dynamic Elastic للصخور تحسنا في توصيف المكامن قيد الدراسة من خلال دمجهما integrated study.

ACKNOWLEDGEMENTS

First and foremost, I would like to give thanks to the God for seeing me through this work Successfully, Secondly, my sincere gratitude goes to the Sudan University of Science and Technology, College of Graduate Studies and College of Petroleum Engineering and Technology for this great opportunity for my master degree and career development.

Thirdly, I want to express my sincere gratitude to my supervisor, Dr. Abbas Musa Yagoub and committee, for guidance, advice, encouragement and valuable comments during this work, also appreciate the support and encouragement for publishing scientific papers in Journal Science and Technology of Sudan University.

Finally, I would like to thanks, Petro-Energy E&P Company, for providing the data, moreover, I would like to extend my appreciation to CNLC geosciences center in Sudan, for their support and help for processing and providing the shear sonic data of Keyi-12.

DEDICATION

To my Father, Mother, and family, also I wish to present my special thanks to my wife, Safa Abubaker, for her strong support to complete this research.

TABLE OF CONTENTS

LIST OF TABLES

LIST OF FIGURES

APPREVIATIONS:

XRD	X-ray diffraction	DENSx	Density of mineral x
SEM	Scanning Electron Microscopy	Vminx	Volume of mineral x
CGR	Corrected gamma ray	PHIE	Effective porosity
OOIP	Original oil in place	DENSSH	Density of shale layer
QFL	Quartz feldspar lithic	DENSW	Density of the water
GR	Gamma ray	DENSHY	Density of hydrocarbon
CAL	Caliber log	a	Tortuosity factor.
BIT	Bit size	m, n	Electrical properties.
K	Potassium	Rt	True resistivity
K	Permeability	Φ_t	Total porosity
Th	Thorium	Rw	Formation water resistivity
U	Uranium	SW	Water saturation
RD	Deep resistivity	Φ_{tsh}	Total Shale porosity
RS	Shallow resistivity	Rsh	Shale resistivity.
RMSL	Micro resistivity log	Qv/CEC	Cation Exchange Capacity
PE	Photo electric factor	KS5	Constant
N	Lithological parameters	DENS	Bulk density
XWAT	Water saturation in flushed zone	DTS	Shear sonic
UWAT	Water saturation in invaded zone	DTC,	Compressional Sonic
XOIL	Oil saturation in flushed zone	PR	Poisson's Ratio
UOIL	Oil saturation in invaded zone	N	Shear Modulus
XBWA	Total bound water.	Kb	Bulk Modulus
LDT	Litho density tool	Y	Young's Modulus
API	unit for natural gamma ray	ρma	Matrix density
PHIT	Total porosity	ρf	Fluid density
PHIE	Effective porosity	Pu	Pu Porosity unit
VCL	Clay volume	DST	Drill Stem Test
Vshale	Shale volume		
Ct	Total rock Conductivity		

CHAPTER ONE

INTRODUCTION

This research attempts to identify the lithology, mineralogy, and therefore accurate porosity, water saturation and permeability models integrated with core data to predict reservoirs quality using wire line logging tools.

This work is integrated petrophysical study constrained by elastic rock properties models.

Conventional logging data, core data analysis, dipole shear sonic data and DST results used to provide comprehensive formation evaluation for Ghazal and Zarga formations.

Available data for this research are conventional logs for three wells (Keyi-4, Keyi-11 and Keyi-12), used for logging interpretation, and only one set of dipole shear sonic data of well Keyi-12, to provide dynamic elastic properties model for the formations.

The core analysis data optioned from two wells, Kyei-4 and Keyi-11, to calibrate the logging interpretation results.

The study area in Keyi field area is about 126 sqkm wide within the western escarpment of Fula Sub-basin of Block-6 of Petro- Energy concession area (Fig. 1-1).

The study area is a part of Muglad rift basin in the south central Sudan, and it is a part of trend of Cretaceous sedimentary basin of apparent rift origin related to the global phenomenon of plate tectonics.

The establishment of the stratigraphic column reflects three cycles of deposition in Muglad basin. The Sharef, Abu Gabra, and Bentiu Formations represent the first cycle, second cycle is the Cretaceous of Darfur Group and is characterized by a coarsening upward sequence, and the third one is Nayil Formation. The ages of these cycles are late Jurassic to Cenomanian, Turonian to Paleocene, and early Tertiary respectively“(Mohamed eta al, 2008).

The geological time ranges from Pre-cretaceous to quaternary corresponding to the Formations (Basement to Zeraf), develops Lower Cretaceous Abu Gabra and Bentiu formation, Upper Cretaceous Darfur Formation which include Aradeiba, Zarqa, Ghazal and Baraka Formation, Upper Cretaceous Amal Formation. The lithology is mainly clay stone interbedded with sandstone in Gahzal, Zarqa and Aradeiba Formation, massive sandstone interbedded with clay stone in Bentiu Formation and thin sandstone and shale in Abu Gabra Formation (Fig. 1-2). Main oil-bearing distributes in Ghazal, Zarqa, Aradeiba, Bentiu and Abu Gabra Formation. Ghazal, Zarqa, Aradeiba and Bentiu formation are heavy oil reservoirs.

Wells and seismic data from the Muglad basin confirmed thick continental facies of cretaceous and younger age“(Mohamed eta al, 1999).

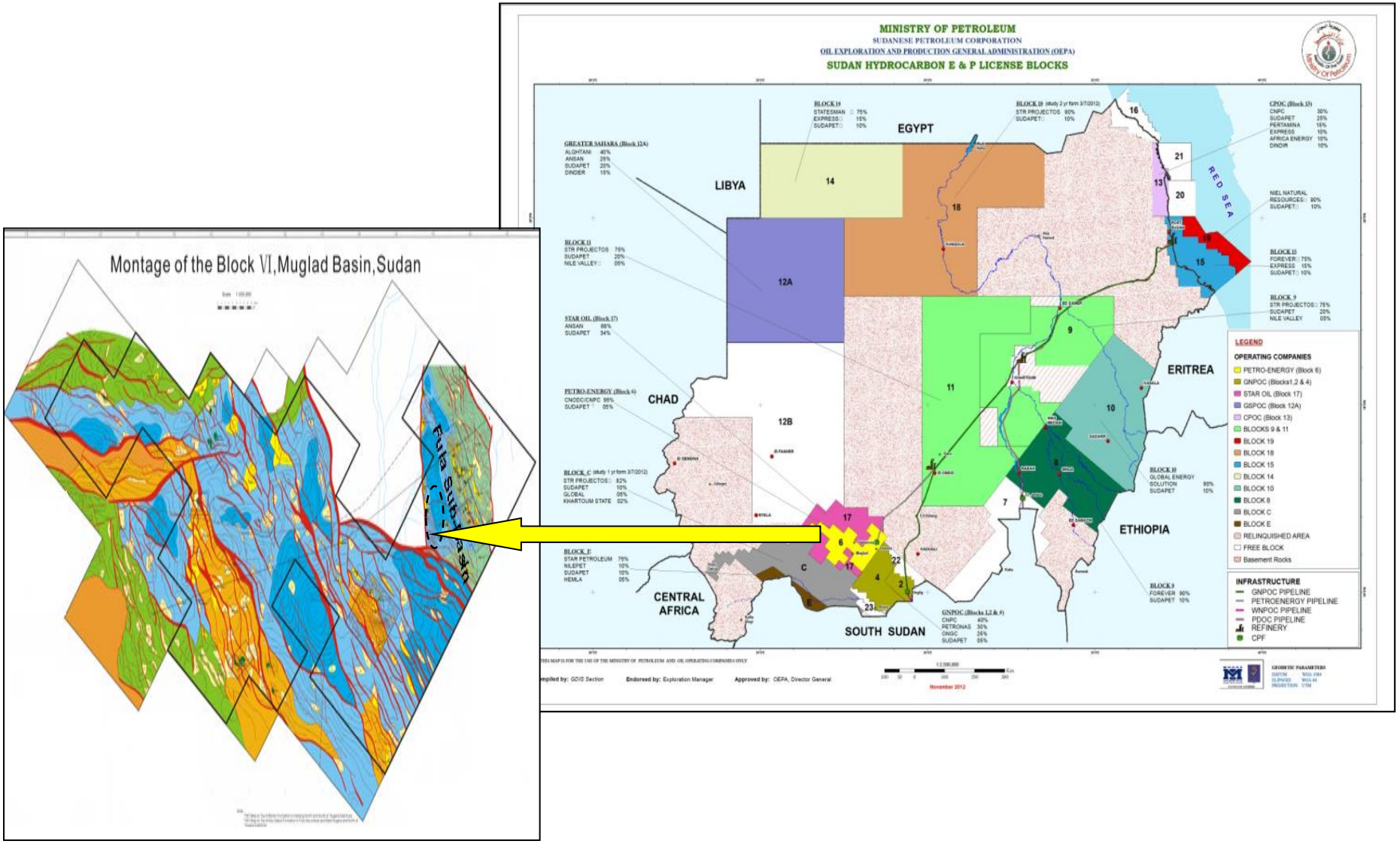

Fig . 1-1 : Location map of Keyi-Oil Field in Fula Sub-Basin, Block-6 , Sudan.

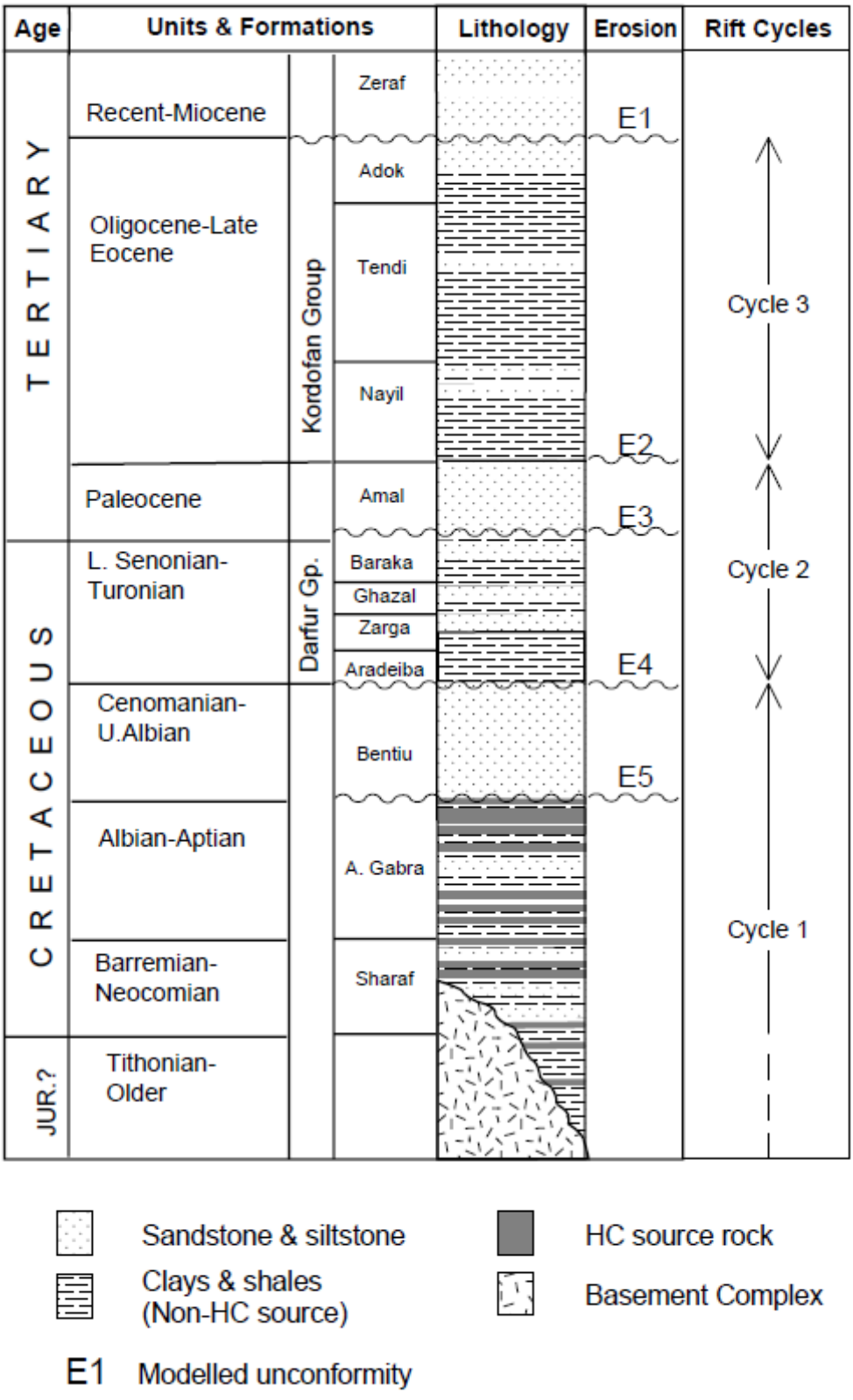

Fig.1-2: Summary of stratigraphic column of the interior Sudan basins with generalized Lithologies showing formation ages"(Mohamed et al, 1999).

1.1 The Problems Description and Challenges

The main purpose of this research is to verify the lithology, mineralogy, accurate porosity, fluid saturations and permeability model of Ghazal and Zarga Formations in Keyi oil field, similar to work objectives done by (Javid, 2013). Another aim is to overcome the uncertainty (radioactive effect of potassium) associated with Gamma ray log, moreover identify the clay type, all these consider as petrophysical challenges to predict reservoirs quality in terms of petrophysical parameters.

The presence of shale content in the rock has an important impact on reservoir quality. It decreases porosity, reduces permeability and may reduce the resistivity and therefore overestimate the water saturation and effect OOIP calculation. Clays and shale affect all logs and make formation evaluation more difficult. They cause porosity tools to read higher and Formation resistivity to read lower, making it more difficult to detect hydrocarbons. This justifies special attention when designing interpretation models and while performing Formation evaluation.

Petrophysical evaluation is the key to predict quality, actual productivity and recovery of hydrocarbon in shaly-sand reservoir, which require a large amount of data and analysis to develop models such as shale volume, effective porosity, water saturation and permeability models, the first challenge is how to estimate reasonable shale volume and clay type identification which cannot be recognized directly from gamma ray measurement, the second challenge is determination of the accurate effective porosity model, and the third challenge is selection of realistic water saturation and permeability models. All these challenges or uncertainties were affected in the petrophysical results and hydrocarbon in place (OOIP).

Mineral identification from logs and core processing and their effect on the reservoir quality is an essential step to describe accurate reservoirs parameters in study area and compare the properties of the different reservoir units.

A rock physics (Elastic constant) characterization based on wireline log data, ,is proposed for identifying elastic rock properties and constraining the petrophysical models such as minerals components of target reservoirs in Ghazal and Zarga Formations, same work done by “(Sharif,2013). For achieving this goal, well logs data, core data, and dipole shear sonic data of well Keyi-12 have been studied for getting precise results.

1.2 Objectives of the Study

This work accomplished under some objectives outlined as the following:

- The main purpose is to obtain petrophysical models, minerals identification, and calibrated with core data.
- Another aim is to obtain elastic dynamic properties of the rocks, through a rock physics modeling.
- Elastic rock constant from well Keyi-12 has been studied and compared with reconstructed dynamic elastic constant to optimize the petrophysical results.
- Finally reservoir characterization and rock quality have been identified for the oil-Field development plan.

1.3 Motivation for the Study

- The combination of photoelectric factor and gamma ray logs is powerful tool to eliminate or remove the potassium effects from gamma ray log, in order to estimate accurate shale volume.
- There is clear reservoir characterization improvement made, by using mineral bas model to explain mineralogy and their effect on the reservoir quality.
- Three rock types or facies had been identified by capillary pressure and core data.
- The selection of probabilistic approach to compute the reservoir components using Elan plus software, rather than traditional method (deterministic).
- Identified the dynamic elastic constant properties of the reservoirs, and constrained the logging interpretation results.

1.4 Exploration and Development History

The area was investigated by Petro-Energy Company and three oil fields were discovered, Keyi main, Keyi north and Keyi south oil field. A thick sequence of Mesozoic to Tertiary sediments has been penetrated in well Keyi-1.

The study area in Keyi main field, which is the main contributor in the Greater Keyi, with total number of 1 exploration well, 7 appraisals and 20 development wells drilled.

The first field development plan study of Keyi-Oil-Field was carried out by Sudapet Company in 2008, with total of seven drilled wells, five wells in Keyi main, one well in Keyi south and one well in Keyi north, and the petrophysical evaluation results of shale volume about 23% and the porosity range of 10-19%, estimated by density neutron cross plot method, for Ghazal and Zarg reservoirs.

The second in -house field development plan study for Keyi main static model, updated in 2011, and the method used for porosity estimation is density neutron cross plot, and the shale volume about 24% and porosity about 17% for good reservoirs properties.

The third full field review study of Keyi field was carried out in 2015 by Geophysical research institute (GRI) in China, the petrophysical analysis results discriminated the shale volume into the different clay types for the studied formations.

All the previous studies didn't attempt to correct for radioactive effect on the total gamma ray logs, and there for overestimate the shale volume in the reservoirs.

Reference to the last full field review study and the geological study completed by geophysical research institute in china 2015; here are some results obtained for Ghazal and Zarag formations as below:

The Ghazal Formation consists of considerable amount of Kaolinite, Smectite and trace of chlorite with 27.71%, 19.1%, and 9.82% respectively. This formation consist of clay stones interbedded with unconsolidated Sandstone, very fine to fine grained, with traces of medium and coarse grained sandstone, Ghazal formation was deposited in fluvial and alluvial fans environment .The thickness of this formation range from 170 m to 426 m.

The petrophysical log response in the type well and reference well is the same formation show the sharp increase in the gamma ray log trend at the base of the formation. However, the type well shows a slight decrease in the density and neutron response, and therefore gamma ray log it was not good lithology indicator to discriminate between shale and sand layers.

The Zarqa formation is a secondary reservoir it overlies the Aradeiba formation, belonged to the Darfur Group (Fig.1.2), this formation consists of mudstone, clay stones silt in parts inter bedded with very fine to fine & medium grained sandstones & siltstone. Zarqa formation was deposited in a flood plain lacustrine environment with fluvial-deltaic channel sands. The Zarqa formation thickness is range from 120 m to 160 m, reference to Keyi main static model update study in 2011.

Resistivity and gamma ray logs look not attractive from quick look evaluation to predict reservoir quality and potentiality. The previous research work concluded Zarga formation consists of Kaolinite as abundant of clay fraction with 86.3 % as volume and trace of chlorite.

CHAPTER TWO

LITERATURE REVIEW

A review of literature is presented here to provide the theory background and previous main work done as the following:

2.1.Regional Geology

The Muglad Basin is part of a trend of Cretaceous sedimentary basins of apparent rift origin, which cut across north central Africa from the Benue Trough in Nigeria, through Chad and the Central African Republic, into Sudan. The evidence for extension further southeast of this trend has been destroyed by Tertiary uplift associated with recent rifts in Ethiopia and Kenya. Regional data are limited, but the aeromagnetic and gravity surveys indicate as much as 5kilometers of sediments. Tectonics in the basin is highly complicated by faulting.

Seismic data suggest large numbers of tensional faults have affected the overall basin and have defined several sub-basins. Structures within these sub-basins show significant variations in age of formation, complexity and size.

Regional stratigraphy indicates that a major East African rift basin had formed in the early Jurassic whose structural axis paralleled the Rudolf Trough in Kenya. The early rift sediments are probably dominated by coarse continental clastics, but some lacustrine or fluvial sediment may also have been deposited. In the late Jurassic the rift basin continued to widen. Lacustrine sediments, with interbeds of coarser rift clastics derived from surrounding basement blocks, may have been the dominant types deposited. To this time, no Jurassic sediments have been penetrated in the area, due to the possibility that the Sudan Interior Basins may have begun forming at this time. Previous wells and seismic data from the Sudan Interior Basins confirmed thick continental facies of Cretaceous and younger age. Control on geometry of deposition is poor, but numerous areas of low-lying basement hills probably supplied the sediments (Mohamed eta al, 2008).

2.2.Theoretical Background

2.1.1 Petrophysics and Formation Evaluation

Petrophysics is the study of rock properties and their interactions with all the fluids in the reservoirs. (Tiab, D and Donaldson,2004).

Today, Formation evaluation has limits, dictated by the available logging technologies, core-analysis expertise, petrophysical models and interpretation methods. Technological advancements in logging measurements, core-analysis or petrophysical interpretations can contribute to widening the horizon of formation evaluation and magnifying its value in the oil and gas business (AlRuwaili,2005).The parameters usually evaluated in the formation evaluation include lithology, clay content, porosity, water saturations and permeability.

Several tools exist for formation evaluation which includes mud log, cores, conventional logging, borehole imaging, and borehole seismic, for example the following conventional tools were used in this study:

2.1.2 The Total Gamma Ray Log

The gamma ray log measures the total natural gamma radiation emanating from a Formation. This gamma radiation originates from potassium-40 and the isotopes of the Uranium-Radium and Thorium series. The gamma ray log is commonly given the symbol GR (Fig.2.1).

Once the gamma rays are emitted from an isotope in the Formation, they progressively reduce in energy as the result of collisions with other atoms in the rock (Compton scattering). Compton scattering occurs until the gamma ray is of such a low energy that it is completely absorbed by the formation.

Hence, the gamma ray intensity that the log measures is a function of:

- The initial intensity of gamma ray emission, which is a property of the elemental composition of the rock.
- The amount of Compton scattering that the gamma rays encounter, which is related to the distance between the gamma emission and the detector and the density of the intervening material. The tool therefore has a limited depth of investigation.

The gamma ray log is combinable with all tools, and is almost always used as part of every logging combination run because of its ability to match the depths of data from each run (Glover, 2014).

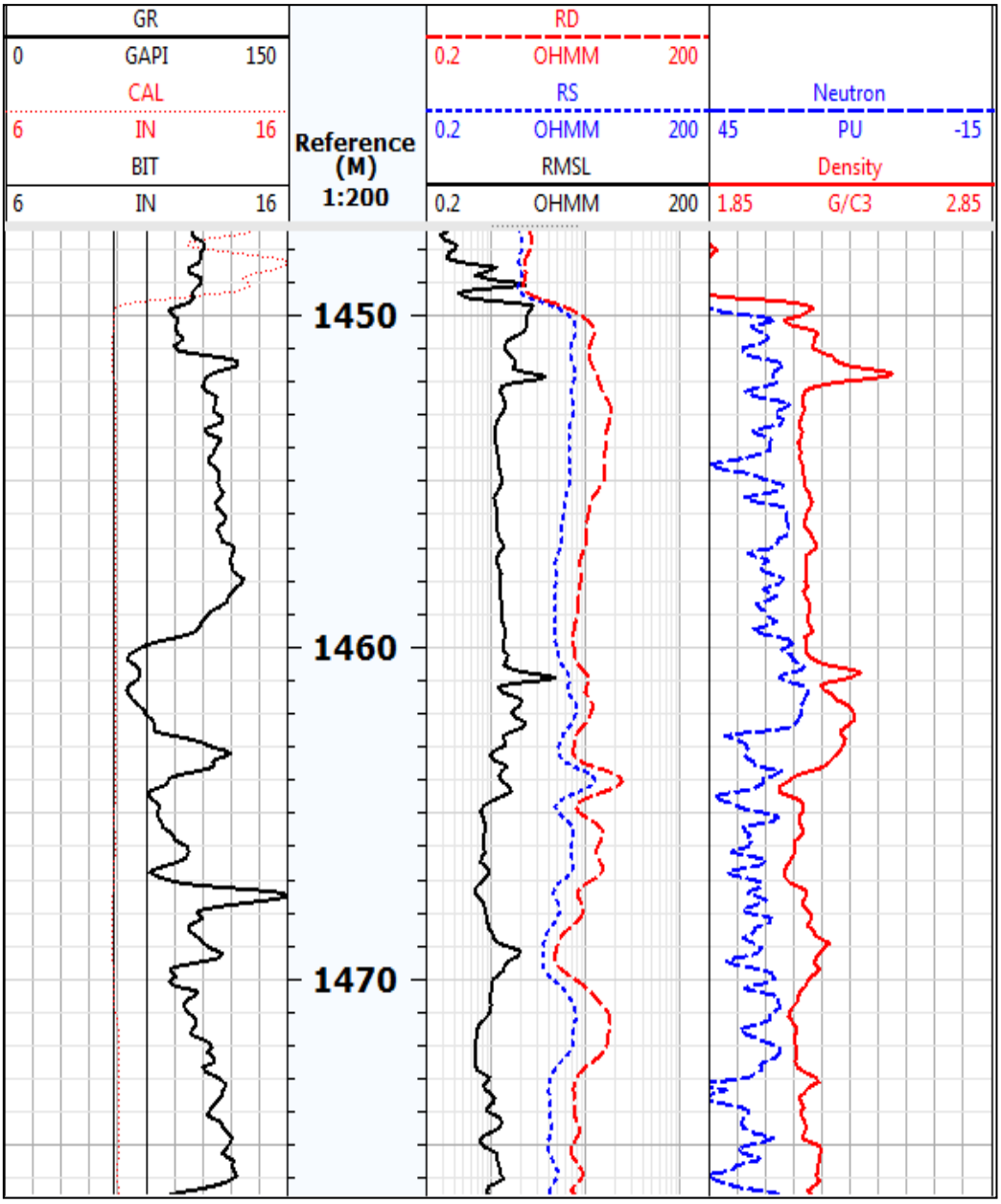

Fig.2-1: A composite log plot display gamma ray in track-1, resistivity in track-3, and neutron-density porosity in track-4 of well keyi-11.

2.1.3 The Natural Gamma Ray Spectroscopy Logs

The natural gamma ray spectroscopy tools measure the total number of gamma rays (SGR) as well as their energy from which is computed the percentage of Potassium (K), Thorium (Th), Uranium (U) and the corrected gamma ray (CGR) which is equal to the total gamma ray (SGR) less the Uranium i.e.Th +K .

2.1.4 Neutron Porosity Log

Reference to Msc thesis by (Che.E, 2011). Neutron porosity logging uses an active neutron source to emit neutrons into the rocks around a borehole. Because free neutrons are almost unknown in the Earth, the flux of neutrons subsequently recorded at the detector in the tool can be used as an indicator of the condition in the surrounding rocks.

The neutrons entering the rocks of the borehole wall from the tool are at high energy and generally have great penetrating power. The exception is when significant concentrations of hydrogen exist. In this case, the neutrons rapidly loose energy due to collisions with the hydrogen nuclei and become what are known as “thermal neutrons” (Fig.2.2). These thermal neutrons behave in many respects like a diffusing gas and form a spherical shell around the source in the probe. The radius of this sphere will depend primarily on the concentration of hydrogen in the environment around the probe. Because the technique is sensitive to lithological differences, neutron porosity logs can be very useful in cross plots with other log data to help determine lithology. The parameter of interested zones, obtained from the neutron porosity log (Fig. 2-1).

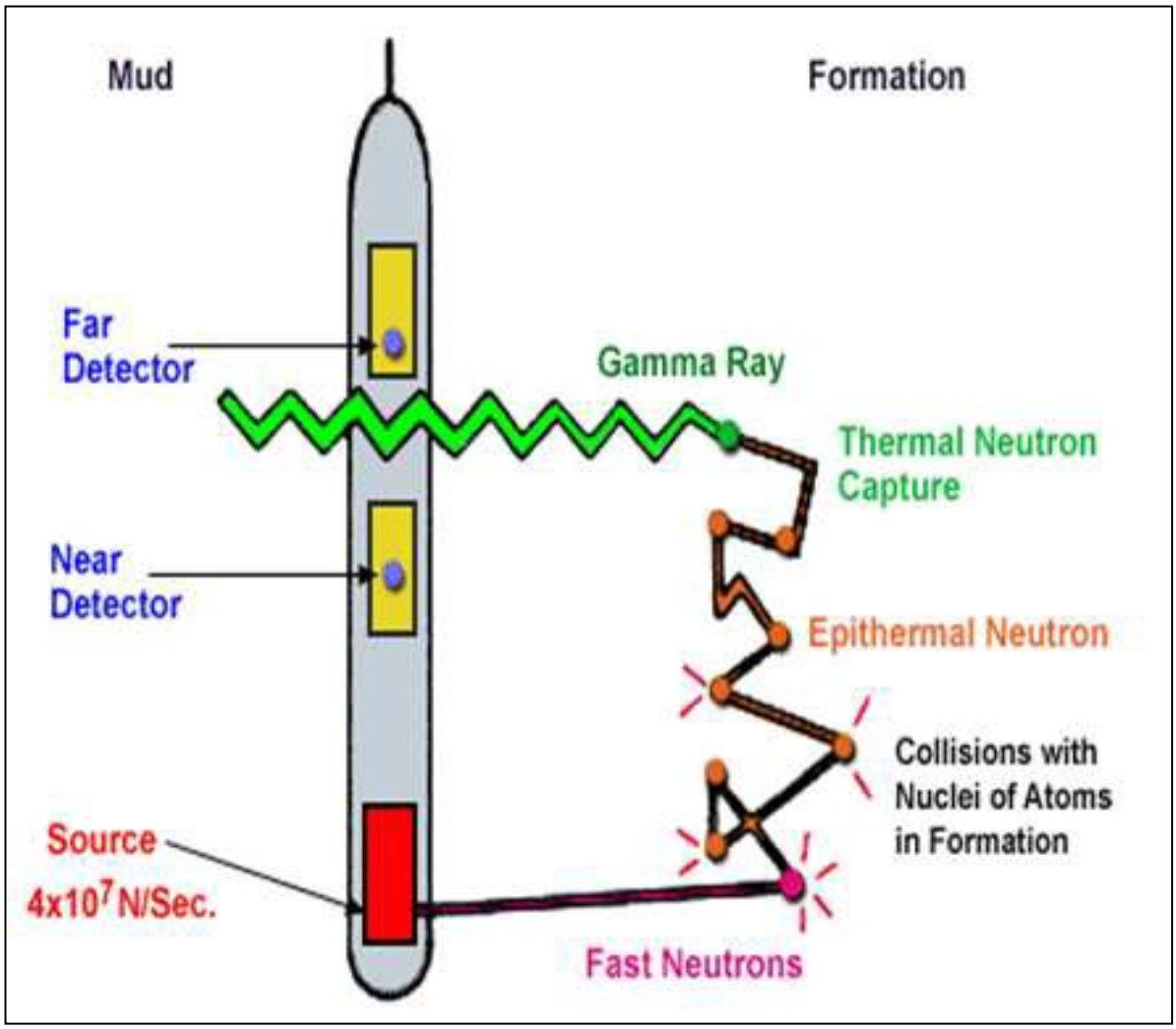

Fig.2-2: Showing the neutron logging tools and how it is works (Che, 2011).

2.1.5 The Litho- Density Porosity Log

The litho-density log is a new form of the formation density log with added features. It is typified by Schlumberger's Litho-Density Tool (LDT). These tools have a caesium-137 source emitting gamma rays at 0.662 MeV, a short-spaced and a long-spaced detector in the same way as the basic formation density tool. However, the detectors are more efficient, and have the ability to recognize and to count separately gamma rays which have high energies (hard gamma rays: 0.25 to 0.662 MeV) and gamma rays which have low energies (soft gamma rays: 0.04 to 0.0 MeV). The hard gamma rays are those that are undergoing Compton scattering. The count rates of these gamma rays (in the energy window 0.25 to 0.662 MeV) are used in the conventional way to measure the formation density. The final density value obtained is more accurate than the basic formation density tool because the harder gamma

rays are less prone to attenuation by borehole effects, and there is a smaller spacing between the two detectors that has reduced statistical fluctuations in the count rates. The soft gamma rays are those that are undergoing photo-electric absorption. This effect can be used to provide a parameter which is dependent upon the atomic number of the formation, and therefore immensely useful in lithological recognition (Glover, 2014).

The density log it is good porosity indicator, to calculate total and effective porosity (Fig. 2.1).

2.1.6 The Resistivity Logs Measurements

Resistivity is the oldest and still in many cases the most important measurement. The different types of resistivity measurements are:

- Focused resistivity devices.
- Laterologs.
- Micro-resistivity Logs.
- Induction Logs.
- Spontaneous Potential.

These measurement need to be combined to obtain Rt and Rxo, the main resistivity parameters for formation evaluation. Resistivity differentiates between water and hydrocarbons in the pore space of the reservoir. Resistivity is our main source of information to determine water saturation (Alian, 2006).

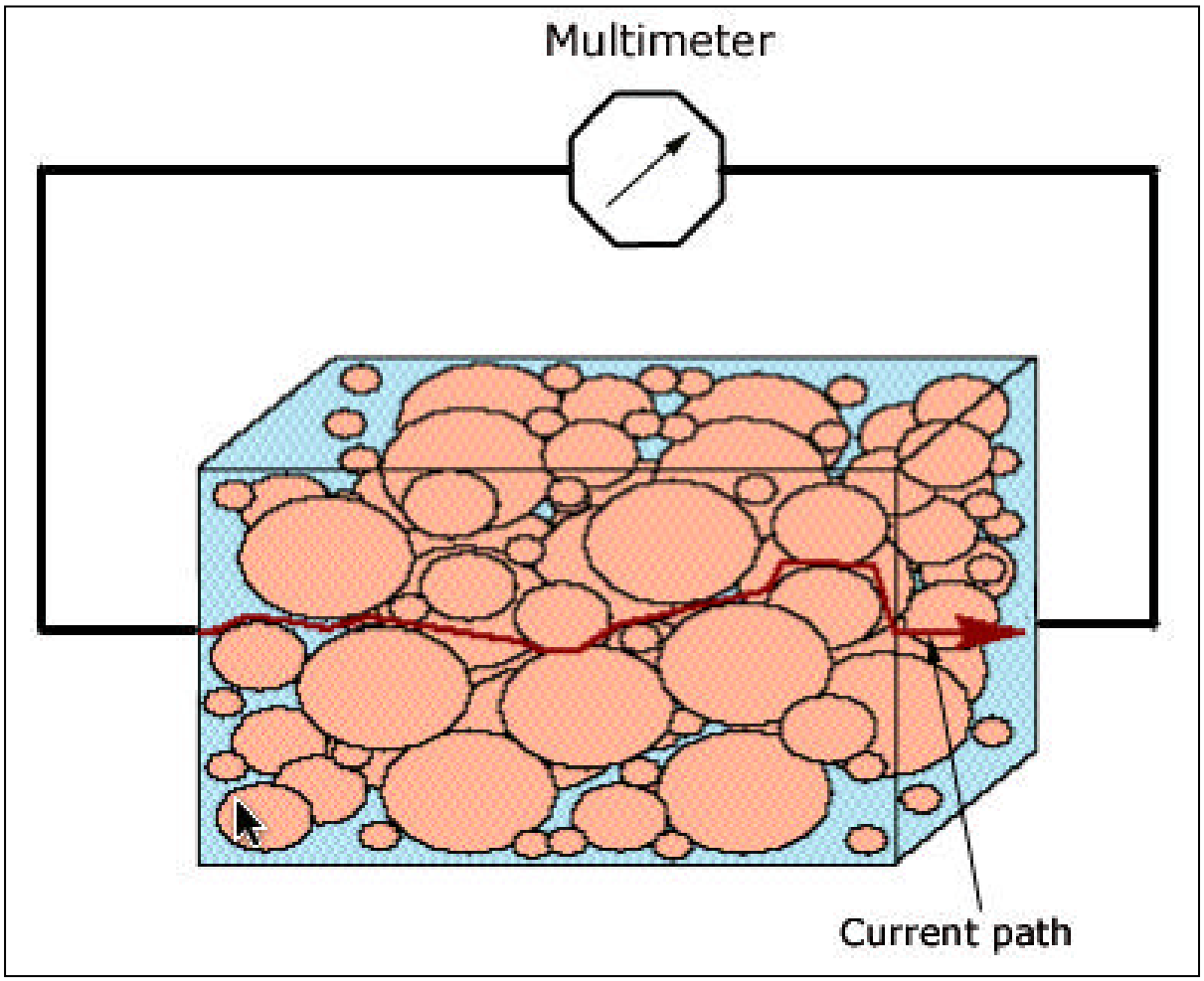

Fig.2-3 : The resistivity measurement and electrical current path way in the formation (Alian, 2006).

The resistivity of a substance is the electrical resistance measured between opposite faces of a unit cube of material.

R = r A/L…….. (1.1)

R = resistivity in ohm-m

r = resistance in ohm

A = area in m2

L = length in m.

Formation resistivity is usually range from 0.2 to 2000 ohm-m. Resistivity higher than 2000 ohm-m is uncommon in permeable Formations, but is observed in very low porosity Formations such as tight carbonates or evaporates. Formation resistivity are measured by

either passing a known current through the formation and measuring the electrical potential or by inducing an electric current into the formation and measuring its magnitude (Fig 2.3).
Resistivity measurements for logging tools are classified into three categories according to their depth of investigation:

• Micro-resistivity: have a depth of investigation of a few inches from the borehole wall.
• Shallow reading: have a depth of investigation of 20 in (0.5 m) to 60 in (1.5 m).
• Deep reading: have a depth of investigation of 50 in (1.3 m) and above.

2.1.7 Elastic Constant Basic (ROCK PHYSICS)

Well logs are often used to determine the mechanical properties of rocks. These properties are often called the elastic properties or elastic constants of rocks. The subject matter and practice of calculating these rock properties is often called "rock physics".
Mechanical properties are used to design hydraulic fracture stimulation programs in oil and gas wells, and in the design of mines and gas storage caverns. In this situation, the mechanical properties are derived in the laboratory or from well log analysis, calibrated to the lab results. In seismic petrophysics, these same mechanical properties are called seismic attributes. They are derived by inversion of time-domain seismic data, calibrated to results from well log analysis, which in turn were calibrated to the lab data. The vertical resolution of seismic data is far less than that of well logs, so some filtering and up-scaling issues have to be addressed to make the comparisons meaningful.
The main purpose for finding these attributes is to distinguish reservoir quality rock from non-reservoir. The ultimate goal is to determine porosity, lithology, and fluid type by "reverse-engineering" the seismic attributes. The process is sometimes called "quantitative seismic interpretation". In high porosity areas such as the tar sands, and in high contrast areas such as gas filled carbonates, modest success has been achieved, usually after several iterative calibrations to log and lab data. Something can be determined in almost all reservoirs, but how "quantitative" it is may not be known.
There are many other types of seismic attributes related to the signal frequency, amplitude, and phase, as well as spatial attributes that infer geological structure and stratigraphy, such as dip angle, dip azimuth, continuity, thickness, and a hundred other factors. While logs may be used to calibrate or interpret some of these attributes, they are not discussed further here. The best known elastic constants are the bulk modulus of compressibility, shear modulus,

Young's Modulus (elastic modulus), and Poisson's Ratio. The dynamic elastic constants can be derived with appropriate equations, using sonic log compressional and shear travel time along with density log data.

Dynamic elastic constants can also be determined in the laboratory using high frequency acoustic pulses on core samples. Static elastic constants are derived in the laboratory from tri-axial stress-strain measurements (non-destructive) or the chevron notch test (destructive).

Elastic constants are needed by five distinct disciplines in the petroleum industry:

1. Geophysicists interested in using logs to improve synthetic seismograms, seismic models, and interpretation of seismic attributes, seismic inversion, and processed seismic sections.

2. Production or completion engineers who want to determine if sanding or fines migration might be possible, requiring special completion operations, such as gravel packs.

3. Hydraulic fracture design engineers, who need to know rock strength and pressure environments to optimize fracture treatments.

4. Geologists and engineers interested in in-situ stress regimes in naturally fractured reservoirs.

5. Drilling engineers who wish to prevent accidentally fracturing a reservoir with too high a mud weight, or who wish to predict over pressured formations to reduce the risk of a blowout.

The elastic constants of rocks are defined by the Wood-Biot-Gasman equations. The equations can be transformed to derive rock properties from log data. If crossed dipole sonic data is available, anisotropic stress can be noticed by differences in the X and Y axis displays of both the compressional and shear travel times. When this occurs, all the elastic constants can be computed for both the minimum and maximum stress directions. This requires the original log to be correctly oriented with directional information, and may require extra processing in the service company computer center.

Elasticity is a property of matter, which causes it to resist deformation in volume or shape. Hooke's Law, describing the behavior of elastic materials, states that within elastic limits, the resulting strain is proportional to the applied stress. Stress is the external force applied per unit area (pressure), and strain is the fractional distortion which results because of the acting force (Fig. 2-4).

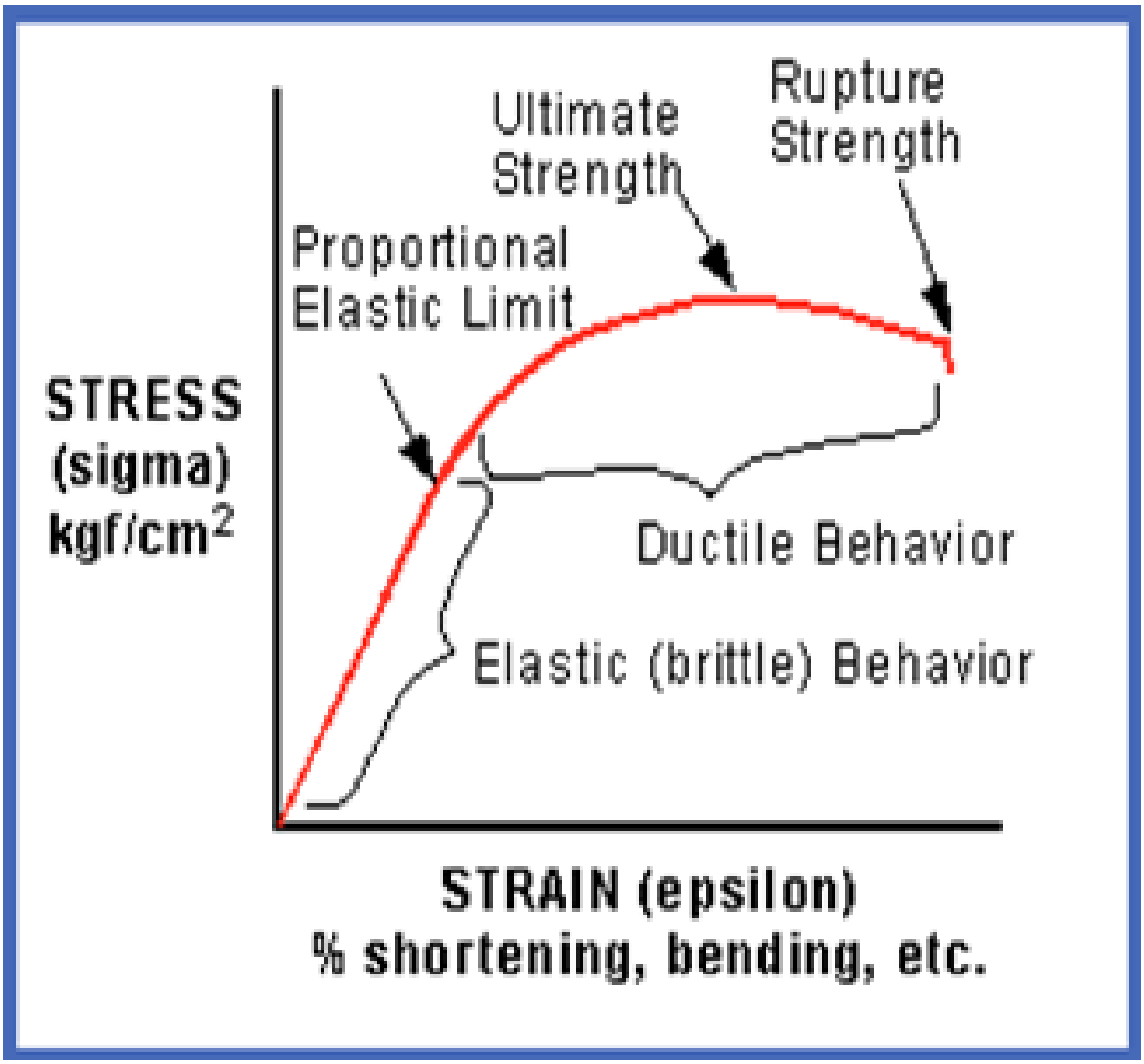

Fig.2-4 : The chart describing the behavior of elastic materials and the modulus of elasticity is the ratio of stress to strain (crain, 1978-2016).

2.3.Previous Work:

It is common to use the standard gamma ray log (SGR) or total contribution from all three elements-uranium (U), potassium (K), thorium (Th)-as an indicator of the clay content. The presence of highly radioactive black organic material and/or natural fracture in the formation results in a big difference from X-ray diffraction data. This causes an overestimate of shale volume and therefore affects the original oil in place (OOIP) and reserves. A novel methodology that combines normal distribution and normalization to predict correct gamma

ray from SGR and deep resistivity, Rt, and across correlation technique applied to validate the methodology, and the model corrected gamma ray (CGR) matches the actual CGR very well. Next, element capture spectroscopy (ECS) logs used to quantify the actual caly volume (Vsh).Then computing techniques to develop a shale volume model using CGR and Rt as independent variables and Vsh from ECS as the dependent variable (Rodolfo, 2010).

Clay minerals are very small particles with layered structure (phyllosilicate) and large specific surface areas. They are the main component of claystones and shales but they are common in sandstones and can affect the reservoir properties. Clay minerals form in different diagenetic environments (eogenesis, mesogenesis) and by weathering of the feldspars. Diagenetic clay minerals can be discrete particles or pore-filling aggregates.
Chlorites are clay minerals which are classified in two different types according to their chemical composition, Fe chlorite and Mg chlorite. Chlorite is a stable clay mineral that occurs in the early stage of mesogenesis and can be remained in the end of the telegenesis regime. The reservoir quality strongly changes with the proportion of pore-filling vs. pore-lining chlorite. The best in terms of reservoir quality is the coarser-grained sandstones, where chlorite forms a thin pore-lining layer that does not hinder significantly the permeability and preserves porosity (Sanaz . J, 2013).

Reservoir description requires that geological and petrophysical data are integrated for input to a dynamic three-dimensional reservoir simulation model (Hurst & Archer, 1986) [previous paper]. Porosity, Φ permeability (K), water saturation (Sw) and the petrophysical parameter volume shale (Vsaale) are routinely evaluated from wireline logs, sometimes without input of geological data. It is emphasized that all the characteristics, Φ , K, Sw and Vshale, are derived indirectly from log measurements using mathematical or empirical formulae. Clay minerals influence all wireline logs; therefore all wireline logs have some potential for identifying clay minerals. Ideally, different clay minerals should be differentiated by their characteristics as measured by wireline logs (Fertl & Frost, 1980; Almon, 1979).
In clastics rocks there is a loose relationship between pore throat size and grain size, and there is a loose relationship between grain size and sorting, therefor there is a loose relationship between porosity, sorting and grain size.
The logs measure bulk properties and have little response to grain size and texture.

These simplifications may be appropriate for clastics, but do not always work and are not necessarily applicable to carbonates or fractured reservoirs (Andrew, 2008).

A rock physics characterization based on wireline log data is proposed for constraining the petrophysical properties of the productive interval in the Marcellus Shale. The method involves two parts, 1) petrophysical interpretation of organic shale from wireline log data, and 2) rock physics modeling utilizing the interpreted log data. A petrophysical interpretation of the more radioactive interval of log data suggests that higher TOC is associated with lower clay content. This interpretation also showed that upper the part of the Marcellus Shale is clay dominated whereas the lower part is quartz dominated. The productive interval did not contain significant amount of pyrite or carbonate minerals. Following the interpreted petrophysical data, the rock physics modeling was performed using differential effective medium (DEM) scheme in an inclusion based model to estimate the effective elastic moduli of the composites. The elastic moduli of the matrix phase in the DEM were provided with the Voigt-Reuss-Hill average for a composition of quartz and clay. Imbedded inclusions were assumed. Three types of inclusion phases were considered; a dry pore (i.e. equant pores or ellipsoidal pores), a water-wet clay pore and kerogen. Dry pores were saturated with pore fluids simulating reservoir situations with the low frequency Gassmann equations. Rock physics modeling suggests that the elastic properties of the Marcellus Shale were controlled by the interplay of clay content, kerogen content and low aspect ratio pores. Low aspect ratio pores (~1/40) also comprise the dominant pore types in the Marcellus Shale and these pores are more common in the lower part of the formation. This proposed rock physics scheme constrains the dominant petrophysical properties to be applied for surface seismic data interpretation (Sharif. M, 2013).

CHAPTER THREE

ANALYTIC APPROACH

In order to describe and compute accurate formation components, multi-mineral analysis is proposed using ElanPlus software. The difference between ElanPlus and traditional petrophysical analysis methods (deterministic method) is that ElanPlus solves a set of equations (formed by logs, formation components volume and parameters) to derive the volume of each formation components.

One of the main benefits of ElanPlus is the ability to customize the formation model (Solver) to match the local mineralogy to produce a more accurate representation of the rock, both in terms of lithology and petrophysical properties. In addition, ElanPlus allows multiple models (Solver and Combine), parameter calibration (ParCal), and reconstructed logs (Schlumberger, GF4,Elan plus manual),moreover ElanPlus results will be QC by re-constricted logs curves and original logs. The petrophysical analysis and methods can be summarized as following:

3.1 Methods and Analysis Workflow

3.1.1. Introduction to the Logging Interpretation Results and Workflow

The minerals and formations components were identified with help of conventional logs analysis, core data, thin-sections and DST results, farther optimized with dynamic elastic properties. The petrophysical data were interpreted using mineral solver model to describe precise minerals and formation components.

The petrophysical and formation evaluations results of three wells (Keyi-4, Keyi-11 and Keyi-12) of Ghazal and Zarga sub layers will be presented in chapter-4, following comprehensive workflow (Fig.3-1) from data collection and quality control of well logging curves.

The logs analysis was the first step, secondly parameters selection (multi wells cross plots and histogram) and petrophysical models selection according to core analysis, thirdly fluid identification base on resistivity, porosity and DST result and finally cut off determination incorporating with DST data to calculate the reservoir properties on summary table results.

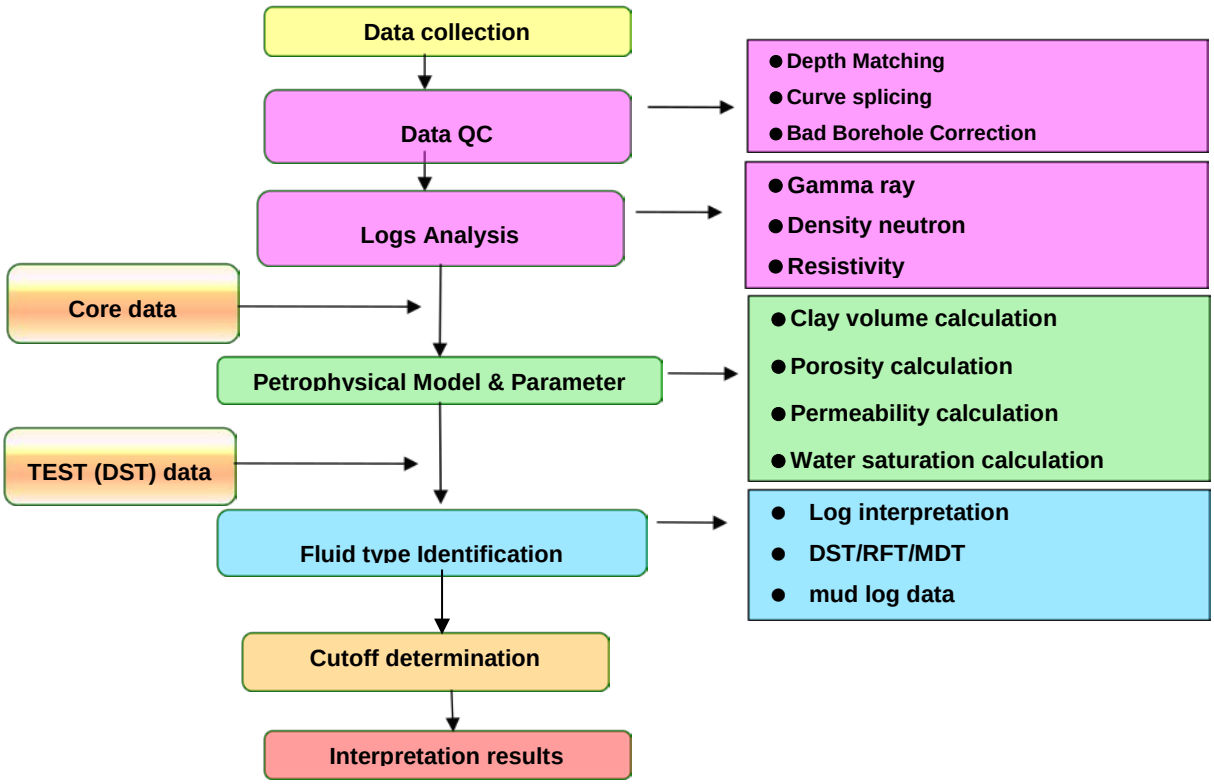

Fig.3-1: Petrophysics and Formation Evaluation Workflow.

The conventional logging data (Las.file format) loading into the software as primary source for display and quick look interpretation for lithology, porosity and fluid saturation. The details petrophysical data were interpreted using Techlog software (version 2014.1.0) running probabilistic programs (Elan Plus-multimineral) approach.

The Elan models of the interpretation composed of:

- Response Equations: GR, RHOB, NPHI, RS, RD and RMSFL.
- Parameters: selected based on cross plot, core and DST.
- Volumes: Quartz, Feldspar, Kaolinite, Smectite, Chlorite, XWAT, UWAT, XOIL and UOIL.

The shale and clay type identification depends on, which program is running for interpretation, for examples:

- Quick look-interpretation- usually Vshale is good enough.

- Deterministic interpretation approach- probably needs V_{cl} and clay types.
- Probabilistic programs – definitely need V_{cl}, clay types and clay end point, and the clay considered as wet clay (Fig 3-2).

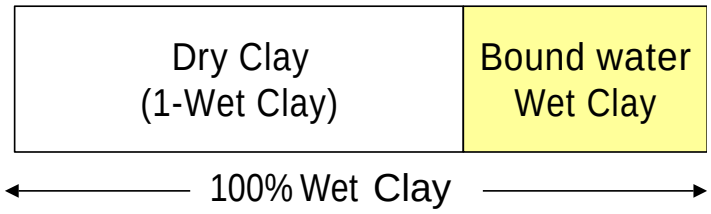

Fig.3-2: Wet clay module

3.1.2. Logs Analysis and Data QC Methods

Log quality control and assessment is usually part of a petrophysicists job description. Modern logs are run and calibrated under control of a computer program, monitored by the logging engineer. Most problems will be related to poor borehole condition and mistakes in recording the log as set out in the logging program found in the well prognosis. Tool failures and missing curves may cause difficulties later during the analysis phase (Crain's Petrophysical Handbook).

The available conventional well logs data from 3 wells (Keyi-4, Keyi-11 and Keyi-12) provided in las file format and loaded using Tech Log software version (2014.1.0).The conventional logs data include, Gamma ray (GR), Caliber (CAL), Bit size (BIT), Micro resistivity (MSFL), Shallow resistivity (R_s), deep resistivity (R_d), Density, Neutron porosity, and special logs is dipole shear sonic from well Keyi-12. All the logs were loaded processed and QC as the following steps:

- The depth matching between logs and core to ensure the depth alignment.
- Identify bad hole, because density and neutron porosity logs are sensitive to washout and hole size.
- Identify tool sticking.
- Logging speed.
- Comparison between the logs measurement in the repeat and main logging section.

3.1.1.1. Gamma Ray Log Analysis Method

Clean sandstone has a high GR (60-75API) reading whereas shale and clay (100-120 API), due to high potassium content, which leads to overestimate the shale volume (Fig. 3.3).

The GR is mostly use as clay indicator, but in our case, GR is bad shale indicator and lithology discriminator.

The shale or clay volume estimated from gamma ray, using equation (3.1) as single clay indicator (deterministic method).

$$\text{Vshale} = \frac{GRL - GRclean}{GRshale - GRclean} \quad \text{..... (3.1)}$$

Where:

Vshale: Shale volume

GRL: Gamma ray log

$GRclean$: clean sand reading.

$GRshale$: 100% shale reading.

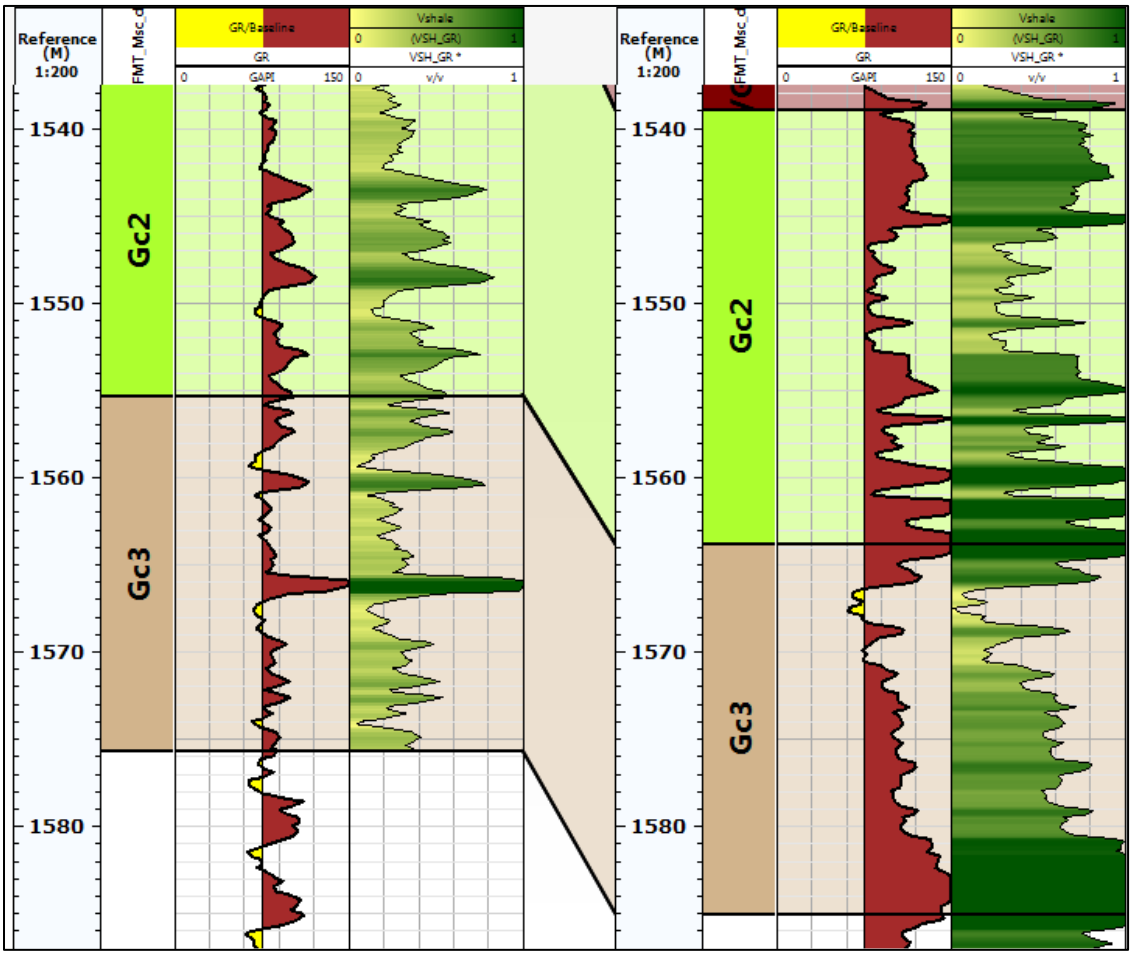

Fig.3-3: Gamma ray responses display relatively high values 60-75 API with high shale volume estimation at depth 1571-1585 m.

The GR is mostly use as clay indicator, but in our case is not good shale indicator to discriminate between shale and sand layers, because the shale volume from gamma ray response is not consistency with other logs like density-neutron and resistivity logs interval (1571.0-1585.0m), the gamma ray read relatively showed high value (105 API) in sand layer, with 60% shale volume, whereas density-neutron and resistivity indicate clean sand with less than 22% shale content in this reservoir (Fig.3-3).

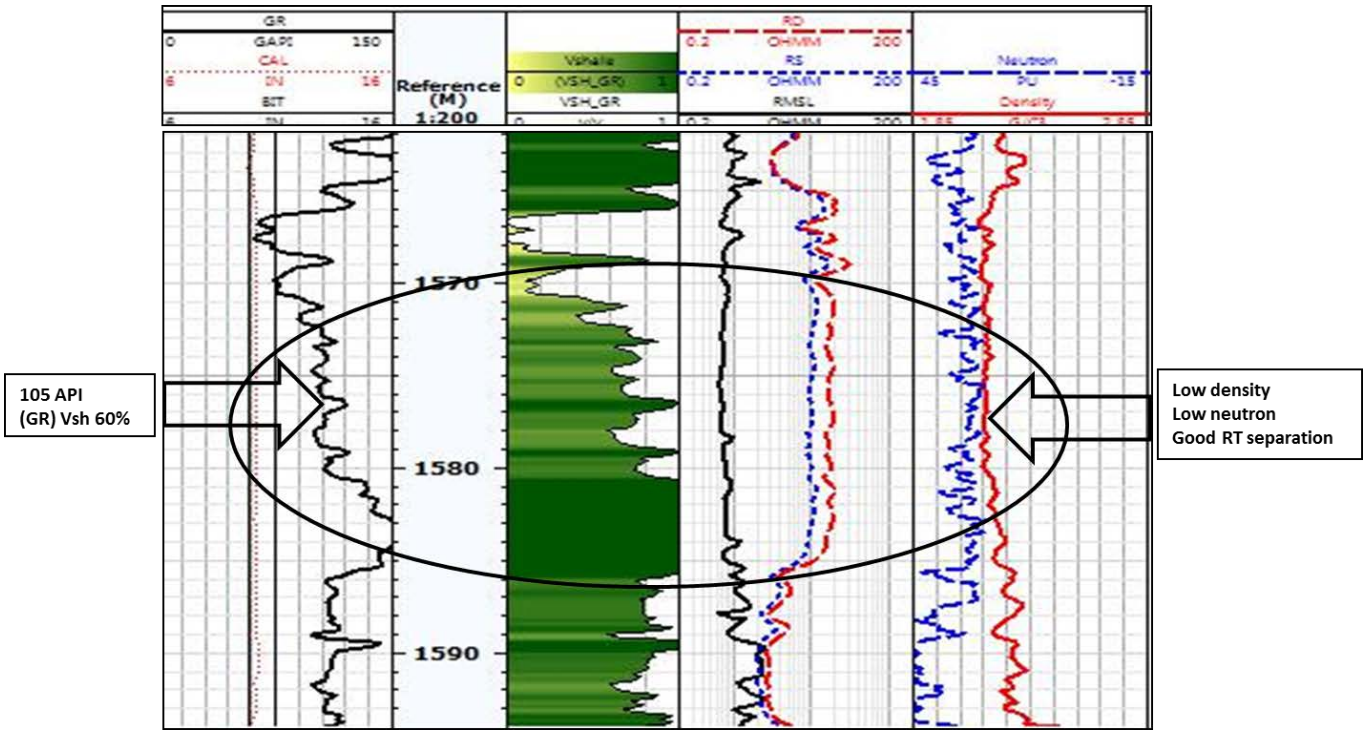

Fig.3-4**:**Comparison between gamma ray response ,density-neutron and resistivity responses in clean sand interval (1571.0-1585.0m) of well keyi-11, the shale content about 60% from GR method.

3.1.1.2. Photoelectric Factor and Gamma ray Logs Combination Method.

Photoelectric factor (PE) and gamma ray logs can be combined into a powerful tool to eliminate the effect of radioactive minerals (K-feldspar) concentration from total gamma ray. Photoelectric factor log has linear relation with gamma ray to some extend and less affected with radioactive mineral. Multi wells cross plot of target zones was generated and plotted GR against PE and regression line extrapolated with upper (149 API, 3.4 PE) and lower(50 API,1.86 PE) limit of lithology was identified (sand-shale end points), then linear equation generated to correct for gamma ray(CGR0) (Fig.3.5),and equation (3.2).

CGR0=57.6*PE-57.4…… (3.2)

Where:

CGR0: Corrected gamma ray

PE: Photoelectrical factor.

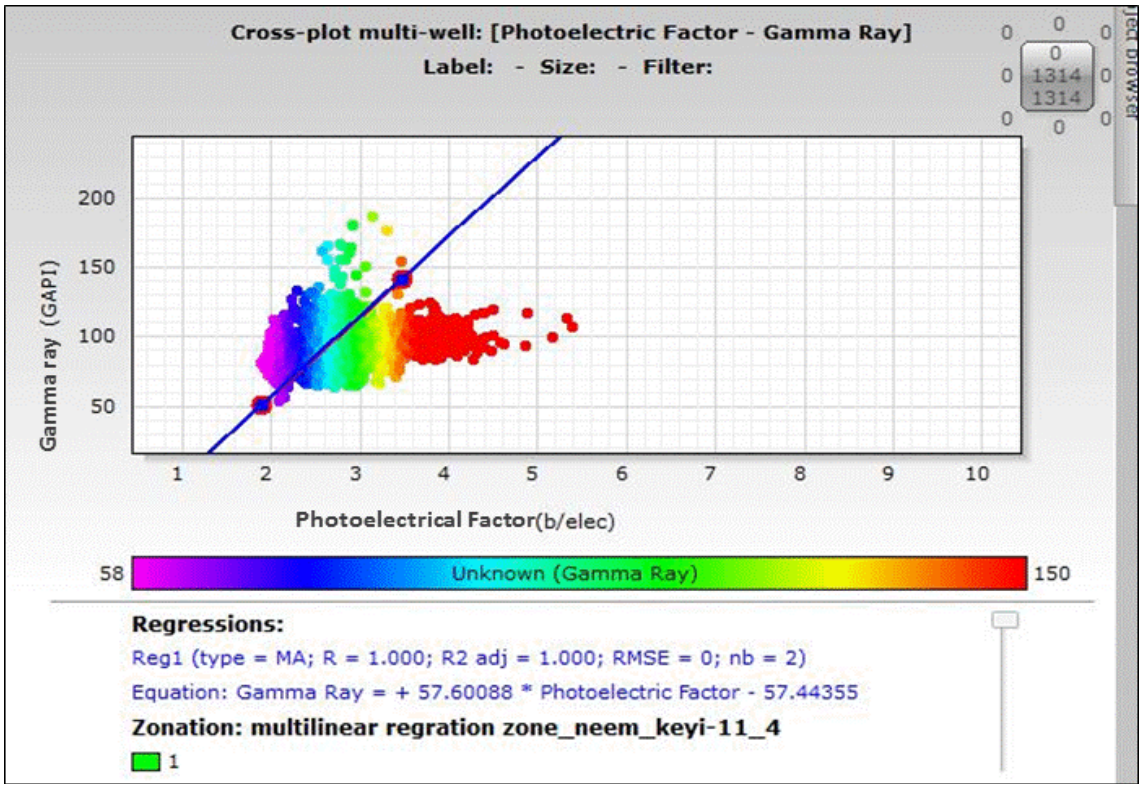

Fig.3-5: The combination of photoelectric factor in x-axis and gamma ray in y-axis to develop a new model to eliminate the effect of the potassium concentration from gamma ray log.

This concept of CGR0 applied to well Keyi-11, that has spectral core gamma and confirmed the effects of potassium on original gamma ray, then the gamma ray correction (CGR0) was done and the result of new method (CGR0) showed clear difference in shale volume estimation from 60% to 29% in some intervals (1571.0-1585.0m) (Fig.3-6).

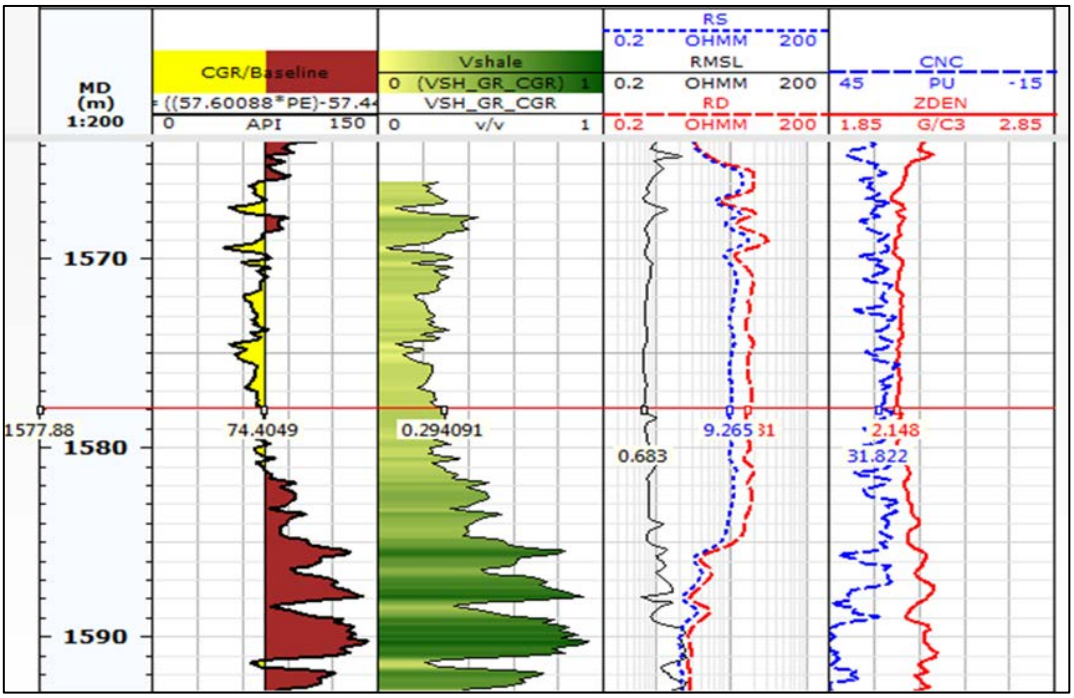

Fig.3-6: Shale volume estimation after gamma ray corrected from potassium effect, using equation(3.2), and calculates reasonable shale content based on gamma ray about 29% of well Keyi-11.

3.1.1.3. Density and Neutron Porosity Analysis

Neutron and density is the main porosity and shale content indicator in this study. They are also sensitive to lithology and fluid type.

Initially a few parameters must be set, and by default a few values are already in place. The matrix density (ρma), fluid density (ρf), and gas correction values should be set early to facilitate the analysis. Matrix density is the density for the primary mineral being analyzed. Usually this is set to sandstone matrix as the following:

- Quartz (sandstone) :ρma = 2.65 g/cm3

Fluid density (ρf) will be the density of the formation water in the reservoir. Normally for evaluation of shaly-sand reservoir the shale endpoint parallel to dolomite line and perpendicular to the dolomite line to sandstone line the shalness decrease (Aaron, D. 2013).

Neutron logs are recorded in porosity units corresponding to a selected matrix lithology and presented with either the density or density porosity logs.

When displayed on the same porosity scale, separation between the neutron and density curves indicate a change of lithology or the presence of gas. In varying and complex lithology, the neutron log is usually displayed in apparent limestone porosity units and the density logs in g/cm3. On logs presented with scales of 1.65 to 2.65 g/cm3 for the density and 48 to 0PU for neutron limestone porosity, both logs overlay in clean sandstone water bearing formations ,this is called a sandstone compatible scale.

The density-neutron cross plot technique for well Keyi-11, it is the main shale/lithology indicator in this study; it is most useful for shaly sands because the shale point is usually well separated from the sandstone line (Fig.3.7). Clean, water-bearing points fall on the main lithology line, as in our case most of points fall below the sandstone line (clean sand); this cross plot did not show very clean sand. Shale points fall to the right of the plot (below purple line). The highest neutron porosity values in shale zones indicate the shale point. The neutron density points cannot be used when either neutron or density log is affected by washout or bad hole conditions.

Density-neutron cross plot is powerful technique compare to gamma ray to discriminate between shale and sand (Fig. 3.7).

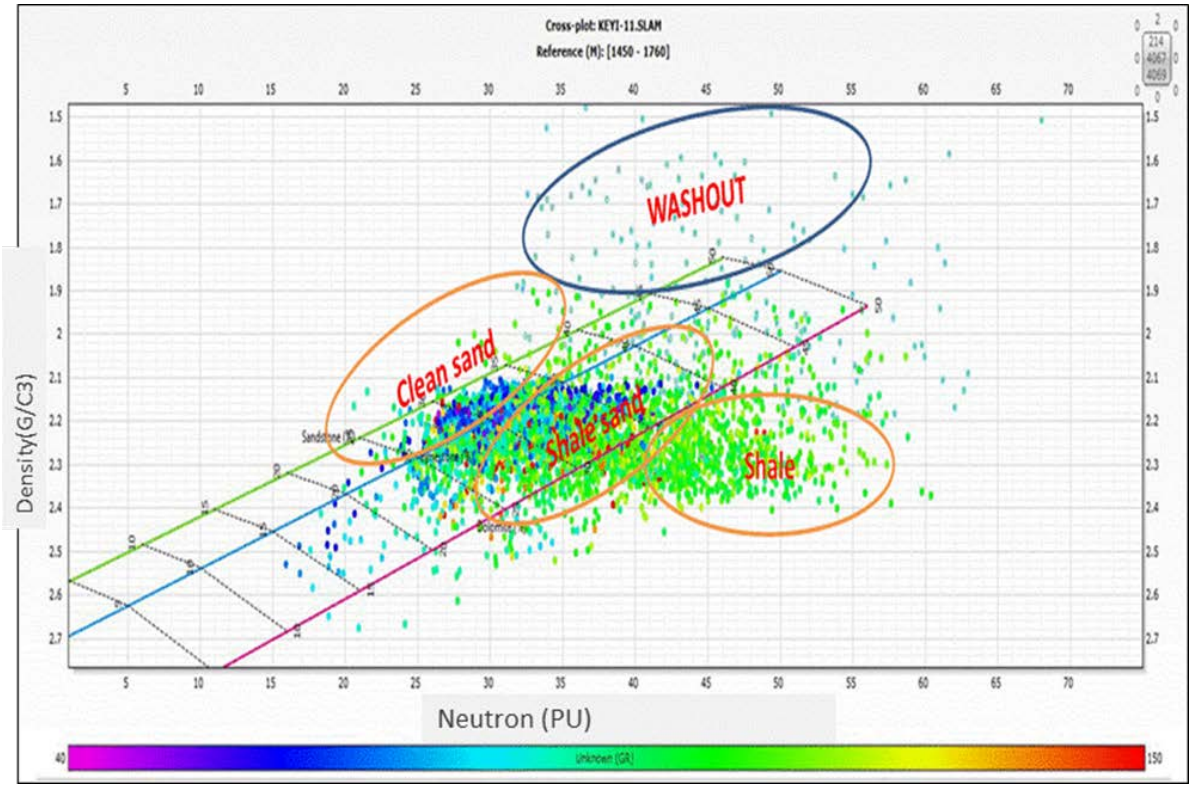

Fig.3-7: The density-neutron cross plot for well Keyi-11, using this technique as lithology ,clay indicator and quality control for the data, which strongly affected by hole conditions.

3.1.1.4. Resistivity and Formation water (R_W) Analysis

Resistivity is the most important measurement to calculate R_w and water saturation. As previously indicated, formation matrices are insulators; thus a formation's ability to conduct electricity is a function of the connate water in the formation. Several methods were proposed for opting formation water resistivity (R_W) values as following:

- R_w calculation from water sample (Table.3.1).
- R_w calculation base on Picket plot technique (Table.3.2).
- Salinity prediction from Gen-9 plot (Fig. 3.8).

Table.3-1: Showing Water Sample Analysis for R_W Identification.

Well Name	Depth (m)	FORMATION	Date Analyzed	Sampling Position	UNIT	OH^-	CO_3^{2-}	HCO_3^-	Cl^-	SO_4^{2-}	K^++Na^+	Ca^{2+}	Mg^{2+}	Salinity	Water Type	T/C	**R_W,ohmm**
Keyi N-4	1329.0-1335.1	Zarqa	Feb 09 2008	Swab outlet	mg/L	0	0	634.61	1906.3	60.04	1386.33	80.2	13.98	3764.16	NaHCO3	56	**0.7**

Table.3-2 : Showing R_W Identification Base On Picket Plot Technique.

Formation	R_w (Range)	R_w (Average)
Ghazal &Zarqa	0.5-1.2	0.85

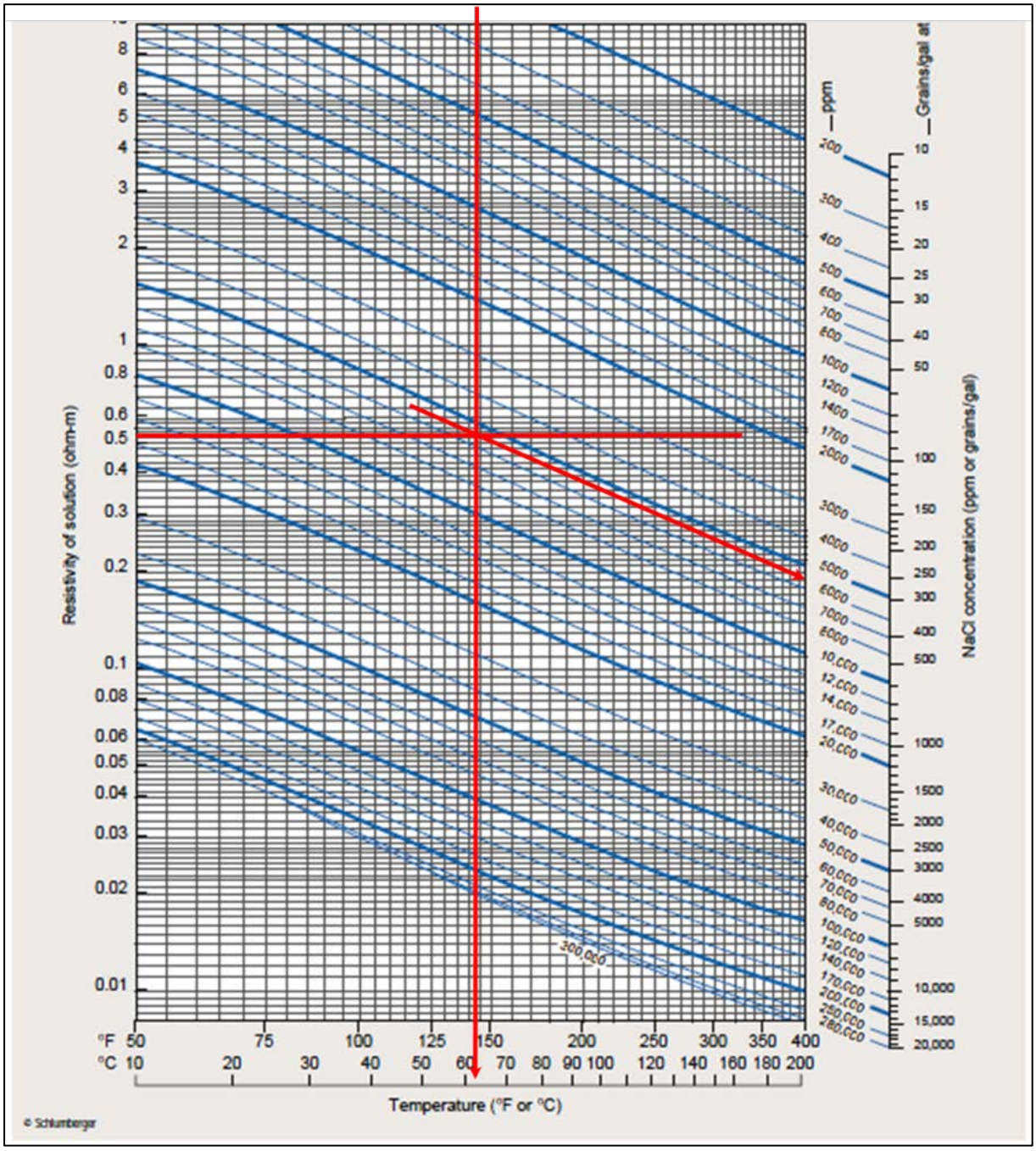

Fig.3-8: Gen.9 plot for salinity about 6000 ppm with minimum R_w 0.5 ohmm-m and formation temperature about 61 c^o

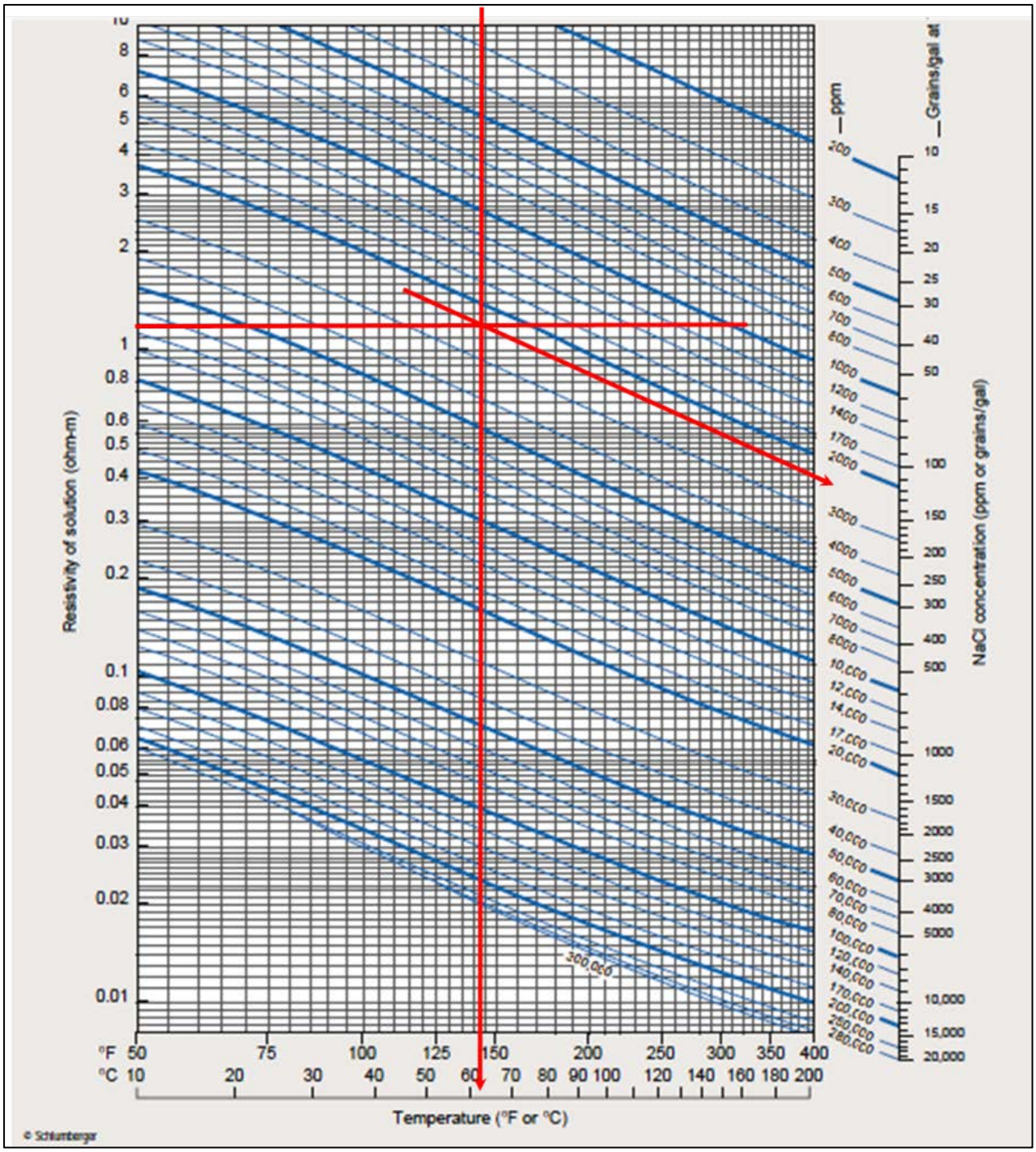

Fig.3-9: Gen.9 plot for salinity about 2500 ppm with maximum R_w 1.2 ohmm-m, and formation temperature about 61 c^o

3.1.3. Core Analysis:

The studied core intervals (1514.50-1516.67m), (1516.67-1518.43m), (1521.01-1524.76m), (1525-1529.20m), (1529.06 -1533.31m), (1529.06 -1533.31m), (1693.06-1700.01m), of well Keyi-11 consist of thick beds of sand stone, which are sometimes intercalated with a few beds of mudstones, and intervals (1510.27-1513.99 m),(1513.99-1516.37 m) and (1688.32-1695.70 m) of Keyi-4 reviewed.

13 samples were used to classify the sandstone of the study area. The quartz: Feldspar: Lithic ratios of the analyzed samples are displayed in QFL (Quartz Feldspar Lithic) sandstone composition diagram (Fig. 3.10).

The challenges in coring include plugs selection, the target interval, handling, preservation and laboratory analysis.

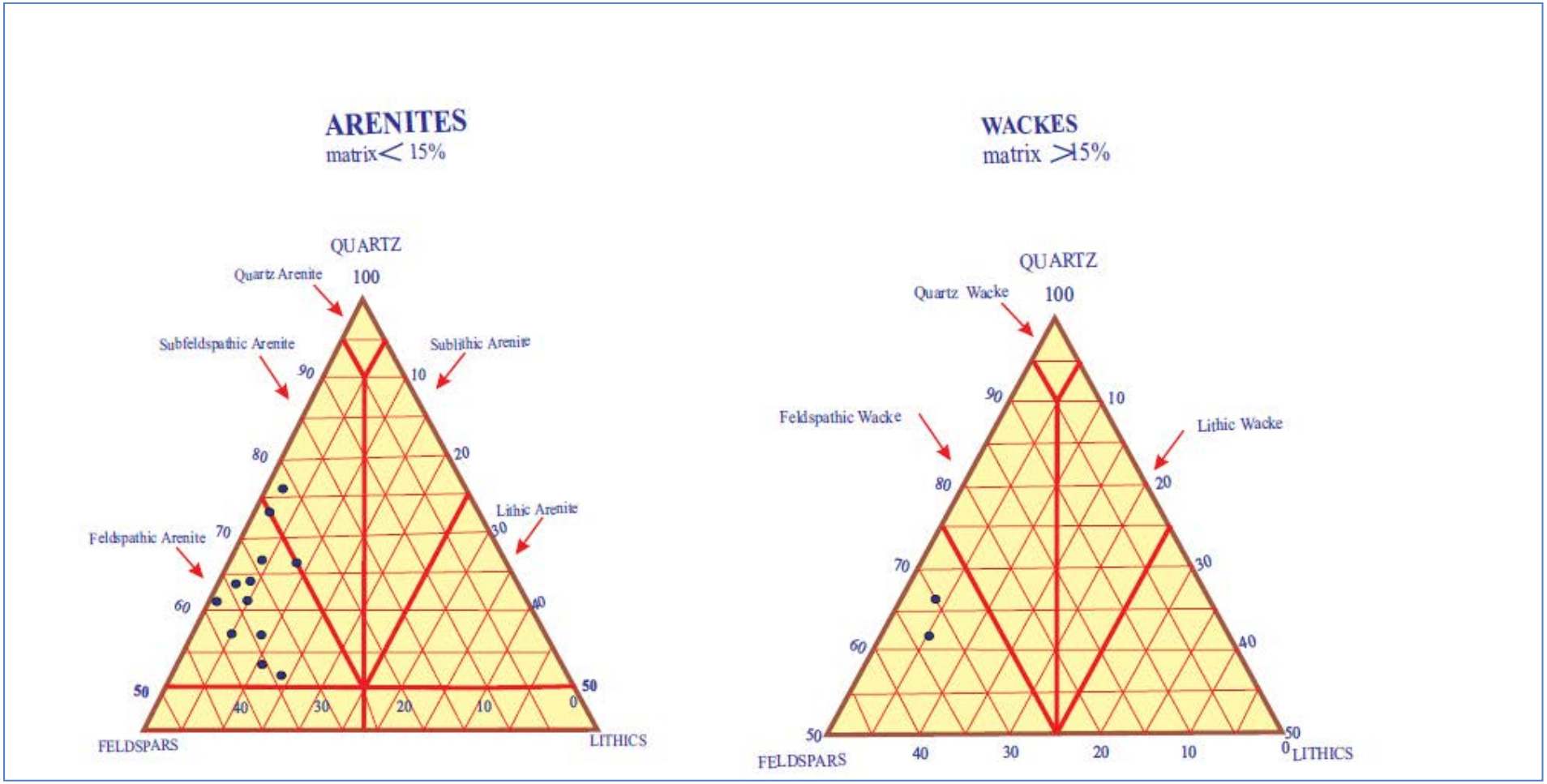

Fig.3-10: The pettijohn classification of sandstone (after pettijohn, 1975). this is an example of the quartz to feldspar ratios and classification in Ghazal reservoir of well keyi-11(CPL, 2014).

3.1.2.1. Spectral Core Gamma Analysis:

The different radioactive minerals emit gamma rays of characteristic energy levels, and based on these levels the contributions from the minerals, Potassium, Uranium and Thorium are specified.

The Thorium (Th) is in ppm, Potassium (K) is measurement in percent and Uranium (U) is measurement in ppm. The thorium, potassium and uranium logs were obtained for better clay types and mineralogy interpretation (Rodolfo, 2010).

In order to verify the presence of the thorium concentration in the matrix, Spectral logs (Potassium, Thorium and Uranium concentrations) were investigated and plotted (Fig.3.11), and cross plot of thorium vs potassium showing also low TH/K ratio equal to zero (Fig. 3.12).

Core description provides calibrating information about the porosity, permeability, and mineralogy and pore type.

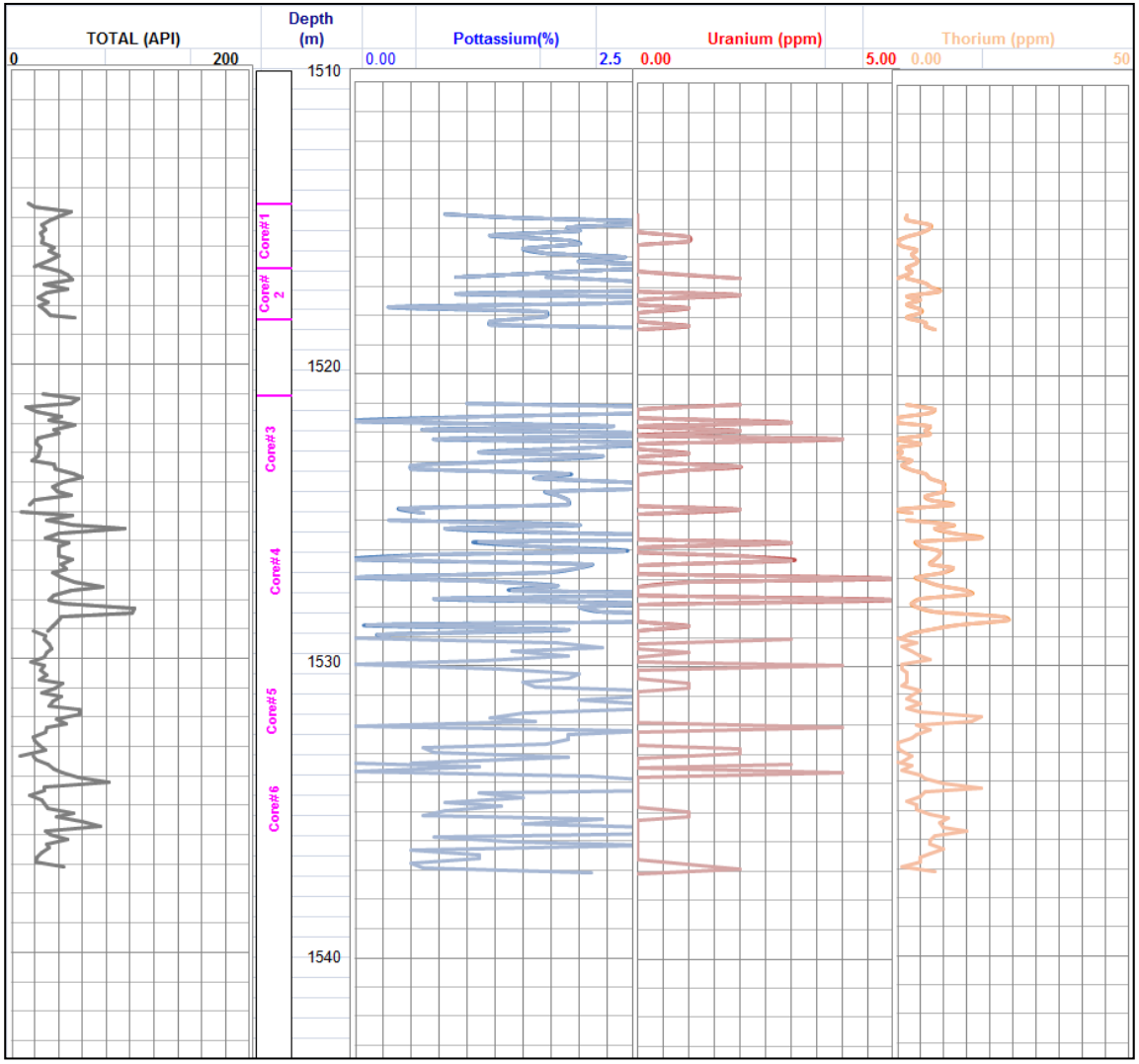

Fig.3-11: The spectral core gammas analysis of well Keyi-11, showing the concentration of K-potassium in the core sample (CPL, 2014).

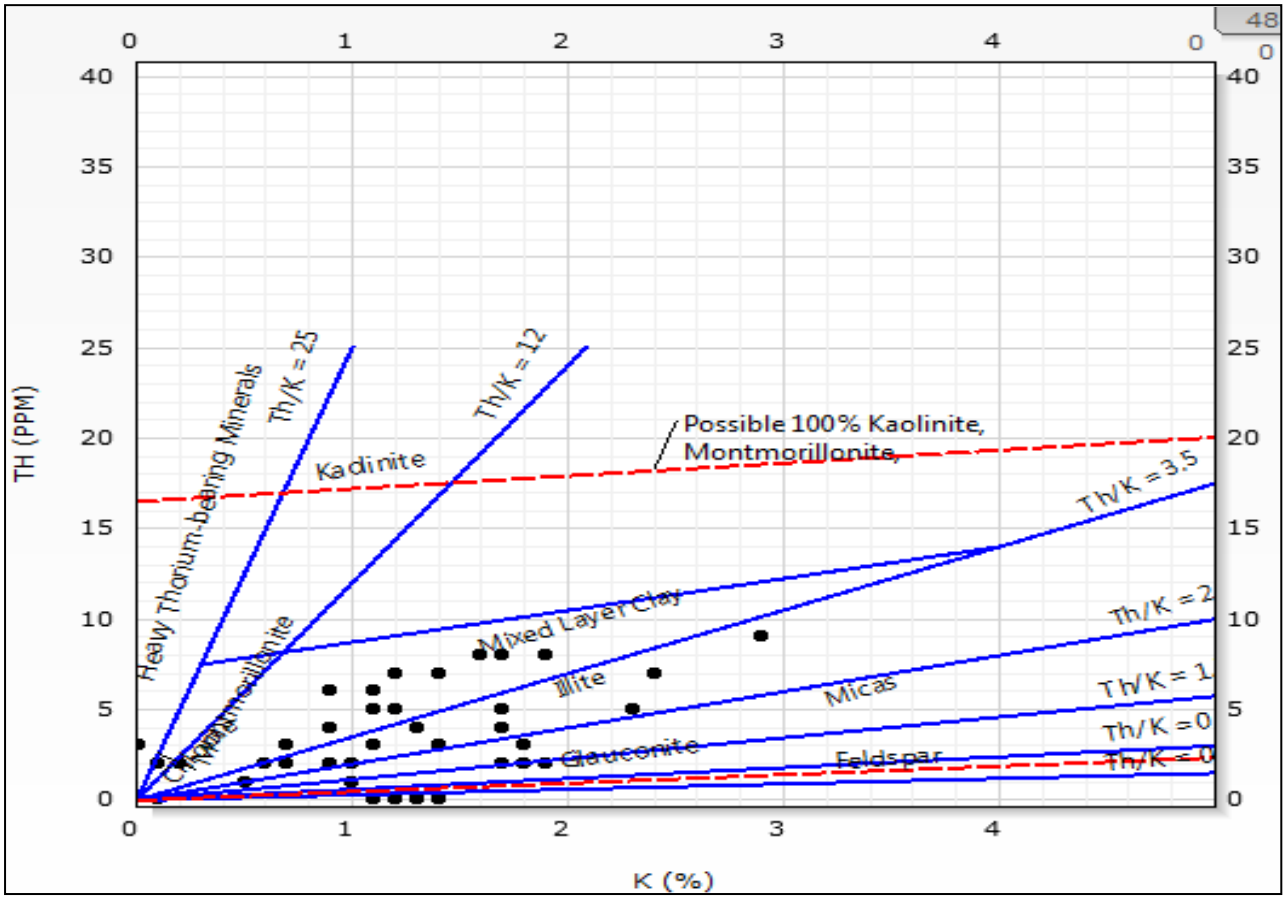

Fig.3-12: Thorium and Potassium cross plot showing low Th/k ratio

3.1.2.2. Clay Mineral Identification from XRD Core Analysis Method

The study of the clay minerals has involved two analytical techniques, X-ray diffraction and Scanning Electron Microscopy (SEM). Four clay rich samples from the studied intervals have been analyzed with the XRD technique. Four clay mineral species were identified from the size fraction less than 2 micron using the procedures of Chamley (1989) as well as Moore and Reynolds (1997). A quantitative estimation of the clay mineral constituents were computed mainly from the ethylene-glycol solvated XRD patterns as suggested by (Schwertmann et al, 1993). The results obtained are shown in (Fig. 3.13), the dominate clay type is **Kolinate,** with traces of Smectite and Chlorite:

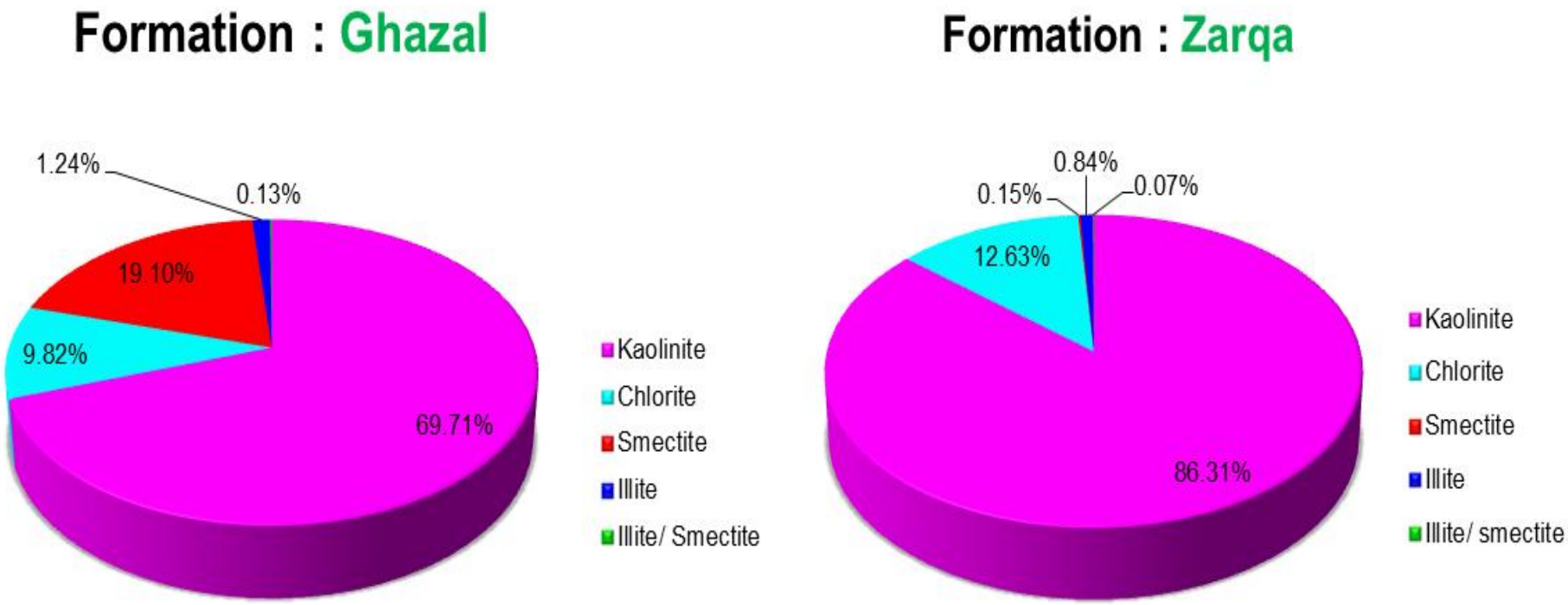

Fig. 3-13: XRD showing the percentages of the clay minerals in the analyzed sample of Ghazal and Zarga formations.

Reference to Petrographic analysis result of thin section of the well Keyi-11 the most common mineral in the reservoirs is quartz with considerable amount of feldspar (Fig.3.12).

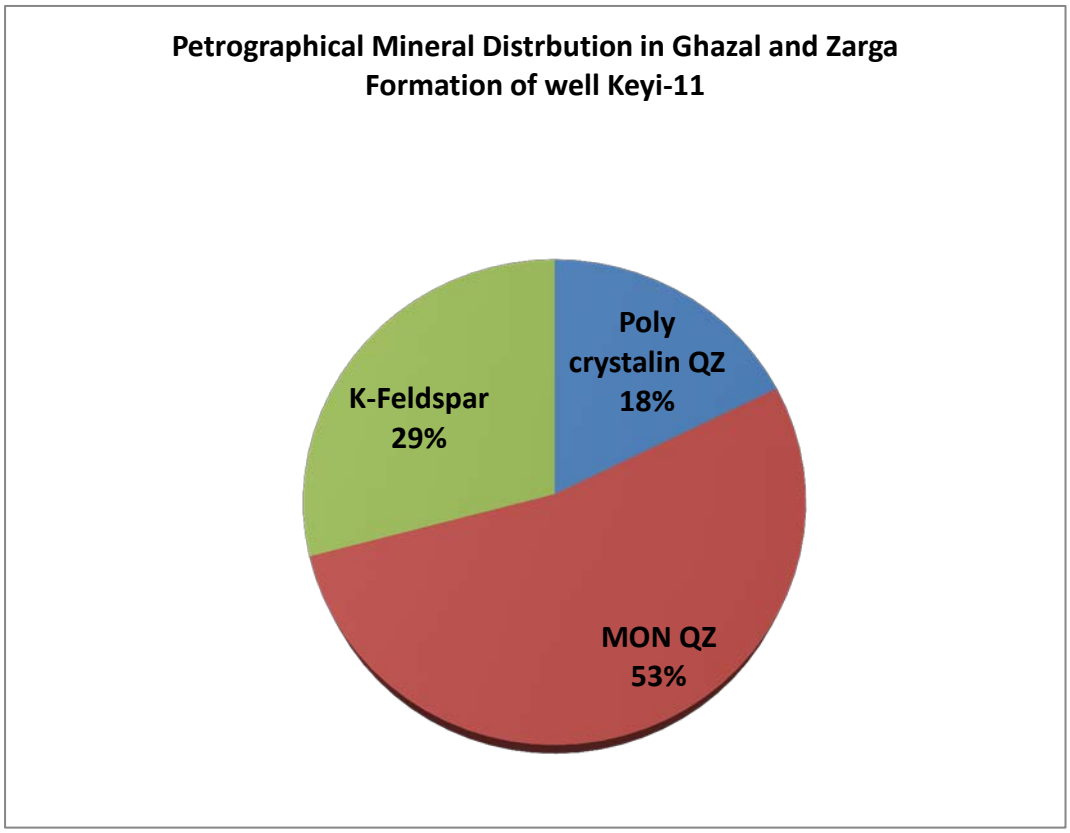

Fig.3-14: The petrographic analysis results, for the studied sample from well keyi-11,showing variable amount of the minerals of Ghazal and Zarga formations.

3.1.2.3. Mineral Identification from Thin Section and SEM Method

The physical properties of the rocks are the consequence of their mineral composition.

The minerals are defined here by thin section photomicrographs and scanning electron microscopy (SEM), and showed that the rocks are composed of mainly quartz and considerable quantities of K-feldspar, Kaolinite ,chlorite, and some amount of plagioclase and few amount of iron oxide (Fig.3.13 to Fig.3.19).

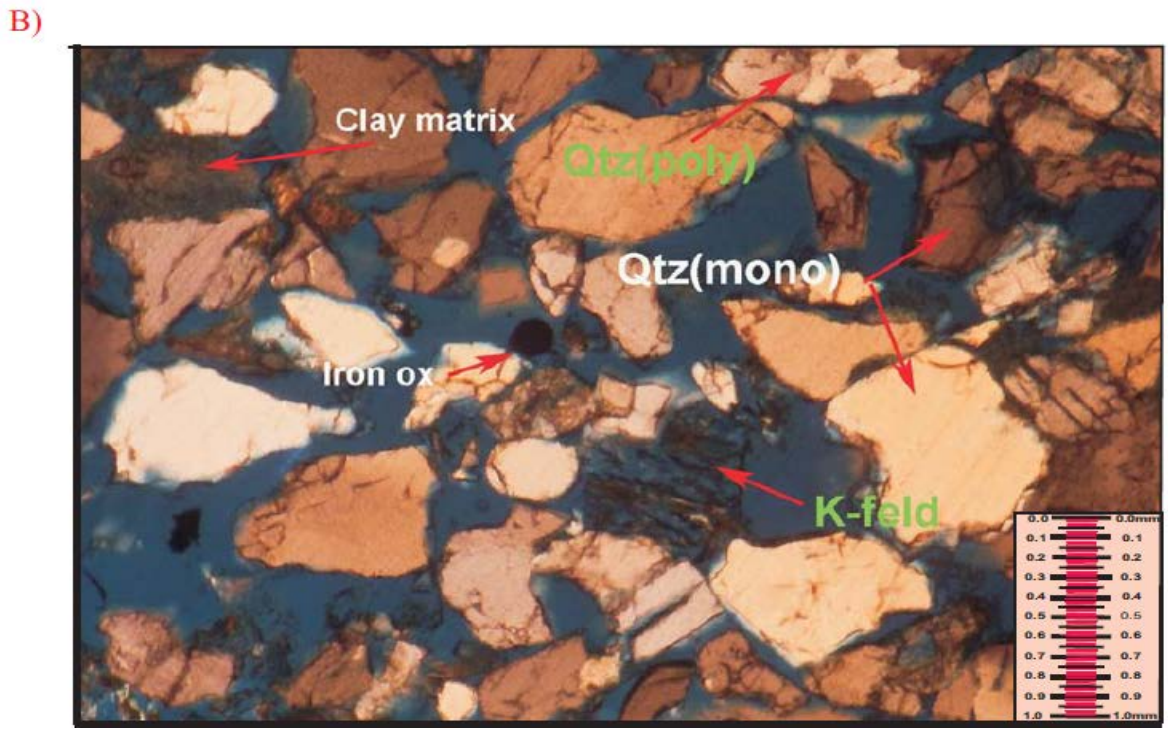

Fig.3-15: Thin section photomicrographs at depth 1698.6m (Zarag formation) of keyi-11well, showing mainly quartz and considerable quantities of k-feldspar (CPL,2014).

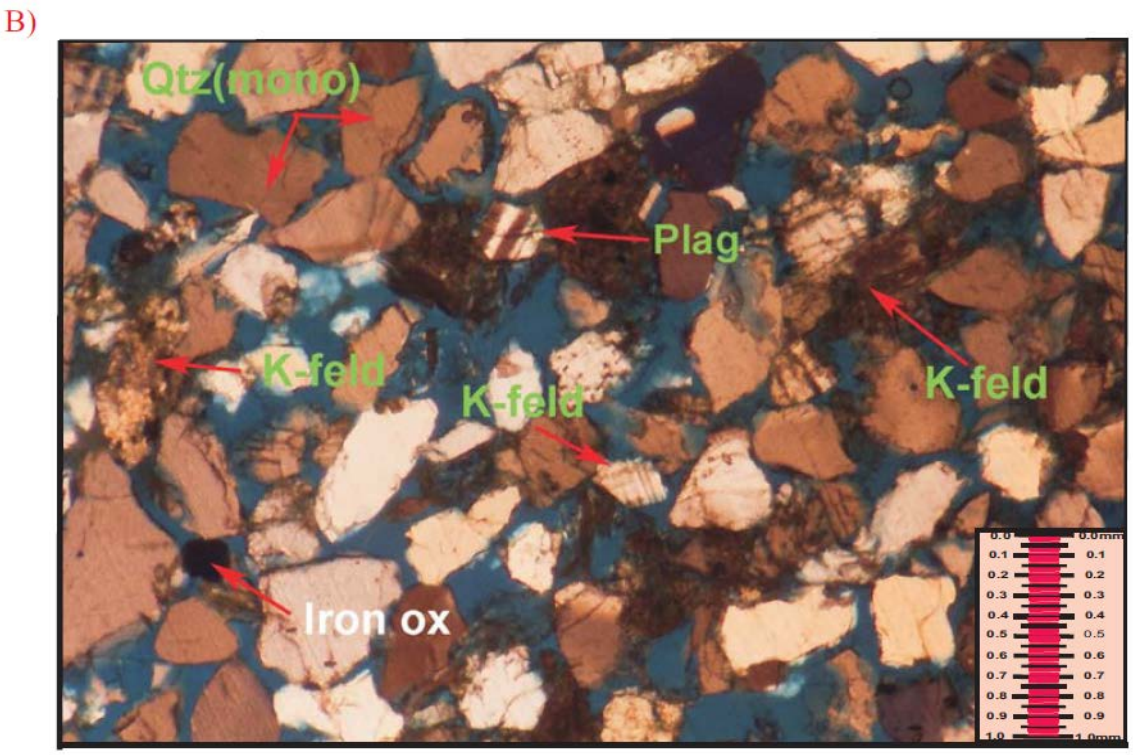

Fig.3-16: Thin section photomicrographs at depth 1534.0m (Ghazal formation) of keyi-11 well, showing mainly quartz and considerable quantities of K-Feldspar (CPL,2014).

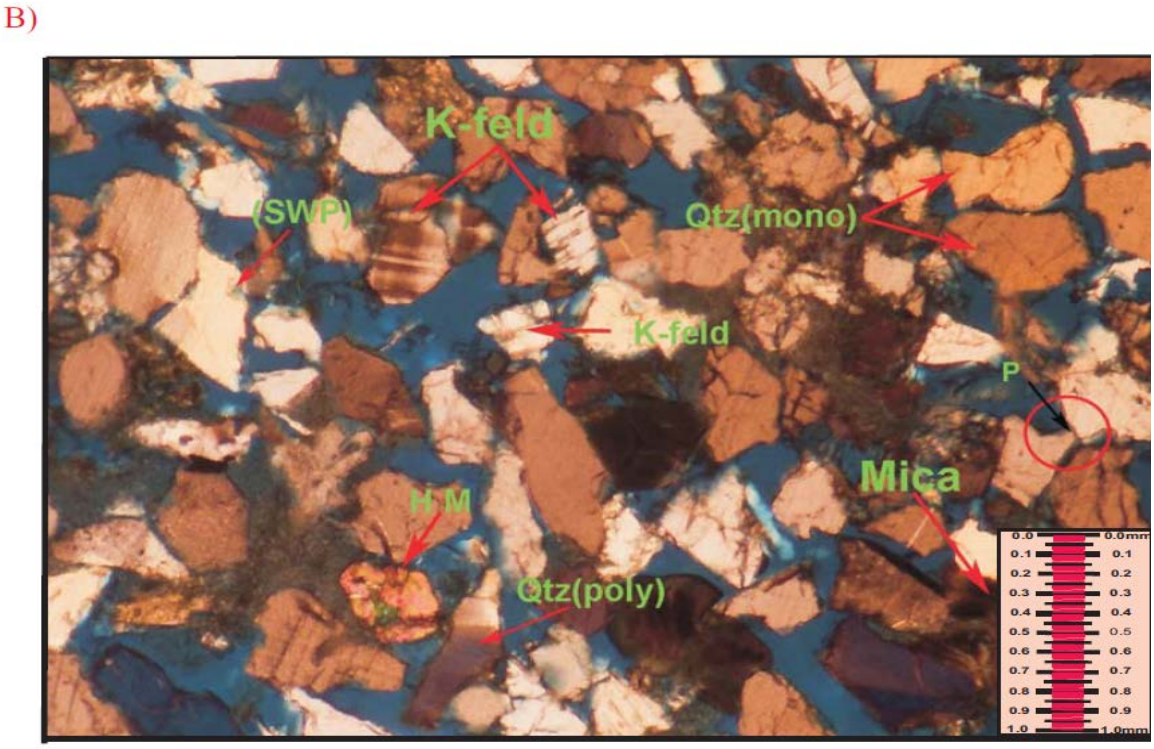

Fig.3-17: Thin section photomicrographs at depth 1521.15m (Ghazal formation) of Keyi-11 well, showing mainly quartz and considerable quantities of K-Feldspar and a few amount of mica (CPL,2014).

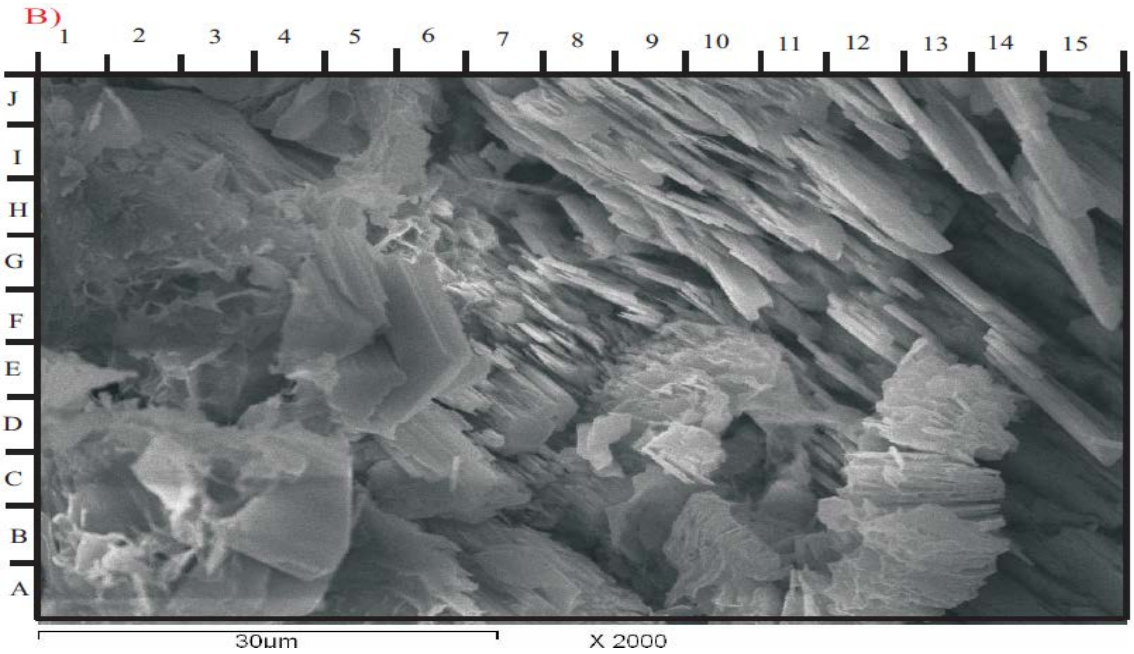

Fig.3-18: scanning electron microscopy (SEM) at depth 1522.4m (Ghazal formation) of Keyi-11 well, showing some authogenic grains of kaolinite (book shape) filling the pores (photo b: h-10 & f-8) & also some detrital grains of kaolinite (photo b: e-10& a-13) (CPL,2014).

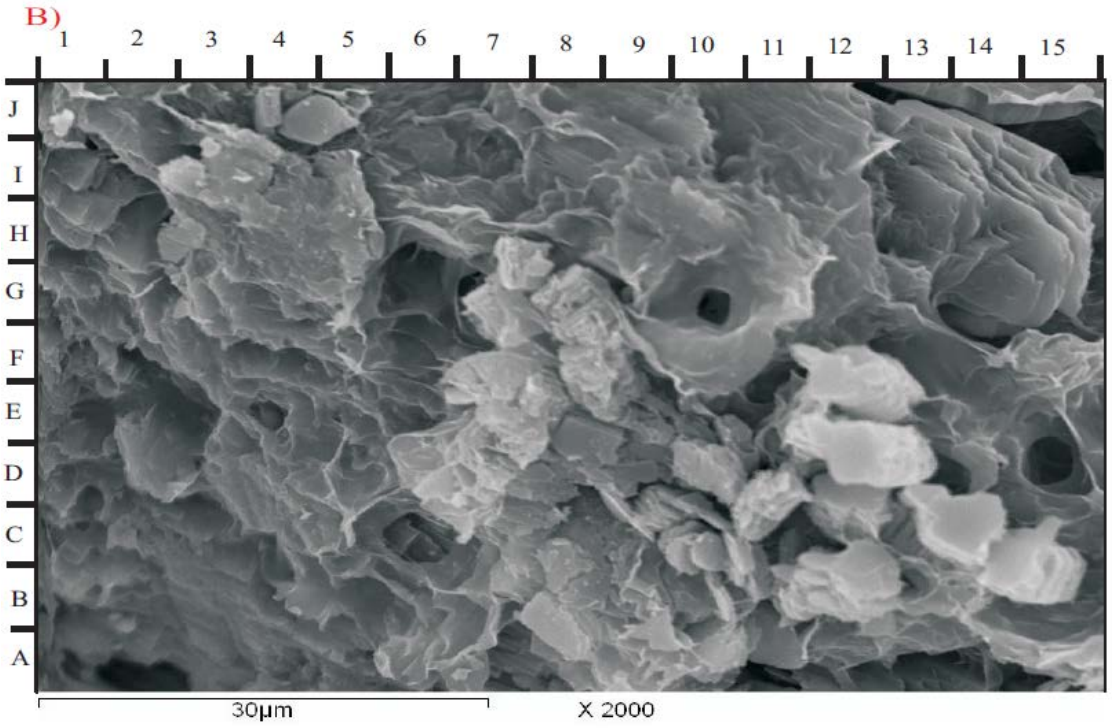

Fig.3-19: Scanning electron microscopy (SEM) at depth 1535.7m (Ghazal formation) of Keyi-11 well, showing filling some pores and partially cover some detrital grains(photo b: i-14)& also some plates of smectite blocked some pores (Photo B:G-10,E-4,D-15 &C-6) (CPL,2014).

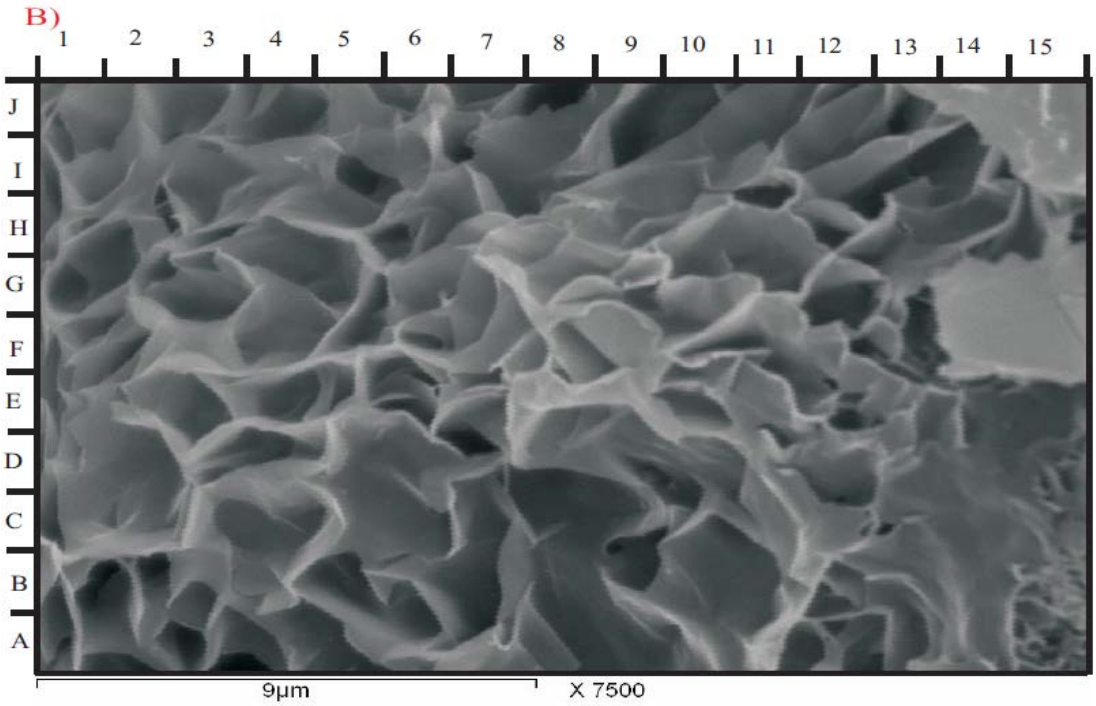

Fig.3-20: Scanning electron microscopy (SEM) at depth 1698.6m (Zarga formation) of Keyi-11 well, showing common authiogenic plates of chlorite arranged like (rose shape) partially filling some pores and blocked it (Photo B: All Over The Photo) (CPL,2014).

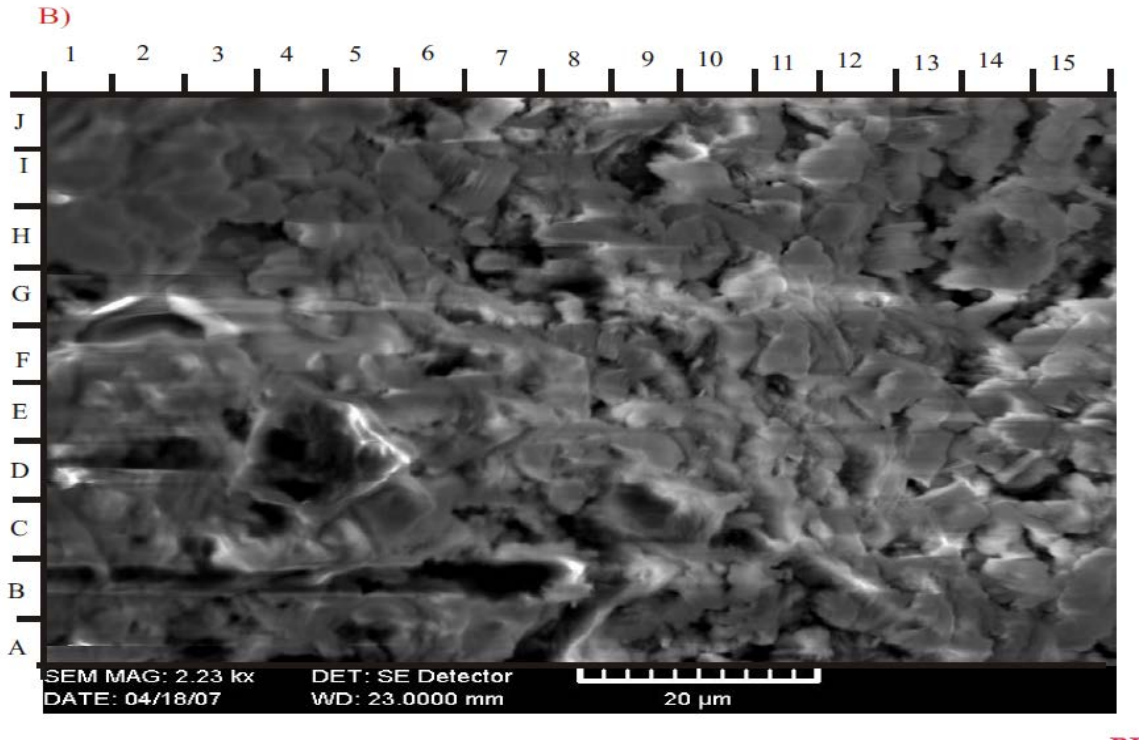

Fig.3-21:Scanning electron microscopy (SEM) at depth 1689.55m (Zarga formation) of Keyi-4 well, showing some clusters of disc-like shape plates of chlorite have also been observed (Photo B: B-D 3-4) (CPL,2014).

3.1.2.4. Porosity and Permeability Core Analysis Method

Core porosity histogram analysis from three wells (Keyi-4, Keyi-11 and Keyi N-9), showed average rang of porosity 10-35% and 20-23% for Ghazal and Zarga formations respectively (Fig.3.22 and Fig.3.23).

The core permeability histogram analysis showed range of permeability 10-1000 md, and 10-10000md, for Ghazal and Zarga respectively (Fig.3.24 and Fig.3.25).

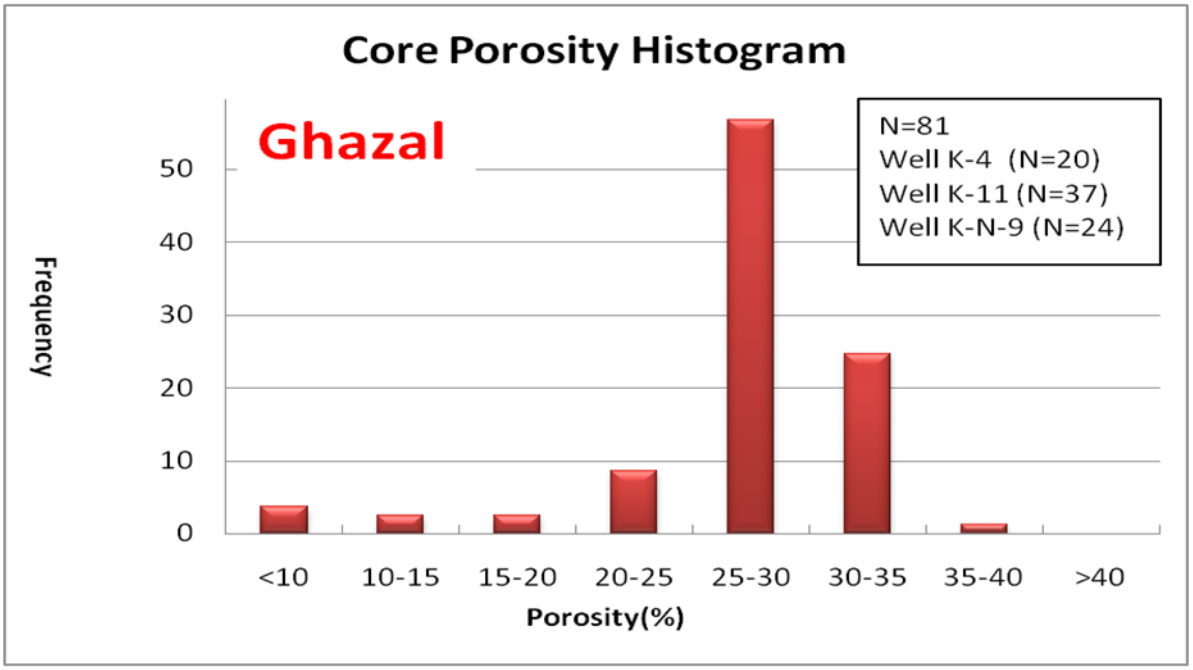

Fig.3-22: The core porosity histogram for Ghazal formation (FFR Study,2015).

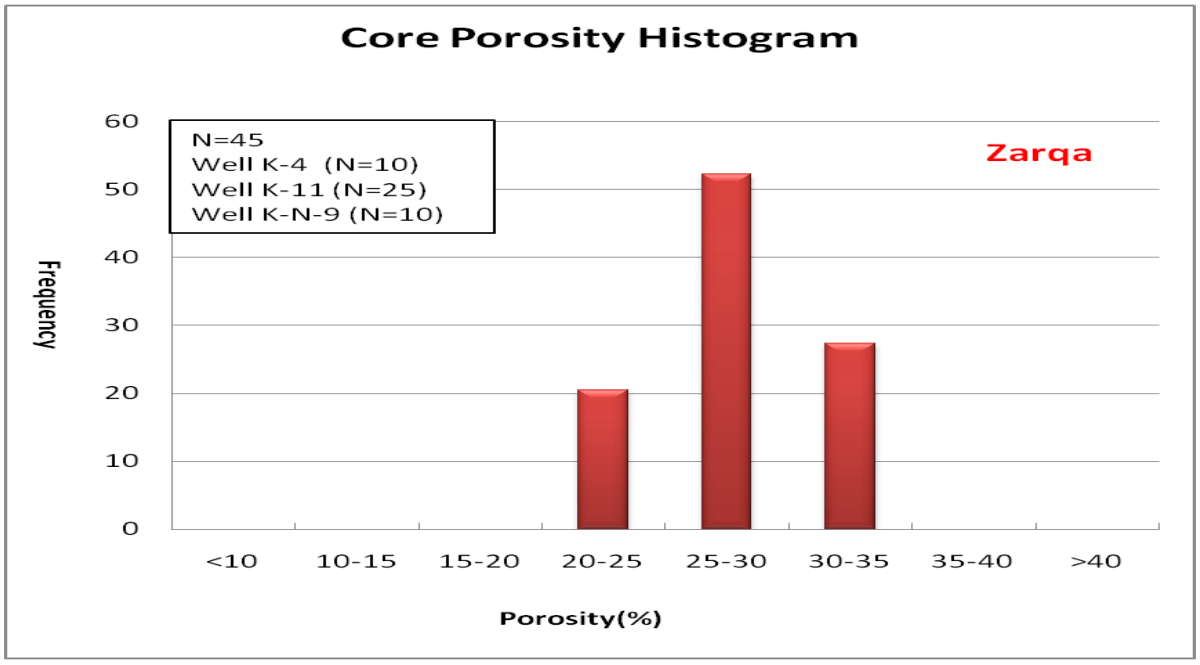

Fig.3-23: The core porosity histogram for Zarga formation (FFR Study,2015).

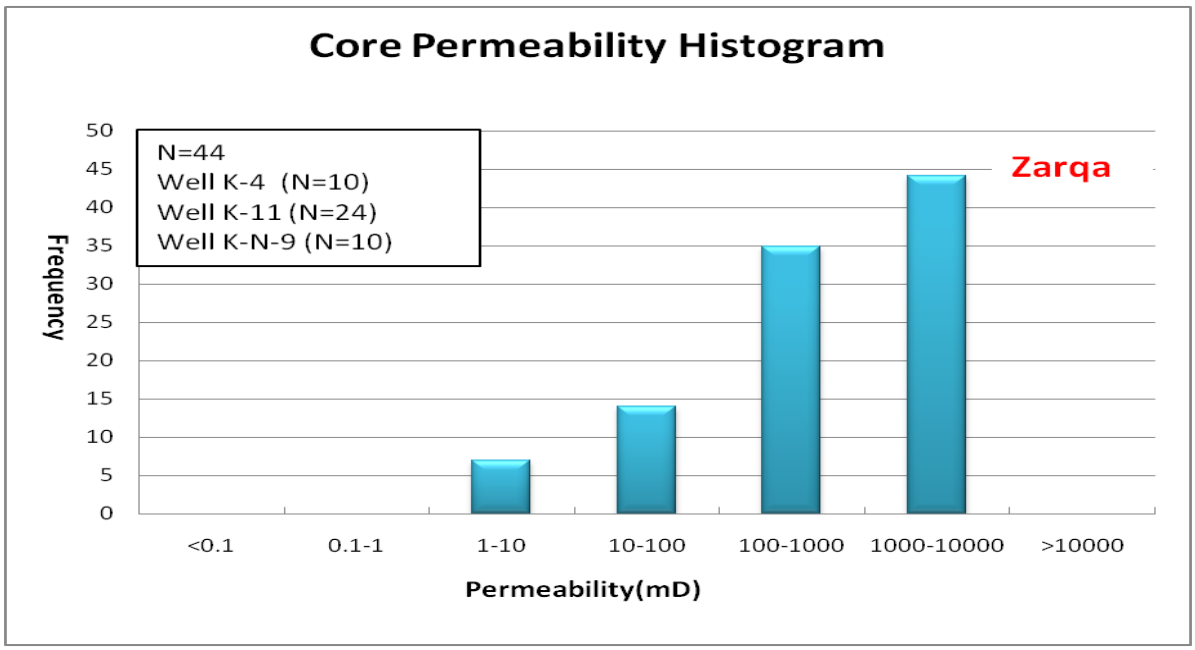

Fig.3-24: The core permeability histogram for Zarga formation (FFR Study,2015).

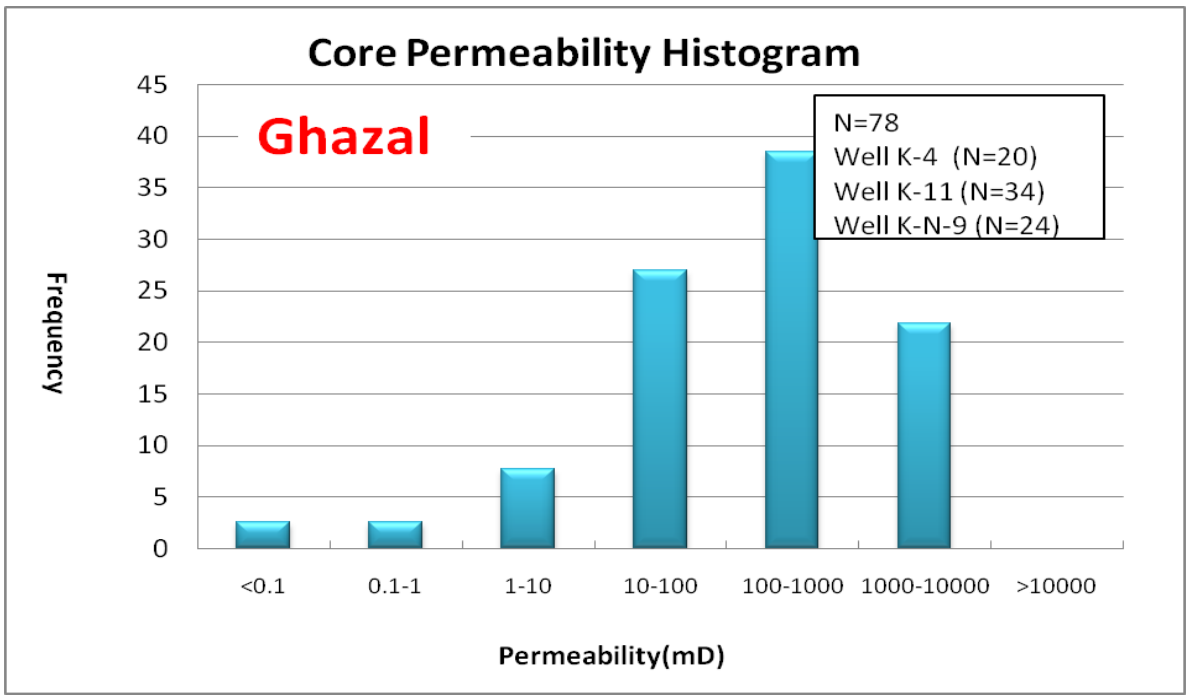

Fig.3-25: The core permeability histogram for Ghazal formation (FFR Study,2015).

3.1.2.5. Porosity and Permeability Analysis

Base on core data from two wells (Keyi-4&Keyi-11) the permeability models established for both formations Ghazal and Zarga, by plotting the permeability in y-axis after corrected from gas effect in the lab, with core porosity in x-axis as showed in (Fig.3-26).

The helium porosity value for the studied plug samples ranged between 23.0% and 39.0%.

The permeability values for the studied plug samples ranged between 695.37md to 2941.93md.

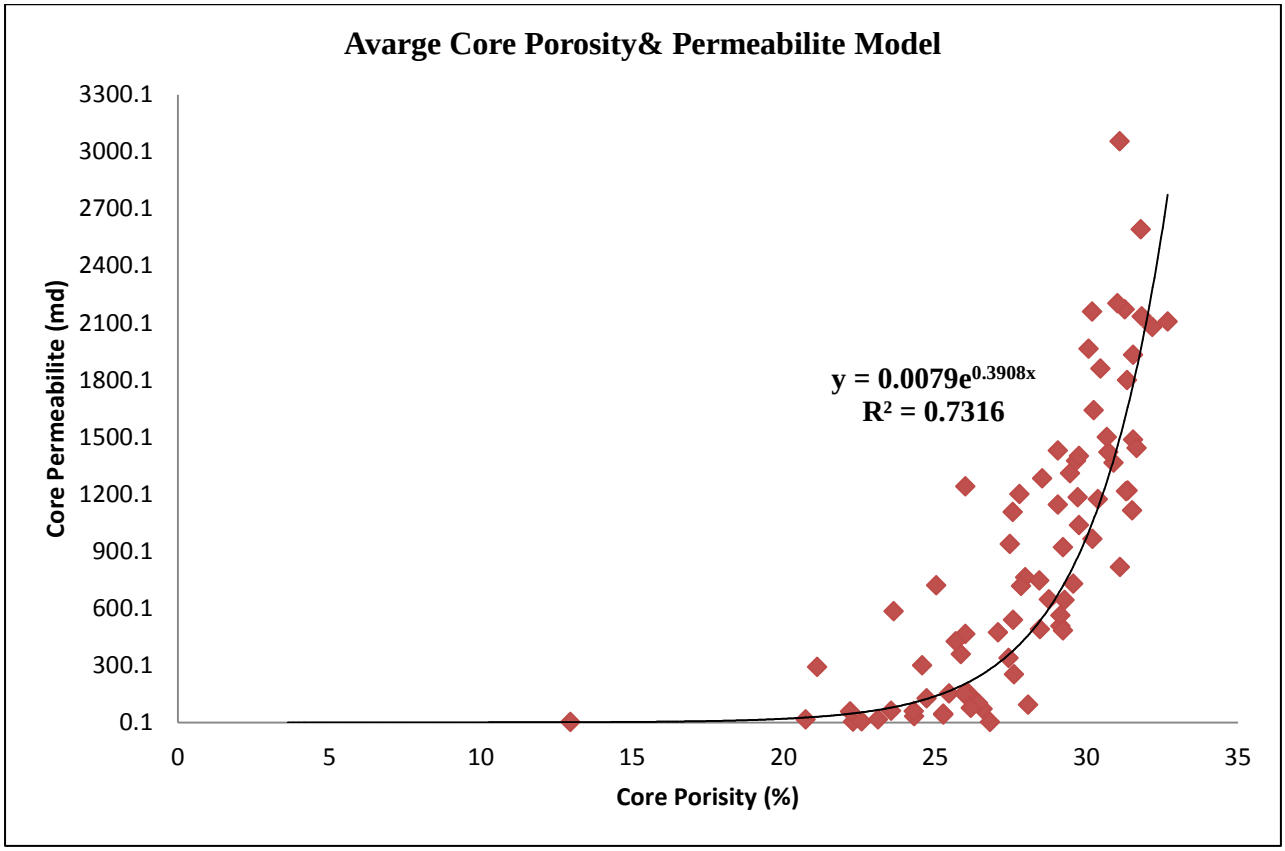

Fig.3-26: Average permeability model for Ghazal and Zarga formation.

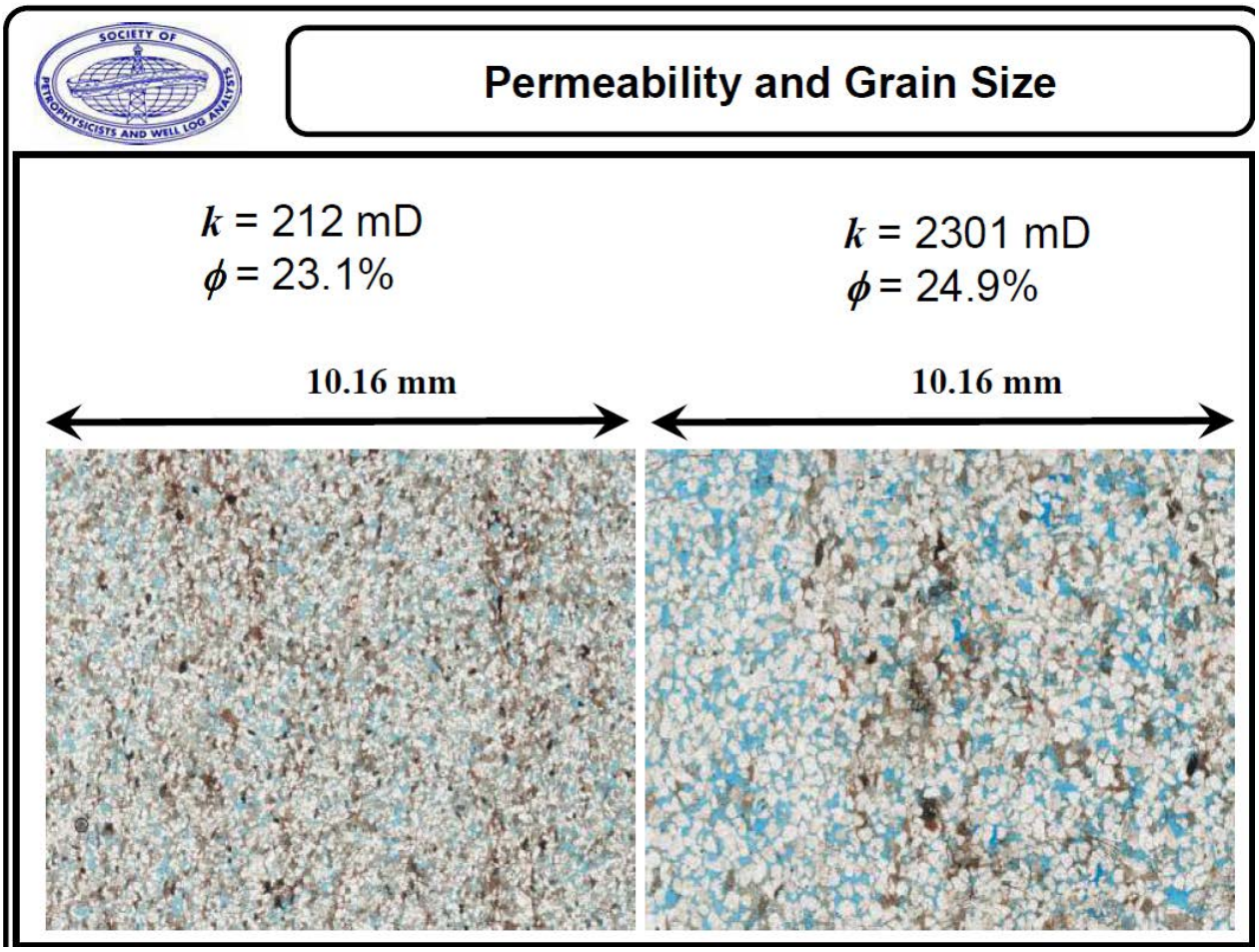

Fig.3-27: The relation between the porosity and permeability control by the grain sizes distributions (Andrew, 2008).

3.1.2.6. Core Porosity Corrections at Overburden Pressure

Normally the overburden pressure reducing the porosity and the permeability and sometimes changing the shape and the size of the rock grain, here we did some porosity analysis base on core data of well Keyi-4 at different formation pressure and small changes to the porosity about (0.8 to 1.1 pu),based on overburdened pressure (Fig.3.28) and (Table.3.3).

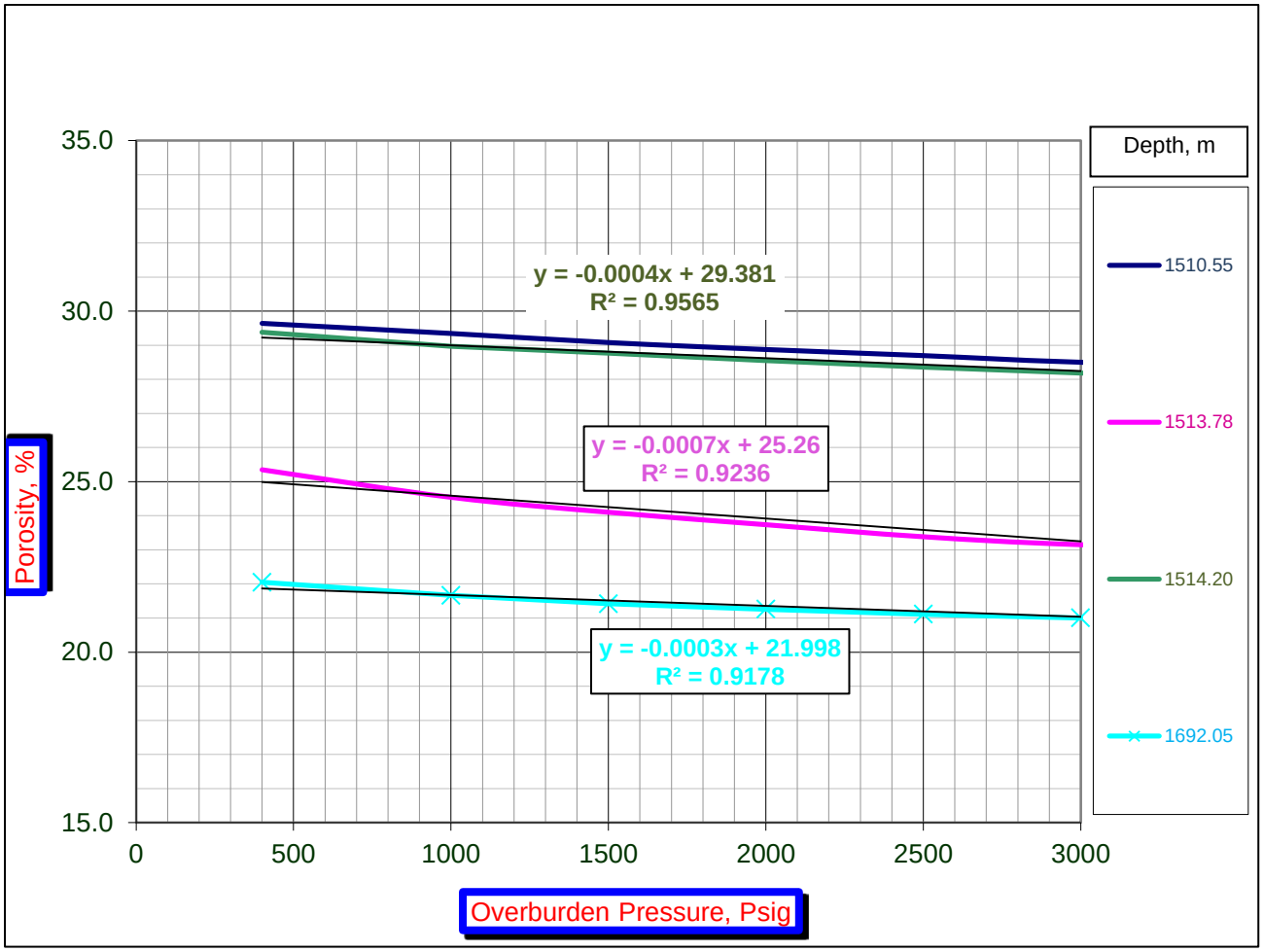

Fig.3-28: Model of porosity as function of overburden pressure for Ghazal and Zarga formation (CPL, 2012).

Table.3-3 : This table showing the effect of overburden pressure (2000 Psi) to the core porosity.

Well name	Form.	No.	Top MID (m)	Bottom MID (m)	Recovery (%)	Length (m)	Samples Num	SELECT MODEL	Core porosity at room %	Core porosity at overburden %	Core porosity diffrence %
KEYI-4	Ghazal	Core#1	1510.27	1514.27	93	3.72	15	2000	29.8	29	0.8
		Core#2	1514.27	1516.95	88.8	2.38	9	2000	29.5	28.6	0.9
	Zarga	Core#3	1688.32	1696.32	92.3	7.38	31	2000	22.1	21	1.1
KEYI-11	Ghazal	Core#1	1514.5	1516.67	100	2.17	9	2000	27.6	26.7	0.9
		Core#2	1516.67	1520.78	24	1.06	3	2000	26.2	25.3	0.9
		Core#3	1521.01	1525	94	3.75	10	2000	28.9	28	0.9
		Core#4	1525	1529.06	100	4.06	4	2000	26.6	25.7	0.9
		Core#5	1529.06	1533.31	100	4.25	7	2000	27.1	26.2	0.9
		Core#6	1533.31	1537.09	100	3.79	5	2000	30.1	29	0.9
	Zarga	Core#7	1693.06	1700.37	95	6.95	10	2000	28.5	27.4	1.1

3.1.2.7. a, b, m, n Determination for Water Saturation Calculation

Reference to the core analysis of Keyi-4 and Keyi-11, the identification of (a, b, m and n) electric parameters is essential step to calculate water saturation equation (Fig.3.29 and Fig.3.30) and (Table.3.4).

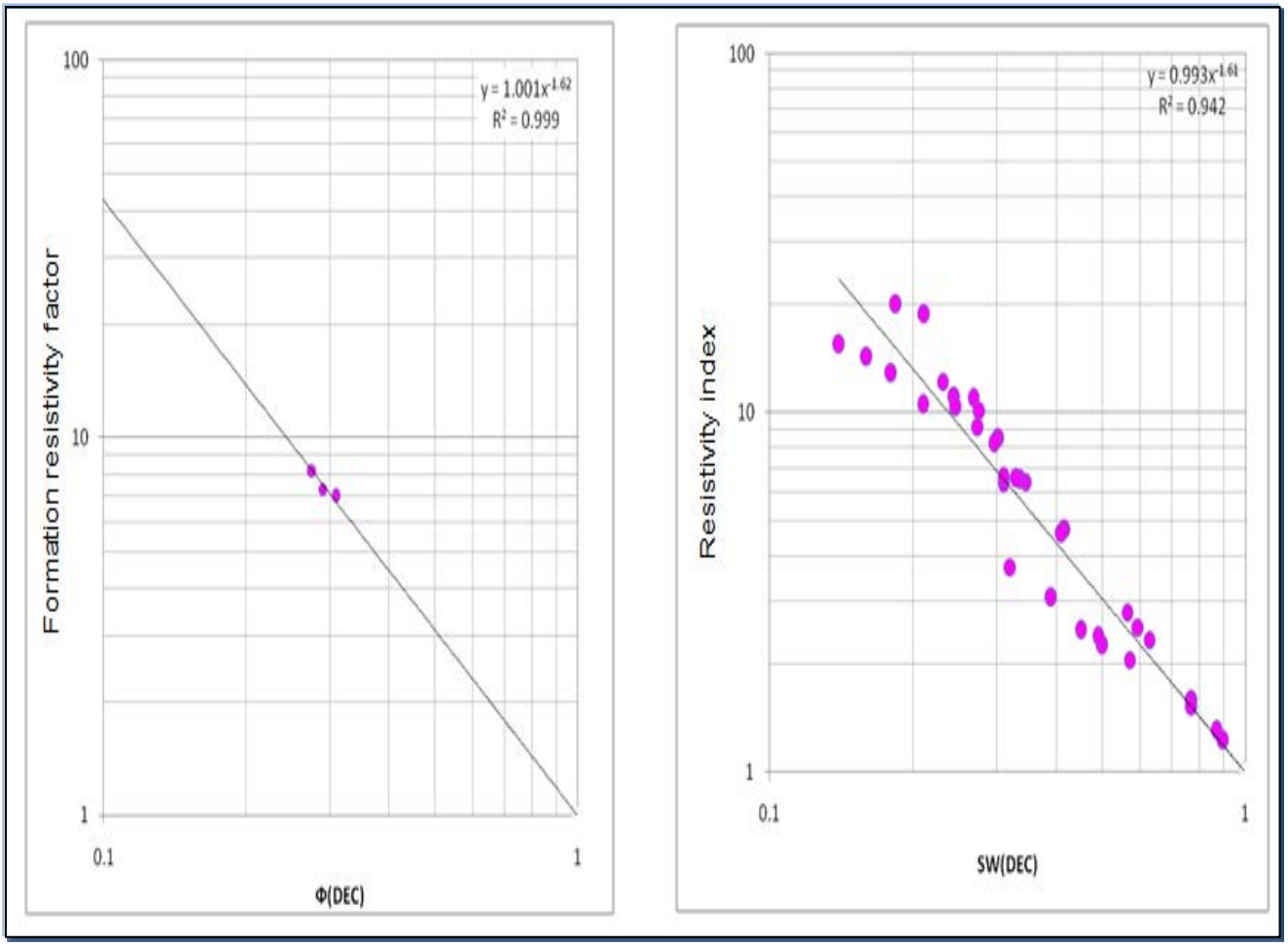

Fig.3-29: Electric property analysis for tortuosity factor (m) and saturation exponent (n),for Ghazal formation(CPL,2012 And 2014).

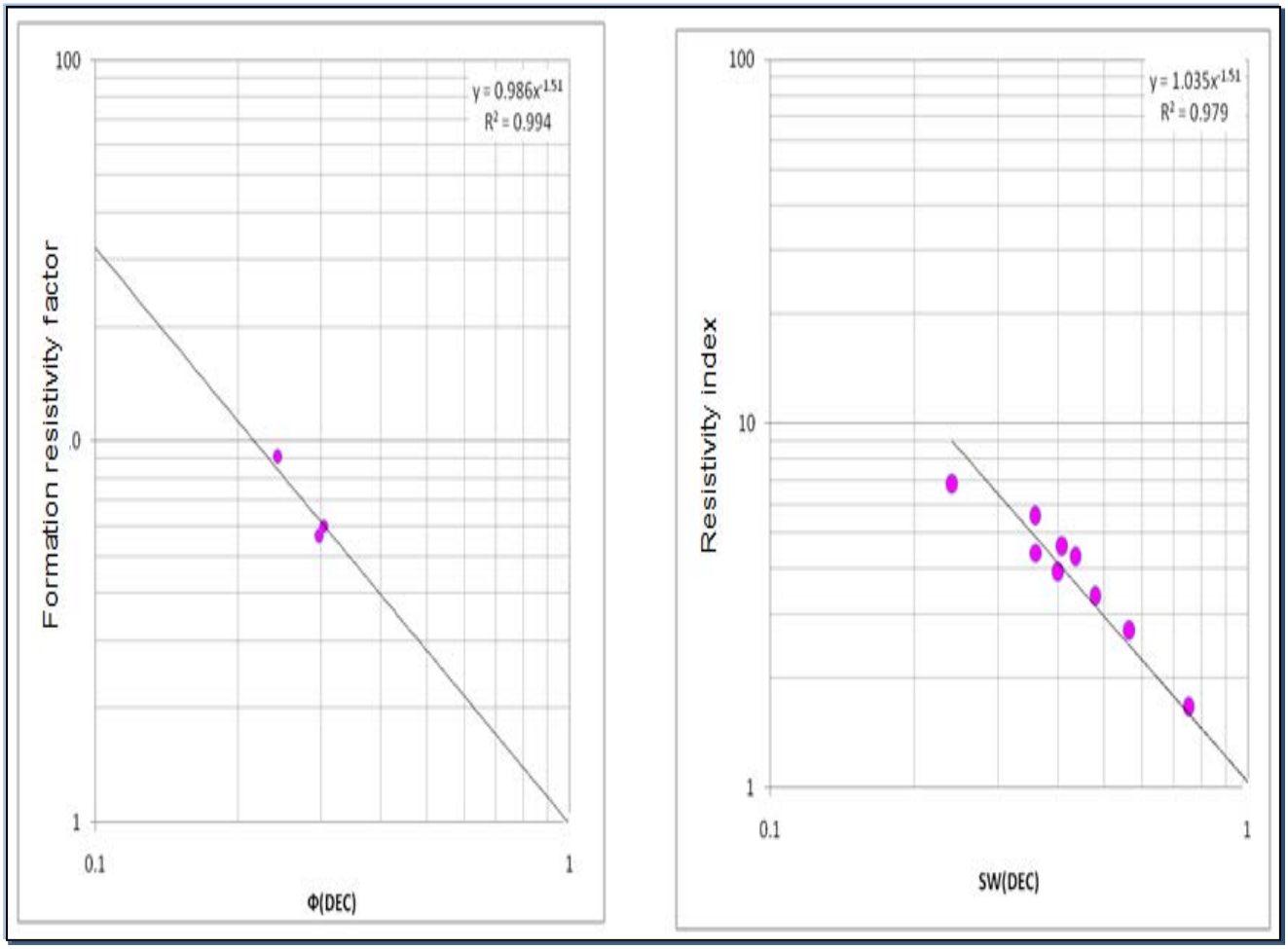

Fig.3-30: Electric property analysis for tortuosity factor (m) and saturation exponent (n),for Zarga formation (CPL,2012 And 2014).

Table.3-4: Summary table for electric rock properties of Ghazal and Zarga formation.

Formation	**a**	**b**	**m**	**n**
Ghazal	**1.001**	**0.993**	**1.62**	**1.61**
Zarqa	**0.986**	**1.035**	**1.51**	**1.51**

3.1.2.8. Capillary Pressure Analysis

Capillary pressure test at overburden pressure has been performed on 8 samples of wells Keyi-4 and Keyi-11(Fig.3.31, Fig.3.32).

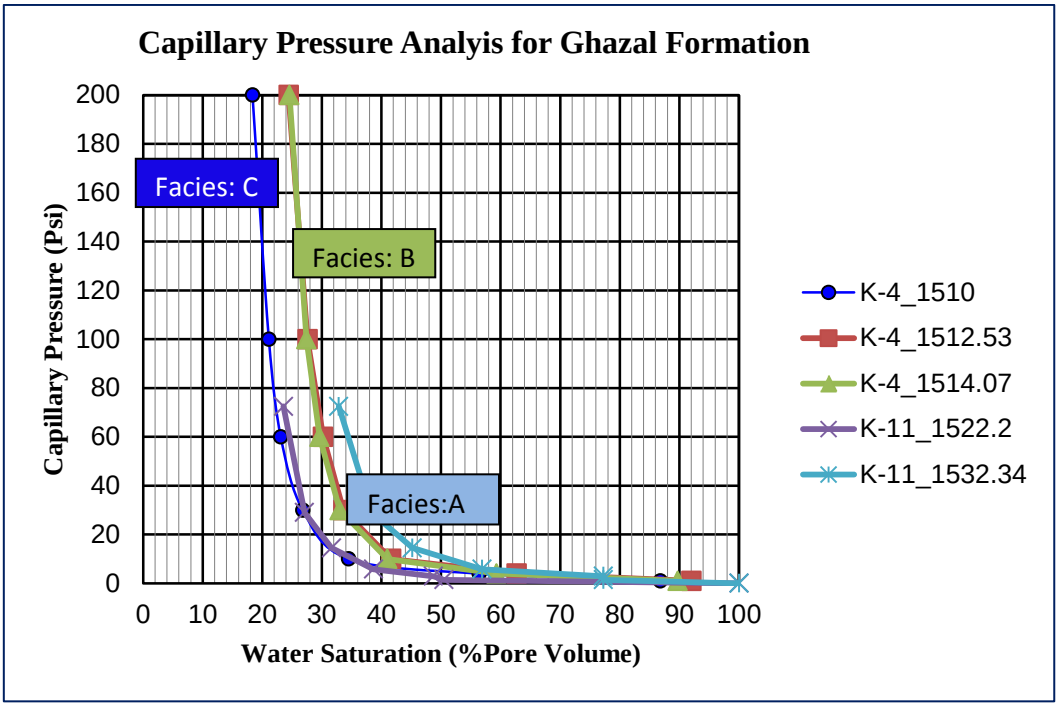

Fig.3-31:Capillary pressure curves versus water saturation results, shown three geologic facies (A, B, C) each with different capillary pressure vs S_w Relationship,for Ghazal formation.

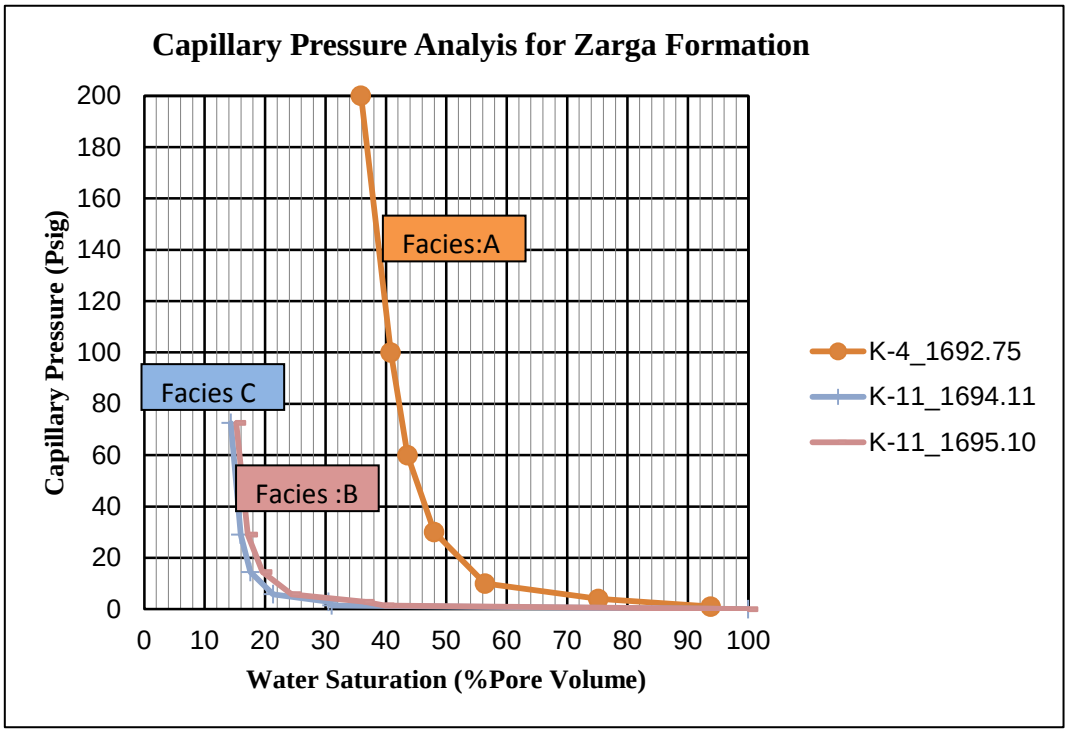

Fig.3-32: Capillary pressure curves versus water saturation results, shown two geologic facies (A, B), each with a very different capillary pressure vs S_w relationship, for Zarga formation.

3.1.4. Water saturation methods

The interpretation problem of water saturation determination for shale formations still lacks a satisfactory solution. A wide variety of S_w models currently are used routinely to evaluate shaly sand. Each model can provide a significant different (S_w) values. None is universally accepted by log analysts.

Resistivity measurements are, the most commonly used measurement to determine S_W, but the presence of clay can suppress the resistivity and sometime mask the hydrocarbon effect.

There are two general groups of water saturation equation methods commonly used today as following:

1- V_{shale} or resistivity model equations (Uses PHIE)

- Laminar
- Simandoux
- Modified Simandoux
- Poupon Leveaux
- Fertl&Hammack.
- Indonesia

2- Cation exchange or conductivity model equations (Uses PHIT)

- Waxman-Smits
- Modified Waxman Smits
- Juhasz
- Dual Water
- Charlebois

3.1.5. Introduction to ElanPlus Software for Logging Interpretation

The ELANPlus computer program is designed for quantitative formation evaluation of cased and open-hole log level by level. Evaluation is done by optimizing simultaneous equations described by one or more interpretation models. Single-well ELANPlus can be run any time after preliminary data editing (such as patching, depth matching, and environmental correction) is complete (Techlog help manual, 2014.0.1).

Most users think the purpose of the ELANPlus application is solving the so-called inverse problem, in which log measurements, or tools, and response parameters are used together in response equations to compute volumetric results for formation components. In reality, that aspect of the program is only one side of a three-way relationship among tools, response parameters, and formation component volumes. The relationship is often presented in a triangular diagram (Techlog help manual, 2014.0.1):

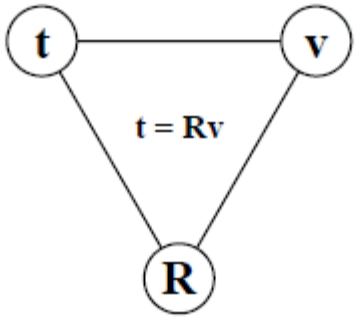

Petrophysical model used by the ELANPlus application.

In this diagram, the **t** represents the tool vector—all logging instrument data and synthetic curves. The **v** is the volume vector, the volumes of formation components. **R** is the response matrix, containing the parameter values for what each tool would read, given 100% of each formation component. Given the data represented by any two corners of the triangle, the ELANPlusprogram can determine the third (Techlog help manual, 2014.0.1).

3.1.4.1.1. Equations and Tools:

Equation and tool will be synonymous in most cases. The more technically correct term is equations, or better, response equations. The term tool comes from the fact that most response equations obtain their input data from logging tools and often use the same mnemonic as the tool data, also the response equations and their associated data are used as tools to produce the desired results. Finally, the term tool has historical roots in the program.

3.1.4.1.2. Formation Components, Volumes:

When setting up an interpretation model, you must tell the ELANPlus program which minerals, rocks, and fluids are likely to be present in the formation. These minerals, rocks, and fluids are the formation components.

Often the primary job of the ELANPlus program is to determine the relative quantities or volumes of the formation components that would most likely produce the set of measurements recorded by the logging instruments. Therefore, the terms volumes and formation components, or just components, are often used interchangeably.

3.1.4.1.3. Model, Interpretation Model:

A model is a way to present information to the ELANPlus program to describe the problem to be solved. A model consists of a set of tools, or equations, a set of formation components, or volumes, and a set of constraints. Implicitly there are associated curves, response parameters, and other global and model-specific parameters.

Abstractly, a model describes program input data and the solution space over which the ELANPlus optimizer can operate (the allowable results). The equations describe the logging data and supplementary response equations that are available. The formation components describe the minerals, rocks, and fluids likely to be encountered in appreciable quantity and provide the geological description of the types of formations to which the model applies.

3.1.4.1.4. Assumptions of the ELANPlus Application:

Most formation evaluation programs impose some sort of interpretation model assumptions about the depositional environment, clay properties, fluid interactions in pore space, and so on. Although the ELANPlus application was designed to be free of such assumptions, it is virtually impossible to design a working computer program without some sort of assumptions some imposed by physics, some resulting from incomplete knowledge of all variables that affect the solution sought.

The assumptions implicit in the ELANPlus program are related to borehole pressure, bound water, curve editing, environmental corrections, flushed-zone and undisturbed-zone relationships, lateral continuity, neutron porosity, summation of fluids, summation of volumes, and vertical continuity(Techlog help manual, 2014.0.1).

3.1.6. Petrophysical Property Computations

Determination of minerals and formation volumes is an important task of formation evaluation. The main objective of lithology identification is to divide the bulk rock volume into effective porosity and solid mineral components (Crain, 2015), so Elanplus software was proposed to handle the petrophysical results base on linear response equation as following equation:

Tool measurement = parameter * volume.....(3.3)

3.1.5.1. Log Response Equations

A response equation is a mathematical description of how a given measurement varies with respect to each formation component. The simplest linear response equations are of the form equation (3.4):

$$measurement = \sum_{i=1}^{nfc} Vi \times Ri \quad \text{………………………………………………..…. (3.4)}$$

Where:

Vi= volume of formation component i.

Ri= response parameter for formation component i

The response equations can be used in several ways. One is to find out what a log would read under a hypothetical set of circumstances. Another way is to calculate one unknown in the equation, for example porosity or shale volume, by using a log reading and assuming the other terms to be known or derivable from some other response equations. A third approach is to use sets of response equations simultaneously to determine as many unknowns as possible from the available log data as in below equations for example (Crain, 2015):

DENS meas= Vsh * DENSSH + DENS1 * Vmin1 + DENS2 * Vmin2 + DENS3 * Vmin3 +PHIE*Sw*DENSW+PHIE*(1-Sw)*DENSHY………………. (3.5)

Where:

DENS meas: Bulk density measurement.

Vsh: Shale volume

DENSSH: Density of shale layer

DENS1: Density of mineral 1

Vmin1: Volume of mineral 1

PHIE: Effective porosity.

DENSW: Density of the water

DENSHY: Density of hydrocarbon

Reference to the above (equations. 3.5), the volumes (Vmin1, Vmin2, Vmin3, PHIE, and SW) are known, and the response of the minerals predicted from cross plot, histogram and core data, whereas (DENS1+DENS2) reconstructed bulk density consider as unknown

3.1.5.2. Shale Volume Computations

A good example is determining the lithology of a shaly sand formation from gamma ray,but in our case it is not usually the best option.
In the first step, shale volume is computed from the formula as below:

$$GR\ measurment = GRshale * Vshale + GRcleansand * (1 - Vshale) \text{.....} (3.6)$$

3.1.5.3. Porosity Computations

In the second step (where V_{shale} is already known) porosity is computed from the density-neutron porosity measurement as below equation:

$$\emptyset N\ measurment = \emptyset N, fluid * \emptyset + \emptyset N, shale * Vshale + \emptyset N, cleansand * (1 - \emptyset - V\text{shale}) \text{.....} (3.7)$$

$$\text{Bulk(Density) measurment} = \emptyset * \text{Dfluid} + (1 - \emptyset) * 2.65 \text{.....} (3.8)$$

3.1.5.4. Total Matrix Volumes/Components Computations

In the last step the using material balance equation yields the volume fraction of sand as in below equation:

$$V\ sand = 1 - \emptyset - Vshale \text{.....} (3.9)$$

Solving an actual interpretation task may be more complicated than this simple procedure. First, some constraints should apply, e.g. neither volume fraction can take negative values. Secondly, a branching can occur: different shale parameters can be applied if the points representing the depth sites separate into groups on a cross plot (Crain, 2016).

3.1.5.5. Water Saturation Computations

Shale is conductive and reduces formation resistivity. Archie's law, which assumes that formation water is the only conductive component in the rock, overestimates water saturation

in presence of shale. Hydrocarbon content is therefore underestimated when using Archie. Specific saturation equations, which account for the presence of conductive shale must be used. Both the Simandoux and Indonesia Equations account for the presence of conductive shale in the rock to compute water saturation. These equations are based on a parallel conductivity model, which assumes that the rock is composed of clean sands and conductive shale layers. For this reason we refer to them as wet shale equations. When the clay fraction is dispersed in the pore space the Waxman-Smits and Dual Water Models are more suitable (Sclumberger, 2006).

Dual water (equation.3.10) and Indonesia (equation.3.11) models adopted to determine water saturation in Ghazal and Zarga formations.

$$Ct = \frac{1}{a}\Phi_t{}^m S^n wt\left[\left(\frac{Swt - Swb}{Swt}\right)Cw + Cbw\frac{Swb}{Swt}\right] \quad \text{..... (3.10)}$$

Where:

a : tortuosity factor.

m, n :electrical properties.

Ct : Total rock conductivity

Φ_t : Total porosity

Swt : Total water saturation

Swb : Bound water saturation

Cw : Formation water conductivity.

Cbw : Bound water conductivity

Swb : Bound water saturation

In the Dual Water Model as in equation (3.10), the bound water and the free water are side by side in the total pore space and their conductivity in parallel, therefore the effective conductivity of the water mixture, also Dual water equation could be expires in resistivity as in below equation:

$$\frac{a}{R_t * \phi_t^m} = \frac{1}{R_w} * S_w^n + Qv * \left(\frac{1}{\phi_{t_{sh}}^2 * R_{sh}} - \frac{1}{R_w}\right) * S_w^{(n-1)} \quad \text{..... (3.11)}$$

$$Qv = \frac{\phi_{t_{sh}} * Vsh}{\phi_t} \quad \text{..... (3.12)}$$

Where:

a : Tortuosity factor.

m, n :Electrical properties.

Rt: True resistivity

Φ_t : Total porosity

Rw: Formation water resistivity.

SW $^{m:}$ Total water saturation

Φ_{tsh} : Shale porosity

R_{sh}: Shale resistivity.

Qv: Cation exchange capacity

$$(water\ saturation)\ S_{W\ Indonesia} = \left\{ \frac{\frac{1}{\sqrt{R_t}}}{\left[\frac{V_{SH}^{\left(1-\frac{V_{SH}}{2}\right)}}{\sqrt{R_{Sh}}}\right] + \left[\frac{\Phi^{\frac{m}{2}}}{\sqrt{a * R_W}}\right]} \right\}^{\left(\frac{2}{n}\right)} \quad \text{..... (3.13)}$$

Where:

Rt -Formation resistivity.

Vsh - Clay volume.

Rsh - Shale resistivity.

a - Tortuosity factor.

m, n -Electrical properties.

Rw - Formation water resistivity.

Rsh - Shale resistivity.

3.1.5.6. Permeability Computations:

Two methods suggested for permeability calculations in Ghazal &Zarga formation as below:

1. First method, the average permeability models for Ghazal and Zarga formations using

core data:

Permeability = 0.007*Exp 0.390*porosity……. (3.14)

2. Second method, K-Lambda permeability expression is referenced to (Herron. M., 1998),using logs data:

$$k = \frac{Z \times \phi^{m^*+2}}{\rho^2 \times (1-\phi)^2 \times \left(\sum_{\square} W_i \times S_{0i}\right)^2} \quad \text{……..…. (3.15)}$$

Where:

k = the intrinsic permeability (mD)

Z = a proportionality constant with a default value of 200000.0 (dimensionless)

φ = total porosity (m3/m3) (PHIT)

m* = the Waxman-Smits cementation exponent (dimensionless)

$$m^* = 1.8 + \left[1.128 \times \gamma + 0.22 \times \left(1 - e^{-17.2 \times \gamma}\right)\right]$$

Where: $\gamma = \frac{Q_v \times \phi}{1-\phi}$.

Qv=QV_GEO, Θ = PHIT

ρg = the grain density (g/cm3)(RHGA_GEO)

Wi = the weight fraction of mineral I (g/g)

S0i = the specific surface area of mineral I (m2/g)

If the initial estimate of k is less than 100 mD, then the calculated permeability is modified using the following expression:

$$k = 0.034325 \times k^{1.714}$$

3.1.5.7. Reservoirs Cutoff Identification:

The cut off analysis values such as shale volume, porosity, and water saturation are very important parameters for reservoir identification and OOIP calculation. The cut-off adopted with DST, log data and log interpretation results, two methods adopted in order to identify the cut off values:

The first method is using sensitivity analysis (Fig.3.33), (Fig.3.34), and the second method, using DST and logging results (Fig.3.35), (Fig.3.36).

3.1.4.7.1. Porosity and Shale Volume Cutoff:

In general the shale volume Cut-off: 50%; and porosity is more than 14.0% for good reservoirs.

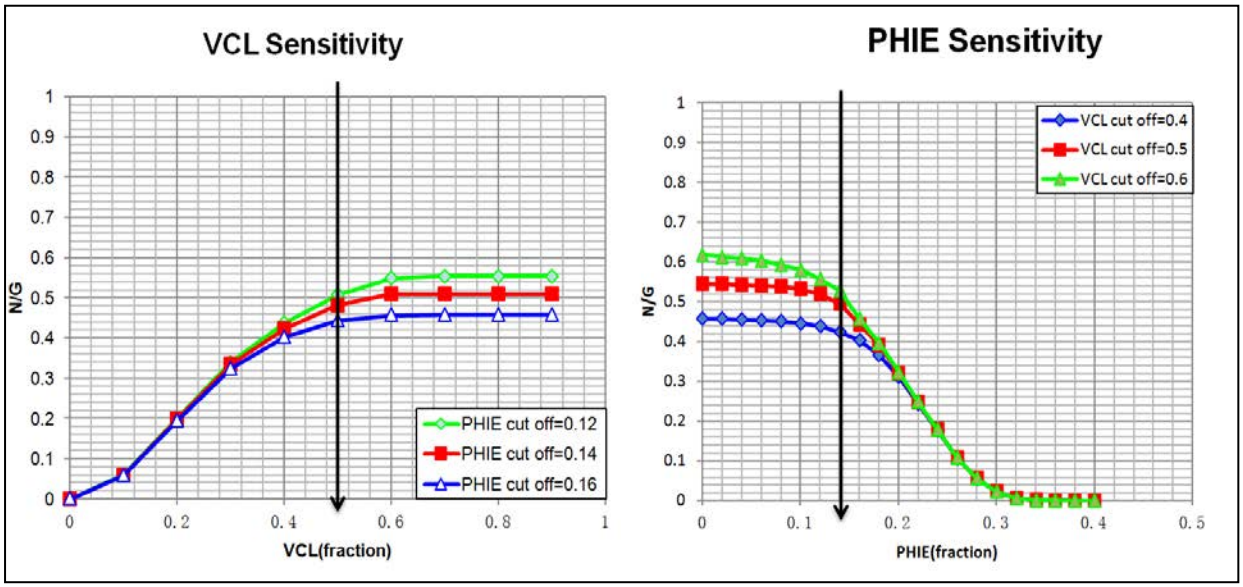

Fig.3-33: Shale volume & porosity cutoff analysis using well log data of Ghazal formation (FFR Study,2015).

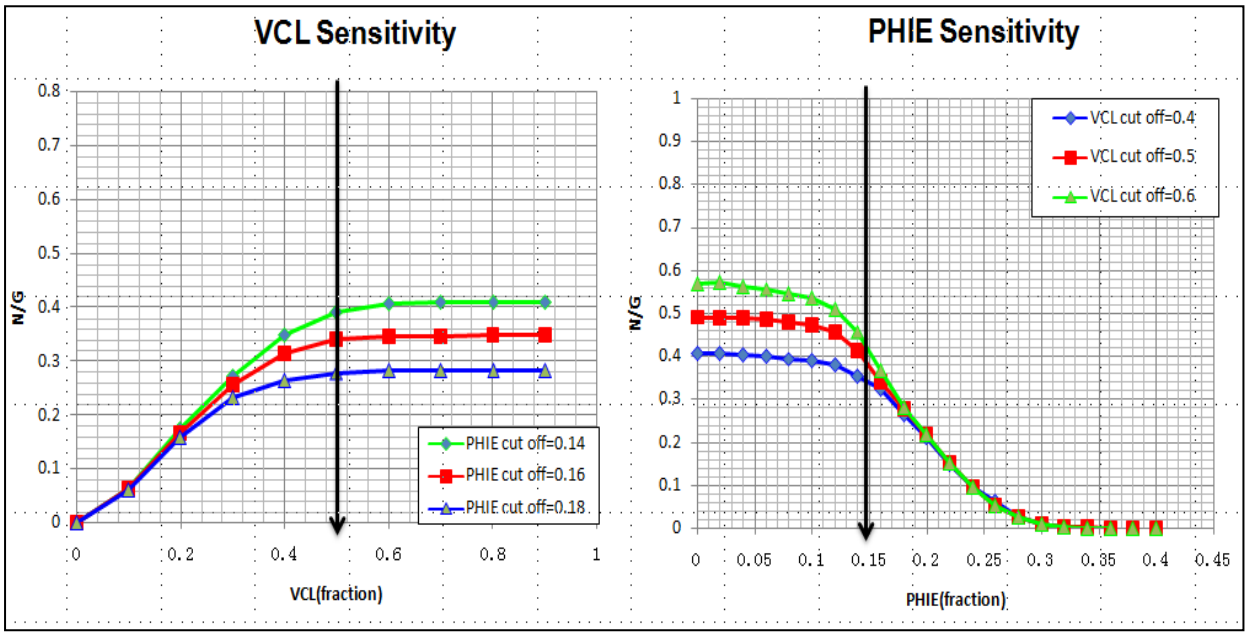

Fig.3-34:Shale volume & porosity cutoff analysis using well log data of Zarga formation (FFR Study,2015).

3.1.4.7.2. Water Saturation Volume Cutoff:

The resistivity of the oil zones in some cases more than (10.0 ohmm.m) and the water saturation is less than 52%, however it is hard to determine one cut off value for porosity and water saturation (Fig.3.34), it could be with range.

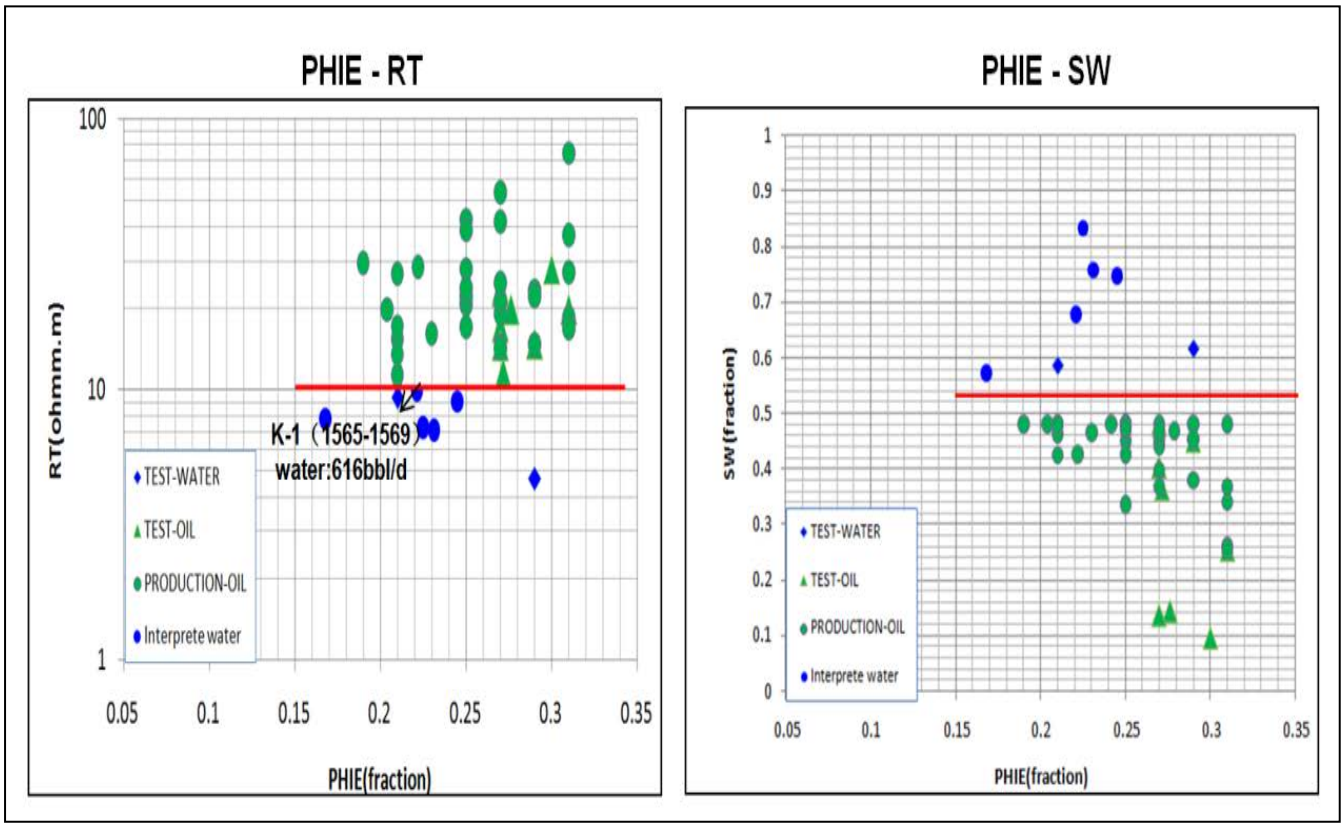

Fig.3-35: Water saturation cutoff analysis using DST data and well log of Ghazal (FFR Study,2015).

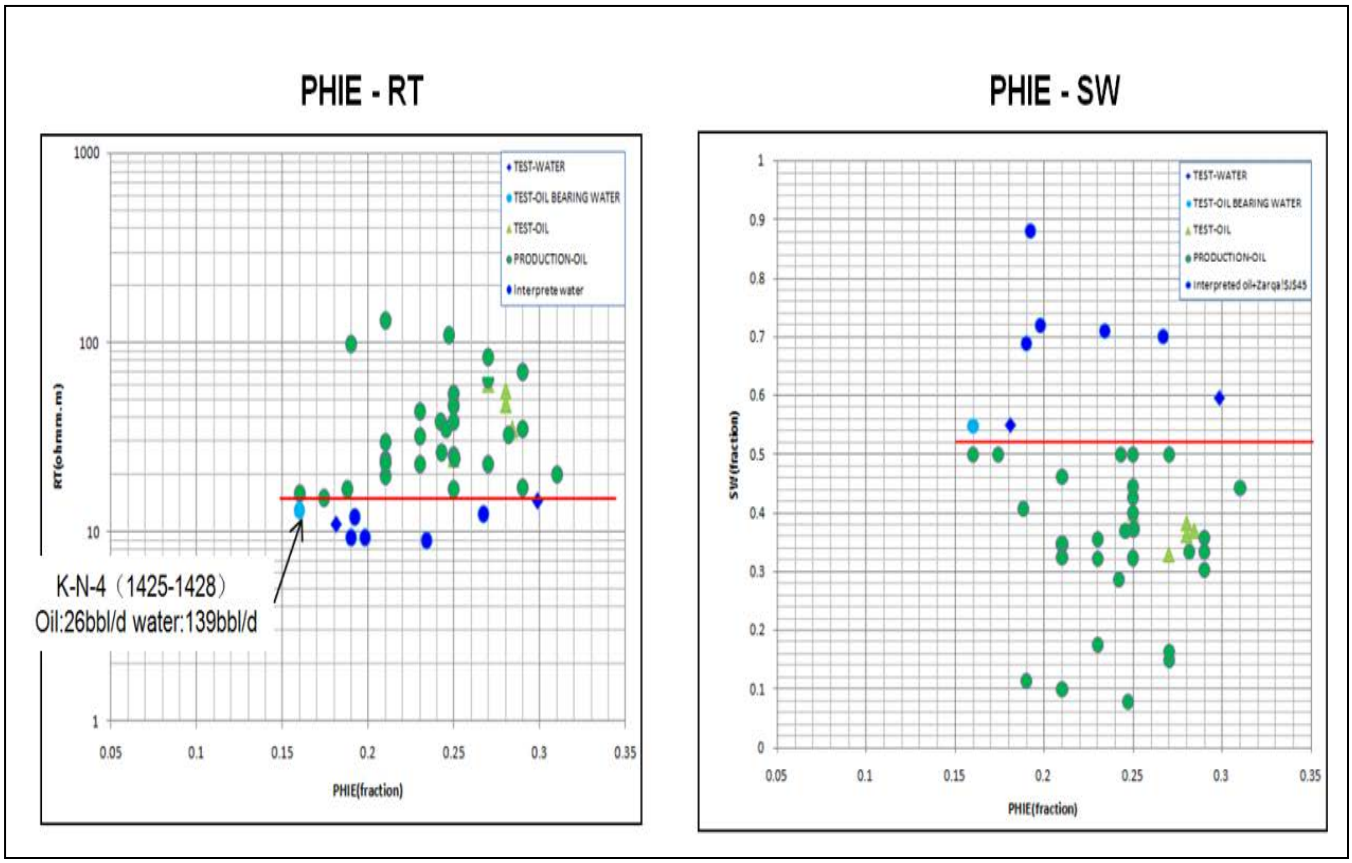

Fig.3-36: Water saturation cutoff analysis using DST data and well log of Zarga formation (FFR Study,2015).

3.1.7. Elastic Constant Basic Computations

The most common approach for calculating these rock properties is to use log data (Density, neutron and acoustic sonic data), after appropriate editing for bad hole and invasion effects, as inputs to the elastic constants equations computed as below equations(Crain,2016):

3.1.5.1. Shear Modulus

N(aka u or mu) is defined as the applied stress divided by the shear strain.

N = KS5 * DENS / (DTS ^2)..... (3.16)

3.1.5.2. Poisson's Ratio PR

The lateral strain divided by longitudinal strain, when shear velocity or shear travel time is available.

R=Vp/Vs

OR:R=DTS/DTC

PR = (0.5 * R^2 -1) / (R^2 -1).....(3.17)

3.1.5.3. Bulk Modulus

The hydrostatic pressure divided by volumetric strain.

Kb = KS5 * DENS *(1 / (DTC^2) - 4/3 * (1 / (DTS^2))).....(3.18)

3.1.5.4. Young's Modulus

Applied uni-axial stress divided by normal strain.

Y = 2 * N * (1 + PR)…….....(3.19)

Where:

KS5: Constant

DENS: Bulk density

DTS: Shear sonic

DTC: Compressional sonic

PR: Poisson's Ratio

N: Shear Modulus

Kb: Bulk Modulus

Y: Young's Modulus

CHAPTER FOUR

FORMATION EVALUATION RESULTS AND INTERPRETATION

4.1.1 Quartz and K-Feldspar Interpretation Results

In order to gain a visual aspect of the amount of quartz, clay, potassium feldspar, or any other mineral that exists within the sample being analysed, across plot technique used.

First 'N' calculated and plotting 'N' versus gamma ray, 'N' is a lithological parameter (Aaron, K. 2013).

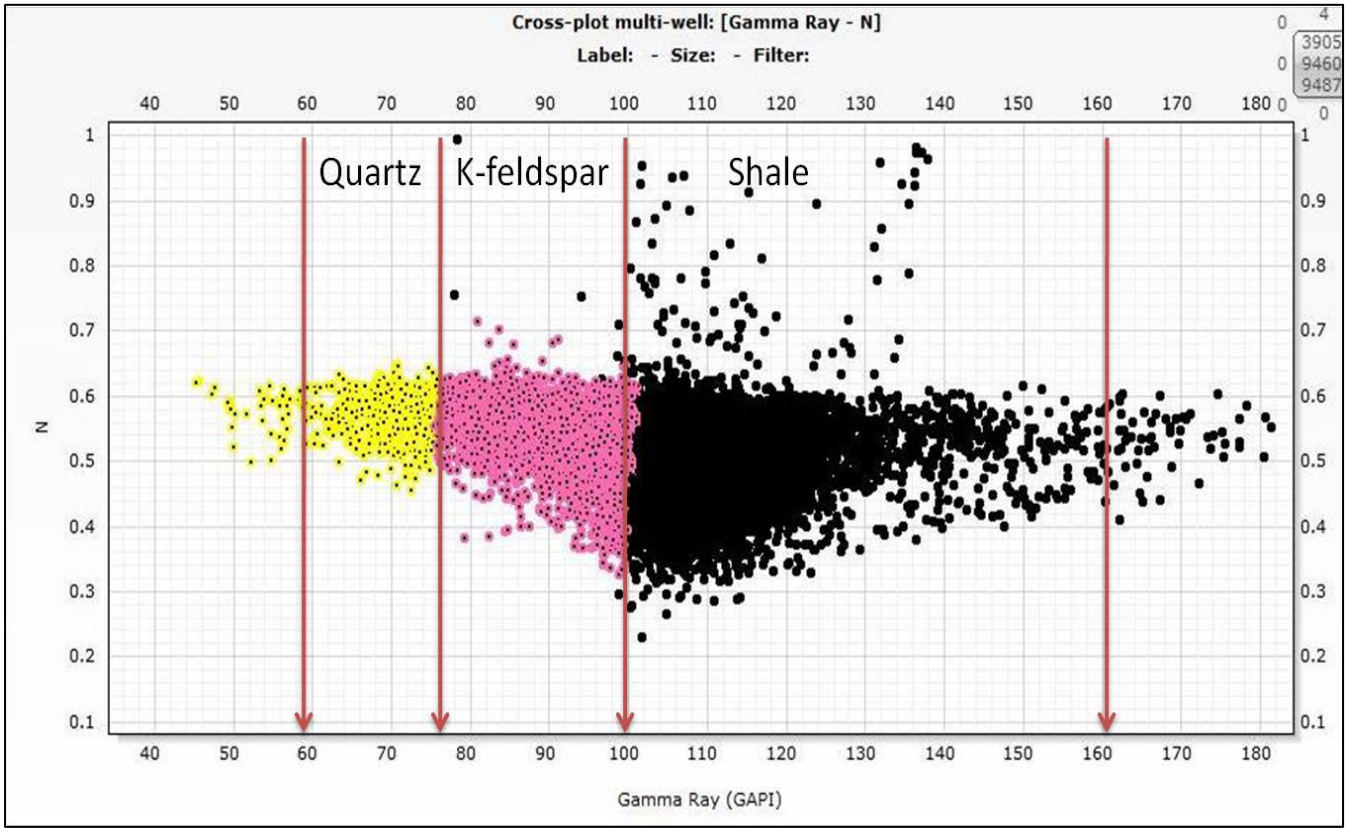

Fig.4-1: 'N' Gamma ray cross plot: illustrating locations of data points that represent different minerals, quartz, feldspar, clay and characteristics of data as gamma ray readings change.

Refer to (Figure.4.1):different parameters can be obtained interactively with the log plot, gamma ray value for clean quartz (60API), feldspar (78 API) and clay (110API), also additional benefit to this cross plot the ability to visualize data points associated with potassium feldspar or clay minerals.

With help of the cross plot in ElanPlus software the solver always get the clay as wet clay, however wet clay response used in this study, and after the solution performed, a post processing step is performing to break clay into dry kaolinite, smectite, chlorite and quartz (Table.4.1).

Table. 4-1: Minerals base model results of dry weight percentage of quartz and k- feldspar distribution, utilizing density-neutron cross plot technique.

Well	Formation	Zones	Top (m)	Bottom (m)	Gross (m)	Av_Volume of K-Feldspar Fraction	Av_Quartz Volume Fraction
KEYI-4	Ghazal	Gc/Gc1	1508.2	1527.4	19.2	0.233	0.15
		Gc2	1527.4	1555.3	27.9	0.288	0.136
		Gc3	1555.3	1575.7	20.4	0.312	0.162
	Zarga	Zc/Zc1	1685	1704.6	19.6	0.242	0.138
		Zc2	1704.6	1726	21.4	0.227	0.127
KEYI-11	Ghazal	Gc/Gc1	1516.5	1538.9	22.4	0.387	0.119
		Gc2	1538.9	1563.8	24.9	0.377	0.077
		Gc3	1563.8	1585	21.2	0.51	0.093
	Zarga	Zc/Zc1	1690	1711.8	21.8	0.299	0.225
		Zc2	1711.8	1729.5	17.7	0.254	0.17
KEYI-12	Ghazal	Gc/Gc1	1518.6	1554.4	35.8	0.407	0.028
		Gc2	1554.4	1579.9	25.5	0.385	0.028
		Gc3	1579.9	1599.4	19.5	0.359	0.023
	Zarga	Zc/Zc1	1723.6	1747.5	23.9	0.396	0.12
		Zc2	1747.5	1769.2	21.7	0.352	0.198

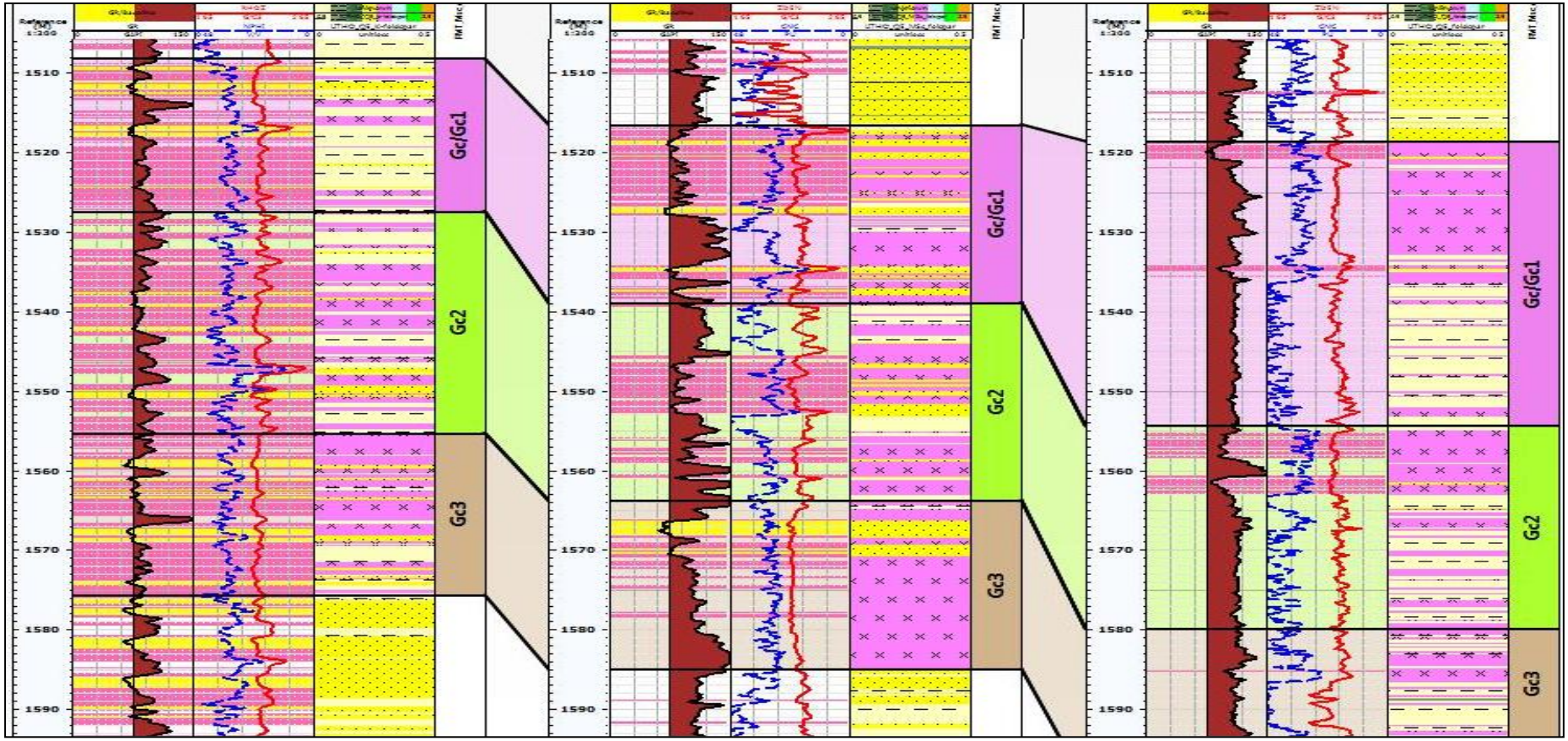

Fig.4-2: log plot display on the first track gamma ray, second track density-neutron, third track minerals components volumes of quartz with yellow shading colour reflect relatively low GR, and orthoclase with pink colour reflected relatively high GR.

4.1.2 The Clay/Shale Volume Model Results:

It is common practice to use the maximum gamma-ray response as the shale point. However, it is not good method in our case here, so that we have applied low wight to the gamma ray log (high uncertainties) because of the potassium concentration in the matrix, the presence of potassium identified from the logs and core analysis. Multi wells cross plot and histogram were generated and the responses of kaolinite, chlorite and smectite were realized, the clay end points identified and the dry weight per cent of the clay minerals components estimated (Table.4.3).

The clay distribution may exist in various ways in the reservoirs laminated or dispersed or form (Fig.4.3)

The clay distribution in Ghazal reservoirs as dispersed clay, and laminar in Zarga reservoirs reference to the difference between total and effective porosity (Table.4.5).

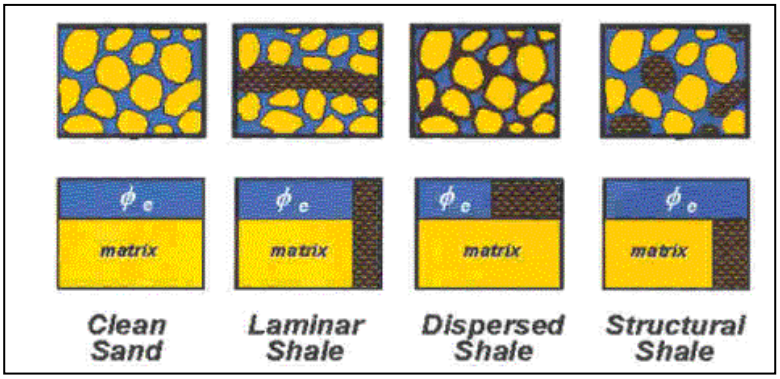

Fig.4-3: Showing how shale is distributed in shaly Sand (Crain, 1978-2016).

Table. 4-2 : The input parameters for clay volume estimation base on the multi wells cross plot technique.

Formation	Sub layer	Clay mineral	Bulk Density	Neutron Porosity	Gamma Ray sand
Ghazal & Zarga	Gc1,Gc2,Gc3 and Zc1,Zc2	Smectite	2.07	0.67	69.7-75.5
		Chlorite	2.24	0.62	
		Kaolinite	2.38	0.57	

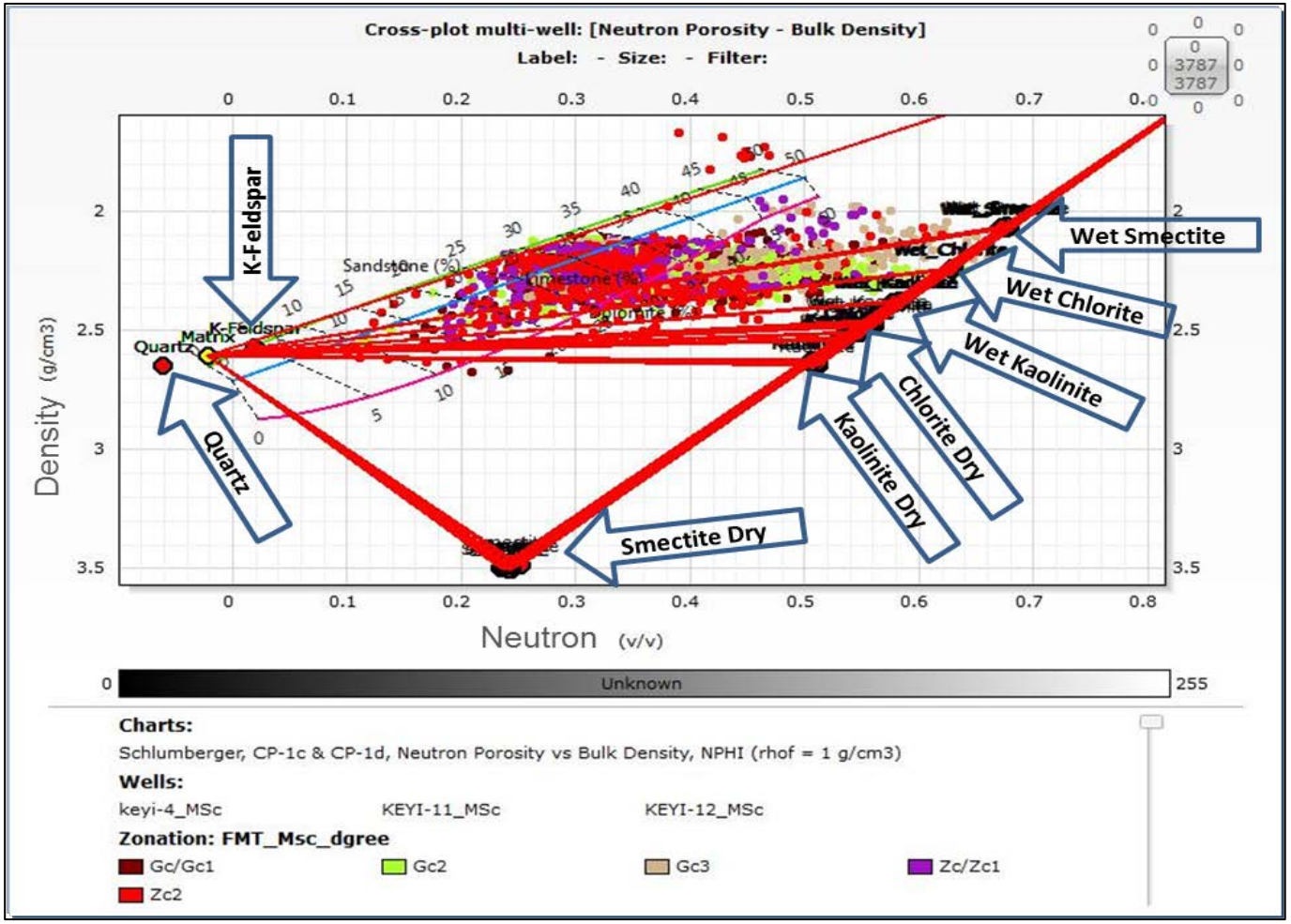

Fig.4-4: Shows multi wells cross plot for lithology and clay mineral end points identification for Ghazal and Zarga sub layers to calculate the volumes of the minerals components (Qz, K-Feldspar, Smectite, Kaolinite, and Chlorite).

Table. 4-3 : minerals base model results of the dry weight percentage of clay mineral disruption, utilizing density-neutron cross plot technique.

Well	Formation	Zones	Top (m)	Bottom (m)	Gross (m)	Av_Kaolinite Volume Fraction	Av_Smectite Volume Fraction	Av_Chlorite Volume Fraction
Keyi-4	Ghazal	Gc/Gc1	1508.2	1527.4	19.2	0.16	0.04	0.00
		Gc2	1527.4	1555.3	27.9	0.19	0.03	0.00
		Gc3	1555.3	1575.7	20.4	0.11	0.04	0.00
	Zarga	Zc/Zc1	1685	1704.6	19.6	0.12	0.00	0.14
		Zc2	1704.6	1726	21.4	0.06	0.00	0.26
Keyi-11	Ghazal	Gc/Gc1	1516.5	1538.9	22.4	0.13	0.06	0.00
		Gc2	1538.9	1563.8	24.9	0.19	0.05	0.00
		Gc3	1563.8	1585	21.2	0.09	0.01	0.00
	Zarga	Zc/Zc1	1690	1711.8	21.8	0.02	0.00	0.22
		Zc2	1711.8	1729.5	17.7	0.06	0.00	0.25
Keyi-12	Ghazal	Gc/Gc1	1518.6	1554.4	35.8	0.25	0.04	0.00
		Gc2	1554.4	1579.9	25.5	0.25	0.06	0.00
		Gc3	1579.9	1599.4	19.5	0.27	0.06	0.00
	Zarga	Zc/Zc1	1723.6	1747.5	23.9	0.09	0.00	0.17
		Zc2	1747.5	1769.2	21.7	0.10	0.00	0.12

4.1.3 The porosity model results:

We consider our porosity model is more precise, because, of accuracy identification of the clay minerals and wet clay porosity, using density neutron cross plot technique.

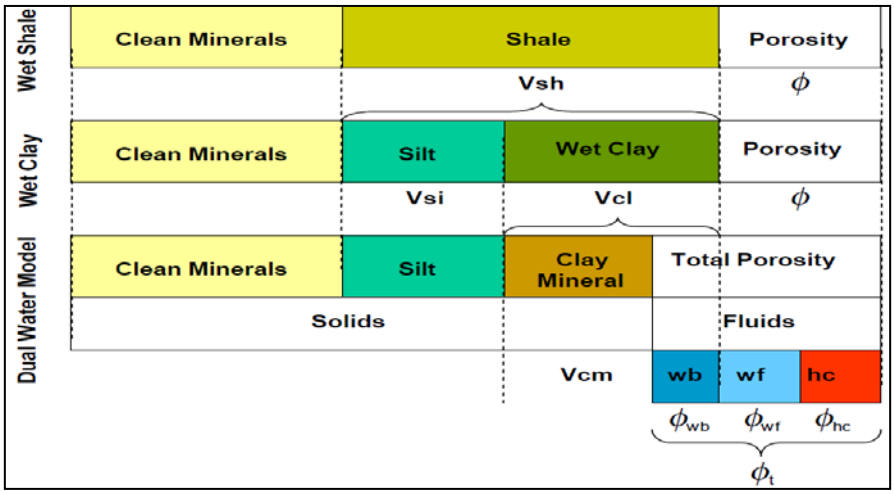

Fig.4-5: Porosity and shale model partitioning into wet clay or wet shale (Schlumberger, 2006).

A new concepts used for partition the rock in individual volumes (Fig.4.5), for porosity consideration as following:

- Wet clay is split into dry clay mineral and bound water porosity (fwb).

The introduction of a second water type next to free water is the characteristic of the Dual Water Model (DWM).

In DWM we define total porosity as the sum of the effective porosity and bound water.

Then:

$V_{cl} = V_{cm} + \emptyset_{wb}$ ..... (4.1)

$\emptyset_t = \emptyset_e + \emptyset_{wb}$ ..... (4.2)

$\emptyset_e = \emptyset_t - (\emptyset_{t\,sh} * V_{cl})$ ..... (4.3)

In the last step, the material balance equation yields the volume fraction of porosity, when the volumes of other components are known (Table.4.4).

Table. 4-4: Minerals base model results of total and effective porosity results of the reservoirs, utilizing density-neutron cross plot technique.

wells	Zones	Top	Bottom	Gross-Sand	Net-sand	Av_Total Porosity	Av_Effective Porosity
		(m)	(m)	(m)	(m)	v/v	v/v
Keyi-4	Gc/Gc1	1508.2	1527.4	19.2	13.4	0.25	0.19
	Gc2	1527.4	1555.3	27.9	18.1	0.25	0.19
	Gc3	1555.3	1575.7	20.4	17.1	0.28	0.20
	Zc/Zc1	1685	1704.6	19.6	12.1	0.22	0.20
	Zc2	1704.6	1726	21.4	9.1	0.23	0.22
Keyi-11	Gc/Gc1	1516.5	1538.9	22.4	19.2	0.25	0.20
	Gc2	1538.9	1563.8	24.9	17.4	0.25	0.21
	Gc3	1563.8	1585	21.2	20.8	0.27	0.25
	Zc/Zc1	1690	1711.8	21.8	17.1	0.22	0.23
	Zc2	1711.8	1729.5	17.7	11.8	0.22	0.25
Keyi-12	Gc/Gc1	1518.6	1554.4	35.8	18.7	0.25	0.21
	Gc2	1554.4	1579.9	25.5	12.6	0.26	0.21
	Gc3	1579.9	1599.4	19.5	9.5	0.26	0.20
	Zc/Zc1	1723.6	1747.5	23.9	17.6	0.23	0.21
	Zc2	1747.5	1769.2	21.7	15.5	0.25	0.23

Table. 4-5 : Minerals base model results of total and effective porosity difference, and clay distributions of the reservoirs, utilizing density-neutron cross plot technique.

wells	Zones	Top	Bottom	Gross-Sand	Net-sand	Av_Total Porosity	Av_Effective Porosity	Porosity Difference	Clay distributions
		(m)	(m)	(m)	(m)	v/v	v/v	v/v	
Keyi-4	Gc/Gc1	1508.2	1527.4	19.2	13.4	0.25	0.19	0.06	Disperse clay
	Gc2	1527.4	1555.3	27.9	18.1	0.25	0.19	0.06	Disperse clay
	Gc3	1555.3	1575.7	20.4	17.1	0.28	0.20	0.08	Disperse clay
	Zc/Zc1	1685	1704.6	19.6	12.1	0.22	0.20	0.02	Laminated
	Zc2	1704.6	1726	21.4	9.1	0.23	0.22	0.01	Laminated
Keyi-11	Gc/Gc1	1516.5	1538.9	22.4	19.2	0.25	0.19	0.06	Disperse clay
	Gc2	1538.9	1563.8	24.9	17.4	0.25	0.21	0.04	Disperse clay
	Gc3	1563.8	1585	21.2	20.8	0.27	0.24	0.03	Laminated
	Zc/Zc1	1690	1711.8	21.8	17.1	0.22	0.21	0.01	Laminated
	Zc2	1711.8	1729.5	17.7	11.8	0.22	0.21	0.01	Laminated
Keyi-12	Gc/Gc1	1518.6	1554.4	35.8	18.7	0.25	0.21	0.04	Disperse clay
	Gc2	1554.4	1579.9	25.5	12.6	0.26	0.21	0.05	Disperse clay
	Gc3	1579.9	1599.4	19.5	9.5	0.26	0.20	0.06	Disperse clay
	Zc/Zc1	1723.6	1747.5	23.9	17.6	0.23	0.21	0.02	Laminated
	Zc2	1747.5	1769.2	21.7	15.5	0.25	0.23	0.02	Laminated

4.1.1 The Water Saturation Model Results:

Indonesia and dual water models showed slide different results of the formations water saturation, affected by shale content (Table.4.6).

If the clay fraction is dispersed, as predicted from (Table.4.5), therefor Waxman-Smits and Dual Water Models are more suitable, also considering the shale distribution and the conductivity of the clay (CEC/QV), whereas Indonesian equation didn’t consider this parameter.

The below tables showed comparison of water saturation results calculated by different models in the same formation of wells, Keyi-4, Keyi-11 and Keyi12.

Table. 4-6: Minerals base model results of water saturation in pay sand ,using dual water and Indonesia models.

Well	Zones	Top	Bottom	Gross	Net Pay	Av_Shale Volume	Av_Effective Porosity	Av_Water Saturation Indonesian	Av_Water Saturation Dual water	Water saturation difference	Standard Deviation	Fluid results
		m	m	m	m	v/v	v/v	v/v	v/v	v/v	%	
Keyi-4	Gc/Gc1	1508.2	1527.4	19.2	10.97	0.25	0.19	0.47	0.04	0.43	30.4	oil
	Gc2	1527.4	1555.3	27.9	9.75	0.27	0.18	0.53	0.09	0.44	31.1	oil
	Gc3	1555.3	1575.7	20.4	12.8	0.24	0.19	0.53	0.13	0.4	28.3	oil
	Zc/Zc1	1685	1704.6	19.6	4.27	0.29	0.21	0.49	0.4	0.09	6.4	oil
	Zc2	1704.6	1726	21.4	2.44	0.14	0.25	0.52	0.51	0.01	0.7	oil
Keyi-11	Gc/Gc1	1516.5	1538.9	22.4	7.24	0.2	0.2	0.51	0.43	0.08	5.7	oil
	Gc2	1538.9	1563.8	24.9	3.66	0.18	0.21	0.51	0.41	0.1	7.1	oil
	Gc3	1563.8	1585	21.2	1.45	0.15	0.25	0.47	0.46	0.01	0.7	oil
	Zc/Zc1	1690	1711.8	21.8	5.18	0.28	0.23	0.47	0.39	0.08	5.7	oil
	Zc2	1711.8	1729.5	17.7	1.75	0.28	0.25	0.51	0.45	0.06	4.2	oil
Keyi-12	Gc/Gc1	1518.6	1554.4	35.8	0	0.22	0.21	0.65	0.5	0.15	10.6	oil
	Gc2	1554.4	1579.9	25.5	0	0.21	0.22	0.66	0.5	0.16	11.3	water
	Gc3	1579.9	1599.4	19.5	0	0.4	0.18	0.78	0.55	0.23	16.3	water
	Zc/Zc1	1723.6	1747.5	23.9	0	0.3	0.22	0.7	0.49	0.21	14.8	water
	Zc2	1747.5	1769.2	21.7	0	0.27	0.21	0.67	0.37	0.3	21.2	water

4.1.2 The Permeability Model Results:

Reference to the capillary pressure analysis, three geological facies identified in Ghazal and Zarga formations, and a new developed permeability models generated to calculated accurate permeability (Fig. 4.6).

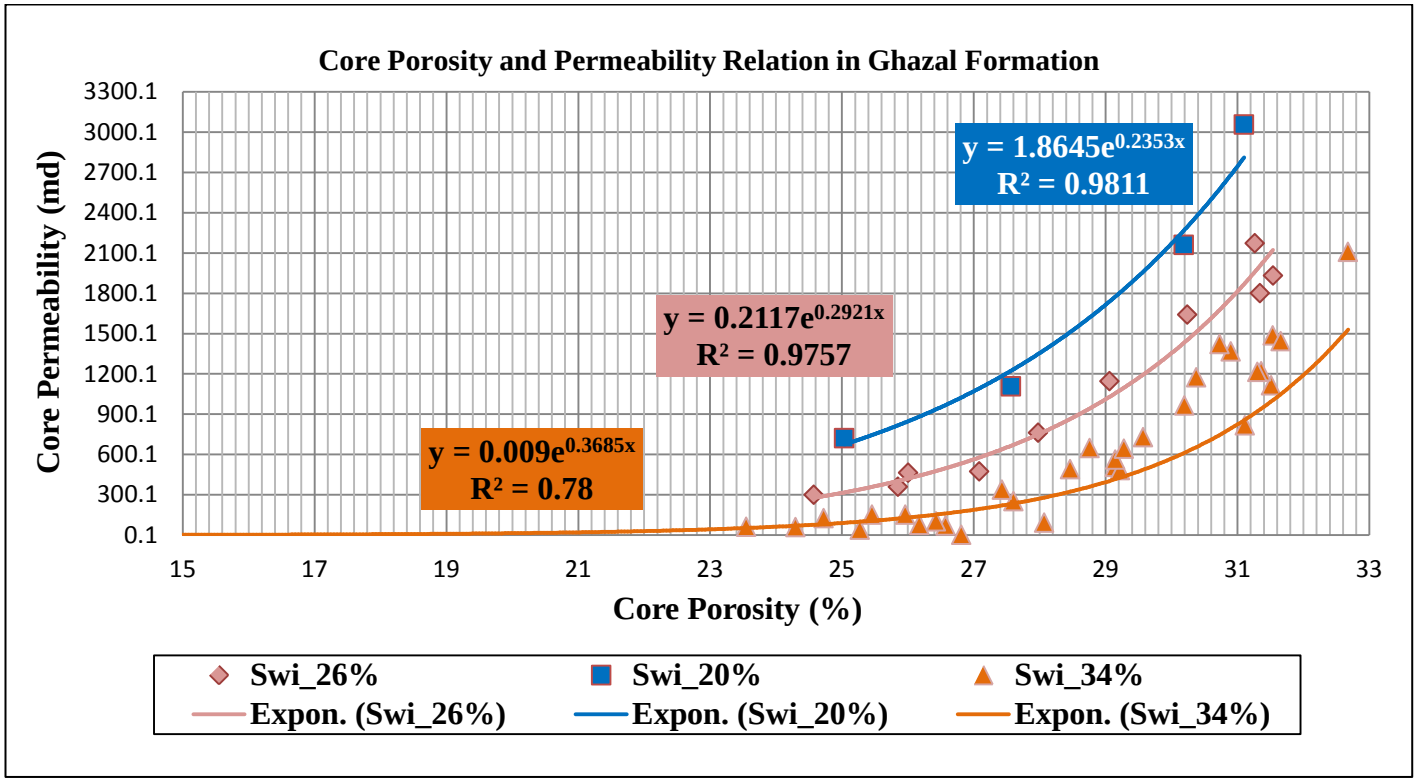

Fig.4-6: Core Porosity and permeability models, distrusted with variety of S_{wi} and facies in Ghazal formation.

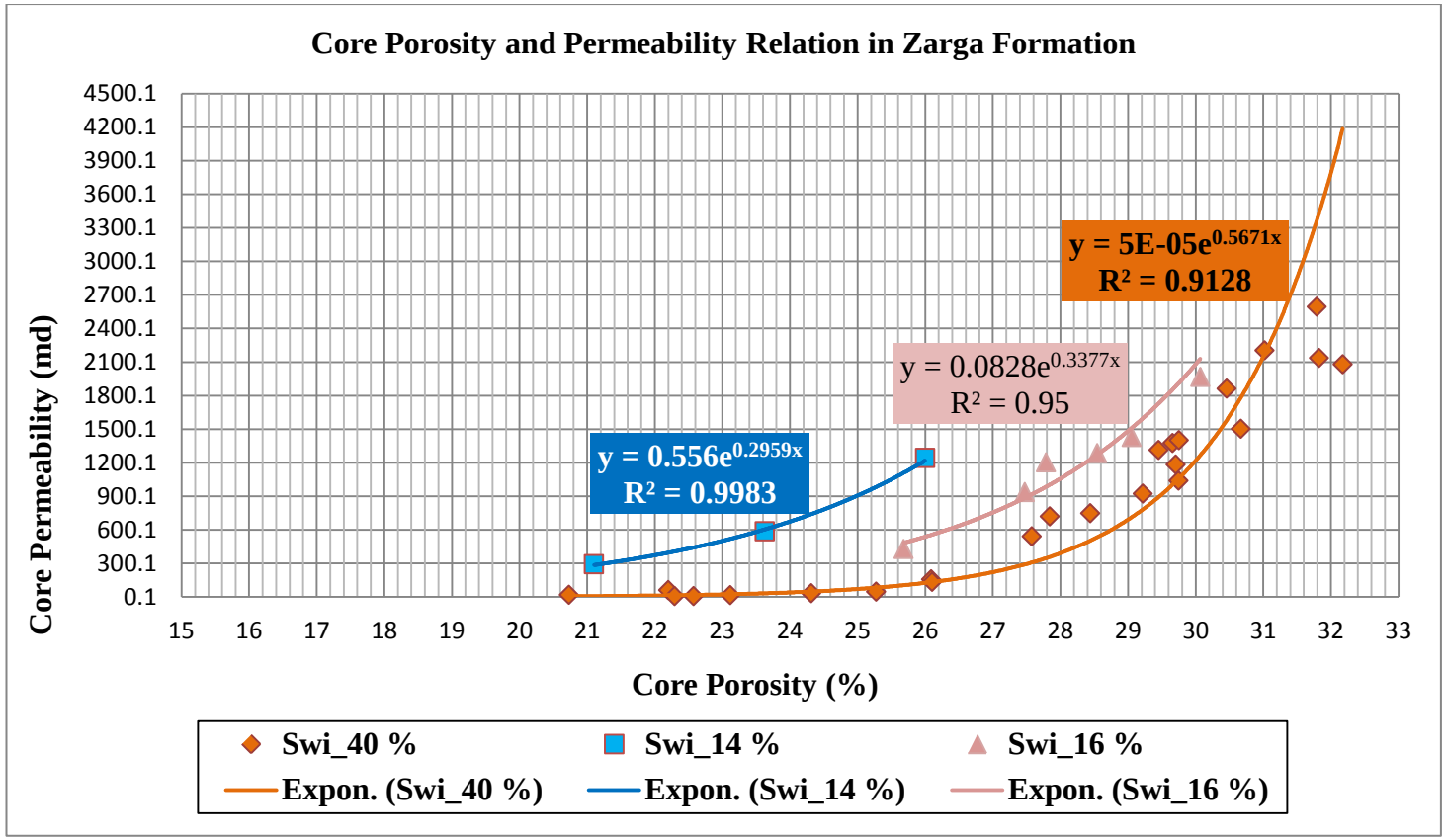

Fig.4-7: Core porosity and permeability models, distrusted with verity with S_{wi} and facies in Zarga formation.

Reference to the above cross plots (Fig.4.6&Fig.4.7), showing different rock types with different characteristic, whoever (6) development permeability equation generated to calculate the accurate permeability (Table 4.7) for each facies as blow equations for Ghazal (equations: 4.4, 4.5, 4.6) and Zarga (equations: 4.7, 4.8, 4.9) formations:

If the $S_{wi} \leq 20\%$ Permeability = 1.8645*Exp $^{0.2353 * porosity}$ ……. (4.4)

If the S_{wi} 20%>26% Permeability = 0.2117*Exp $^{0.2921 * porosity}$ …… …. (4.5)

If the $S_{wi} \geq 34\%$ Permeability = 0.009*Exp $^{0.3685 * porosity}$ …….. (4.6)

If the $S_{wi} \leq 14\%$ Permeability = 0.556*Exp $^{0.2959 * porosity}$ …….. (4.7)

If the S_{wi}14%>16% Permeability = 0.0828*Exp $^{0.3377 * porosity}$ …… …… (4.8)

If the $S_{wi} \geq 40\%$ Permeability = 5E-05*Exp $^{0.5671 * porosity}$ ……. (4.9)

Table. 4-7 : The Permeability results, using core and logging interpretation to identify the reservoirs properties.

Well	Zones	Top	Bottom	Gross	Net-Sand	Av_Shale Volume	Av_Effective Porosity	Av_Total Porosity	Av_log Permeability	Av_core Permeability if (Swi 20%>26%)	Av_core Permeability if (Swi >34%)
		m	m	m	m	v/v	v/v	v/v	md	md	md
Keyi-4	Gc/Gc1	1508.2	1527.4	19.2	13.4	0.24	0.19	0.25	911.81	54.45	9.88
	Gc2	1527.4	1555.3	27.9	18.1	0.24	0.19	0.25	728.57	54.45	9.88
	Gc3	1555.3	1575.7	20.4	17.1	0.22	0.20	0.28	826.92	72.92	14.29
	Zc/Zc1	1685	1704.6	19.6	12.1	0.24	0.20	0.22	812.85	72.92	14.29
	Zc2	1704.6	1726	21.4	9.1	0.21	0.22	0.23	1043.81	130.79	29.86
Keyi-11	Gc/Gc1	1516.5	1538.9	22.4	19.2	0.25	0.19	0.25	307.44	72.92	14.29
	Gc2	1538.9	1563.8	24.9	17.4	0.24	0.21	0.25	1573.32	97.66	20.66
	Gc3	1563.8	1585	21.2	20.8	0.14	0.24	0.27	7115.50	314.16	90.19
	Zc/Zc1	1690	1711.8	21.8	17.1	0.28	0.21	0.22	213.93	175.16	43.16
	Zc2	1711.8	1729.5	17.7	11.8	0.29	0.21	0.22	99.26	314.16	90.19
Keyi-12	Gc/Gc1	1518.6	1554.4	35.8	18.7	0.21	0.21	0.25	1679.99	97.66	20.66
	Gc2	1554.4	1579.9	25.5	12.6	0.20	0.21	0.26	1244.32	130.79	29.86
	Gc3	1579.9	1599.4	19.5	9.5	0.34	0.20	0.26	424.85	40.66	6.84
	Zc/Zc1	1723.6	1747.5	23.9	17.6	0.21	0.21	0.23	1350.57	130.79	29.86
	Zc2	1747.5	1769.2	21.7	15.5	0.18	0.23	0.25	25592.00	97.66	20.66

4.1.1 Reservoirs Cutoff Summary Results:

Base on the DST, log interpretation and sensitivity analysis results the below cut-off had been identified for Ghazal and Zarag formation (Table.4.8).

Table. 4-8 : Reservoirs cut-off summary, using sensitivity and DST techniques, to identify net sand, and net pay of Ghazal and Zarga reservoirs.

Formation	PHIE(fraction)	VCL(fraction)	SW(fraction)	Resistivity(ohm.m)
Ghazal	≧ 0.14	≦0.5	≦0.55	10
Zarqa	≧ 0.15	≦0.5	≦0.55	15

4.1.2 Logging Interpretation Summary Results:

This part summarizes the petrophysical properties of the formation of three drilled wells (Keyi-4, 11 and Keyi-12) for Ghazal and Zarga formations of Keyi field (Table. 4.9).Comprehensive evaluation was carried out as main part of this study, to determine clay volume, porosity, water saturation and permeability based on core data, DST and masterlog as reference.

Table. 4-9: Summary of the logging interpretation results, using Elan plus Software

Reservoir parameters										Net Pay parameters				
Well	**Zones**	**Top**	**Bottom**	**Gross-sand**	**Net-sand**	**Av_Shale Volume**	**Av_Effective Porosity**	**Av_Water Saturation**	**Av_Core Permeability**	**Net Pay**	**Av_Shale Volume**	**Av_Effective Porosity**	**Av_Dual Water Saturation**	**Results**
		m	**m**	**m**	**m**	**v/v**	**v/v**	**v/v**	**md**	**m**	**v/v**	**v/v**	**v/v**	
Keyi-4	Gc/Gc1	1508.2	1527.4	19.2	13.4	0.24	0.19	0.15	54.45	11.0	0.25	0.19	0.04	Oil
	Gc2	1527.4	1555.3	27.9	18.1	0.24	0.19	0.40	54.45	9.8	0.27	0.18	0.09	Oil
	Gc3	1555.3	1575.7	20.4	17.1	0.22	0.20	0.29	72.92	12.8	0.24	0.19	0.13	Oil
	Zc/Zc1	1685	1704.6	19.6	12.1	0.24	0.20	0.63	72.92	4.3	0.29	0.21	0.40	Oil
	Zc2	1704.6	1726	21.4	9.1	0.21	0.22	0.73	130.79	2.4	0.14	0.25	0.51	Oil
Keyi-11	Gc/Gc1	1516.5	1538.9	22.4	19.2	0.25	0.19	0.50	72.92	7.2	0.20	0.20	0.43	Oil
	Gc2	1538.9	1563.8	24.9	17.4	0.24	0.21	0.66	97.66	3.7	0.18	0.21	0.41	Oil
	Gc3	1563.8	1585	21.2	20.8	0.14	0.24	0.67	314.16	1.5	0.15	0.25	0.46	Oil
	Zc/Zc1	1690	1711.8	21.8	17.1	0.28	0.21	0.61	175.16	5.2	0.28	0.23	0.39	Oil
	Zc2	1711.8	1729.5	17.7	11.8	0.29	0.21	0.74	314.16	1.8	0.28	0.25	0.45	Oil
Keyi12	Gc/Gc1	1518.6	1554.4	35.8	18.7	0.21	0.21	0.67	97.66	0.0	0.22	0.21	0.46	water
	Gc2	1554.4	1579.9	25.5	12.6	0.20	0.21	0.71	130.79	0.0	0.21	0.22	0.50	water
	Gc3	1579.9	1599.4	19.5	9.5	0.34	0.20	0.79	40.66	0.0	0.40	0.18	0.50	water
	Zc/Zc1	1723.6	1747.5	23.9	17.6	0.21	0.21	0.76	130.79	0.0	0.30	0.22	0.49	water
	Zc2	1747.5	1769.2	21.7	15.5	0.18	0.23	0.73	97.66	0.0	0.27	0.21	0.37	water

4.1 Elastic Constant Basic Results:

According to actual corresponding geological and laboratory analysis data, one processing result have been done (shear sonic) based on reliable data processing and interpretation. One composite result plots (scale 1:200) displayed as in Fig.4.8 and Fig.4.9, below details descriptions about this plot:

Track 1: Depth (m).

Track 2: Sub layers/zones name.

Track 3: CAL (inch), BIT (inch), SP (mv) and GR (API).

Track 4: DTC _Compressional wave slowness (us/ft), ZDEN: Bulk density (g/cc).

Track 5: DTS _Shear wave slowness (us/ft).

Track 6: BMOD_Bulk modulus (Mpsi).

Track 7: SMOD _Shear modulus (Mpsi).

Track 8: YMOD _Young’s modulus (Mpsi).

Track 9: POIS _Poisson's Ratio.

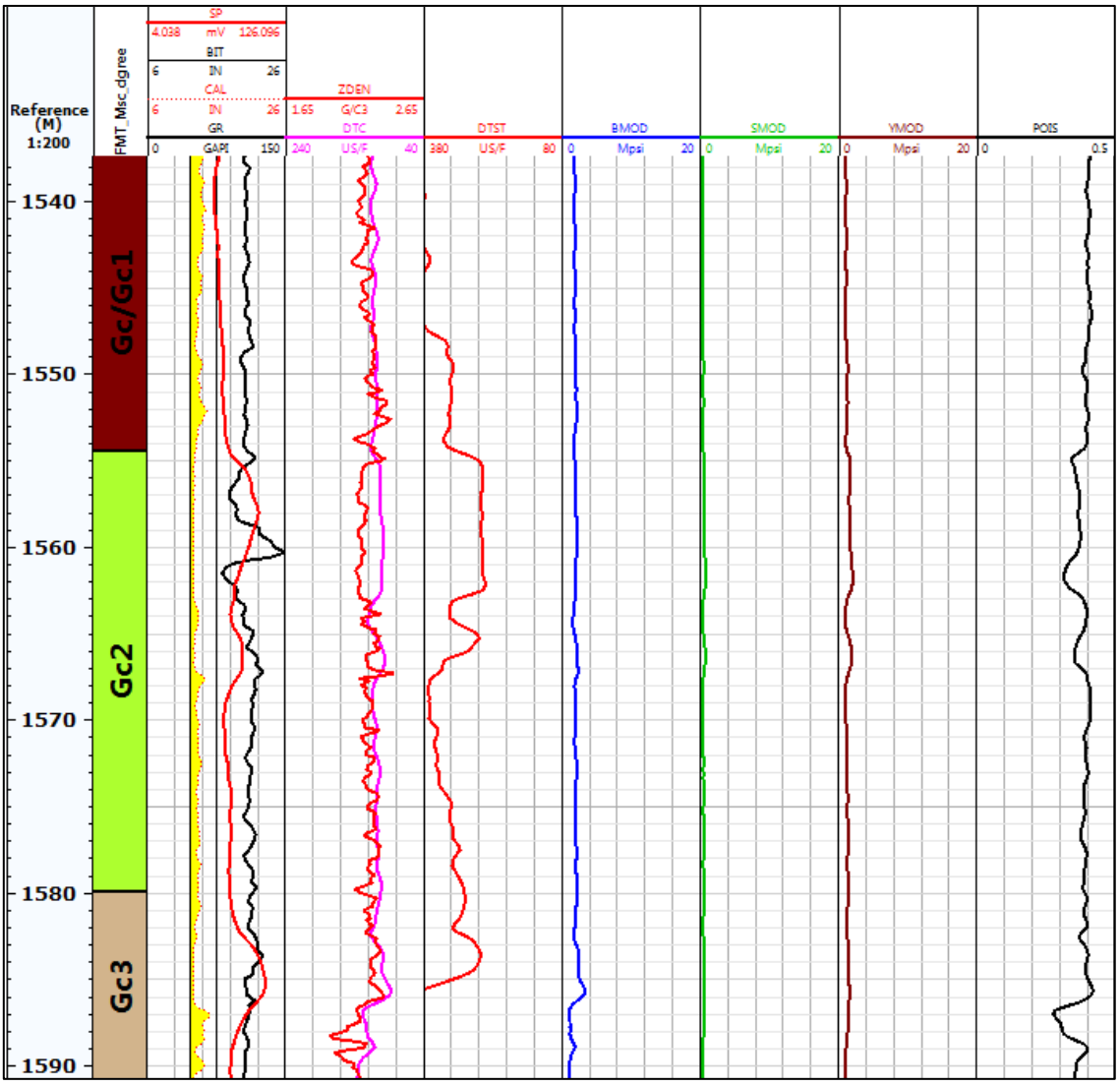

Fig.4-8: This log plot with scale 1:200 m, for Ghazal formation, displayed with raw data(SP,CAL,BT,ZDEN,DTC,DTST) as in track 3,4 and 5, and calculated results of elastic dynamic modules (BMOD,SMOD,YMOD And POIS) in track 6,7,8 and 9.

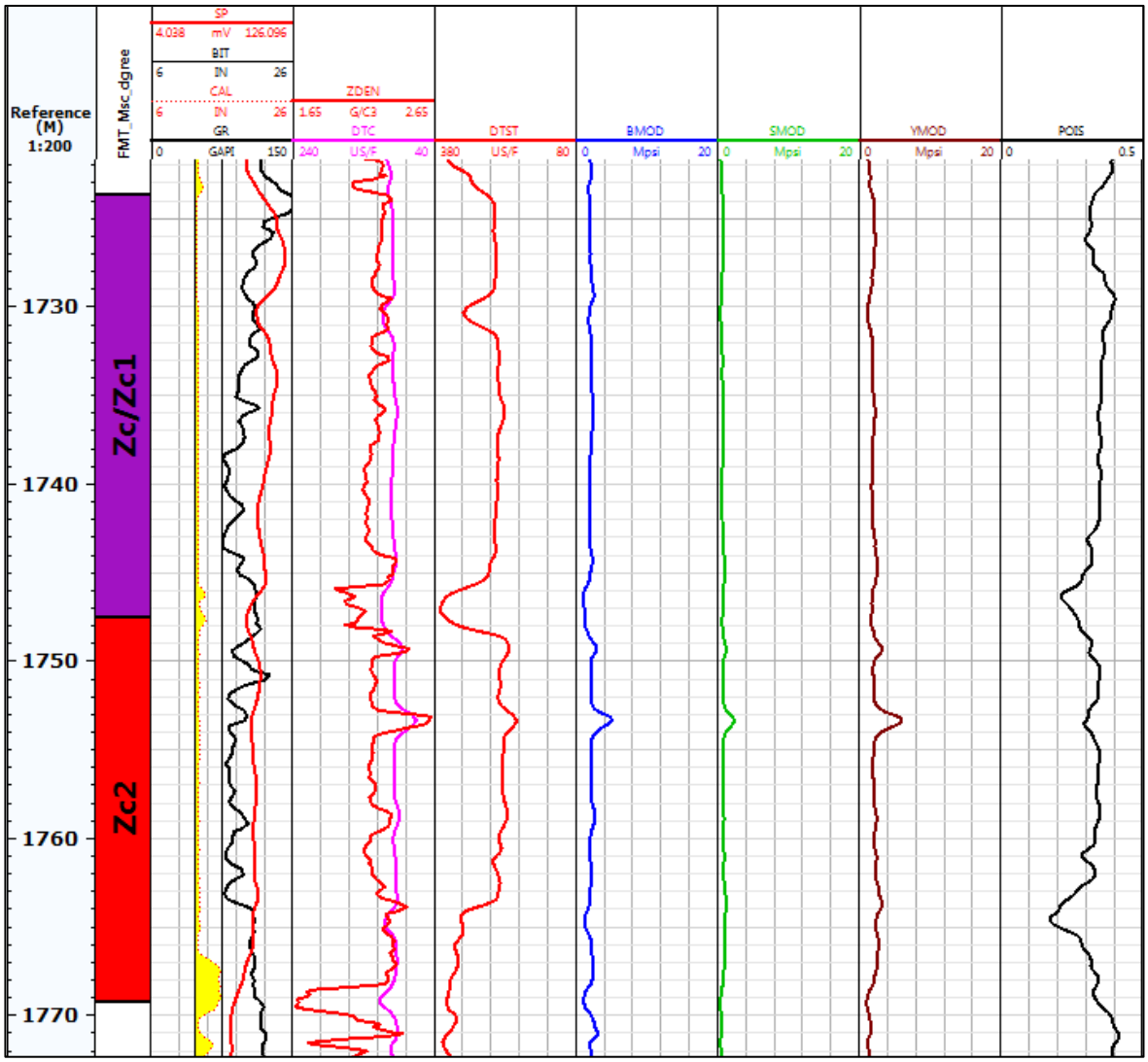

Fig.4-9: This log plot with scale 1:200 m, for Zarga formation, displayed with raw data(SP,CAL,BT,ZDEN,DTC,DTST) as in track 3,4 and 5, and calculated results of elastic dynamic modules (BMOD,SMOD,YMOD And POIS) in track 6,7,8 and 9.

The below (Table.4.10) showing rock mechanical properties results of the Ghazal and Zarga formation.

Table. 4-10: Dynamic rock mechanical properties results of well Keyi-12,using elastic modules

Well	Formation	Sub layer	Top (m)	Bottom (m)	Av_Bulk Modulus (Dynamic) Mpsi	Av_Shear Modulus (Dynamic) Mpsi	Av_Young's Modulus (Dynamic) Mpsi	Av_Poisson Ratio (Dynamic) Mpsi
Keyi-12	Ghazal	Gc/Gc1	1518.6	1554.4	1.96	0.55	1.49	0.37
		Gc2	1554.4	1579.9	1.99	0.53	1.44	0.38
		Gc3	1579.9	1599.4	1.79	0.53	1.42	0.36
	Zarga	Zc/Zc1	1723.6	1747.5	2.04	0.73	1.95	0.34
		Zc2	1747.5	1769.2	2.21	0.93	2.44	0.31

4.2 Interpretation Results and Discussions.

4.3.1 Ghazal sub layer Interpretation Results.

In the target sub layers (Gc/Gc1, Gc2 and Gc3) of Ghazal formation there are two different clay minerals have been recognized, with average volume about 19%, composed of kaolinite as dominant, with trace of Smectite.

Reference to gamma ray response of clean sand as displayed in the histogram (Fig.4.10), characterized by relatively high gamma ray measurement, about (60-75.5) API, with considerable amount of K-feldspar and quartz, with 28% and 16% respectively (Fig.4.11).

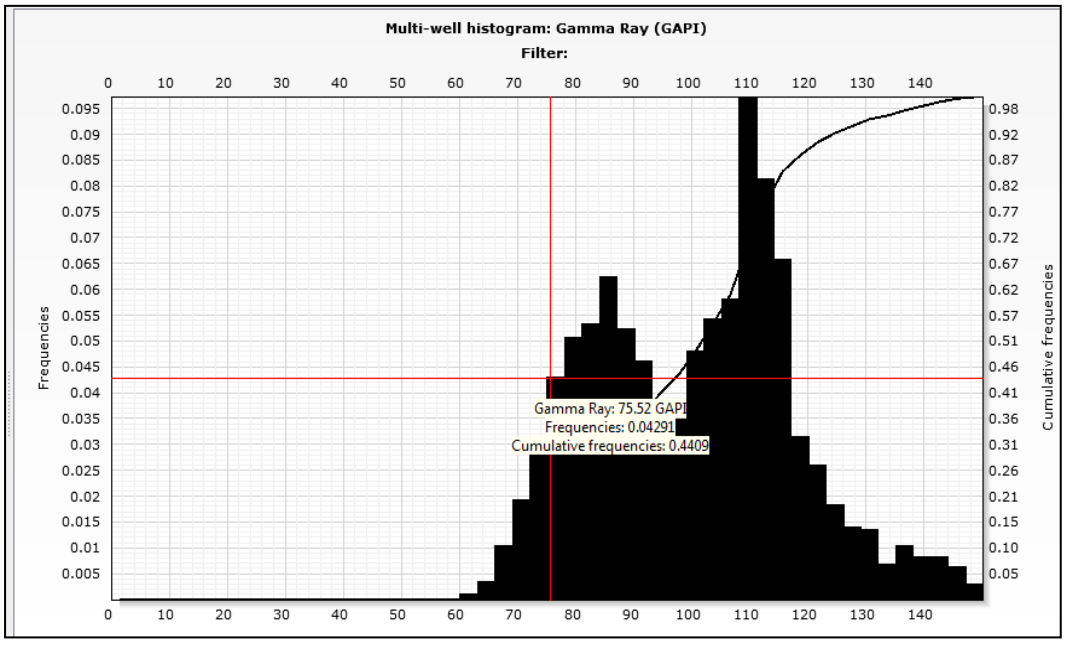

Fig.4-10: Gamma ray multi well histogram in Gahzal sub layers.

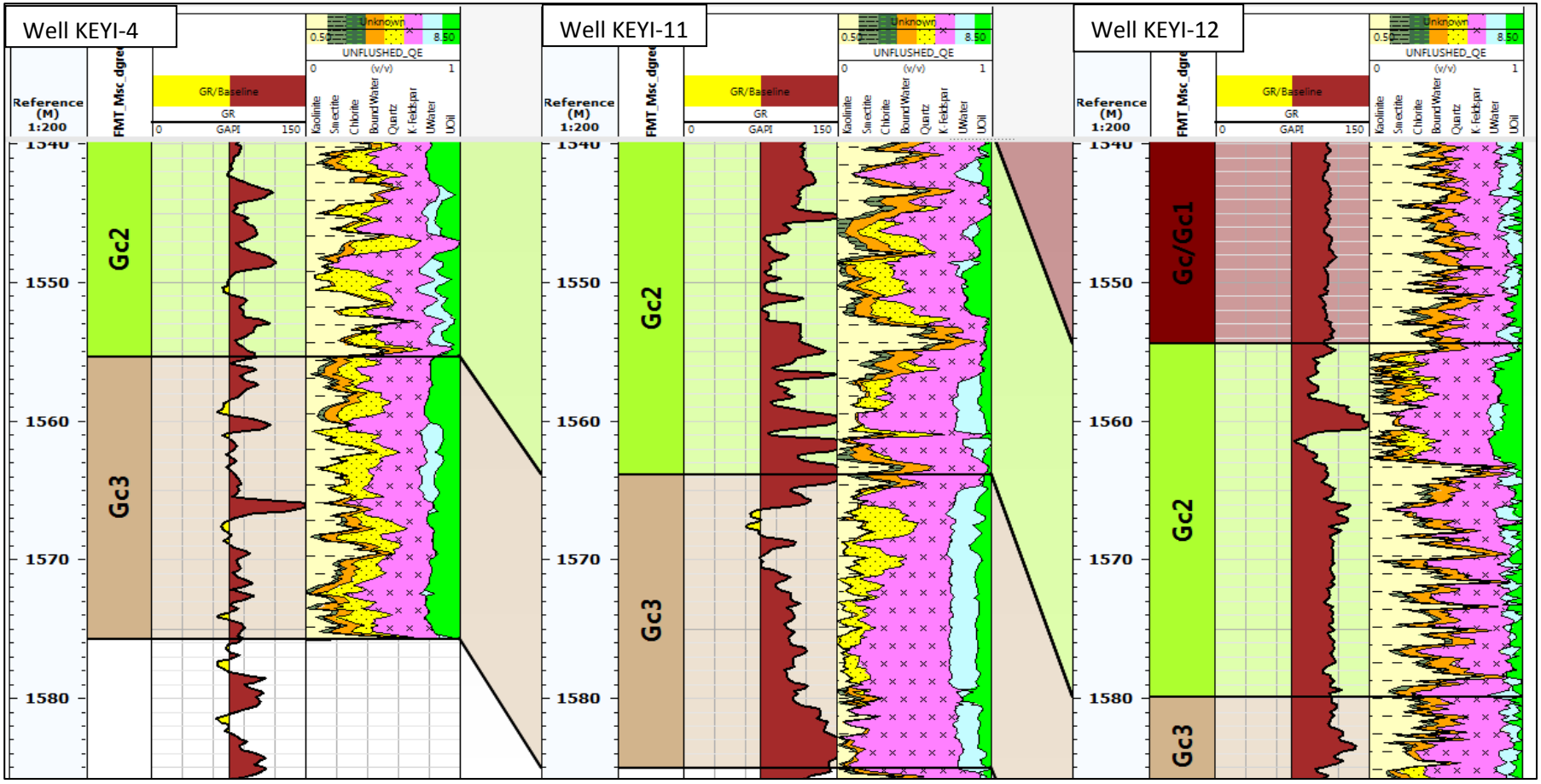

Fig.4-11: Volume fraction of the minerals components in Ghazal sub layers, showing relatively high k-feldspar compare to quartz volume, with considerable amount of Kaolinite.

Reference to the above section of the wells (Fig.4.11),demonstrated an example of K-feldspar rich zone (51%), with high gamma ray measurement (104 to 120 API),and gradually increasing of quartz volume up to (20%),from bottom to top interval (1572.0-1584.0m) of well Keyi-11.

If the shale volume estimated base on gamma ray only (deterministic), then the volume about 57-60%, whereas the corrected or actual shale content is less than 12%, however the main causes of the over estimation of the shale is the K-feldspar concentration.

The dominant minerals are K-Feldspar, with considerable amount of Kaolinite (Table.4.3).

There is good correlation between gamma ray measurement and reconstructed or model gamma ray (Fig.4-12), if the K-feldspar considered as dominant minerals in the matrix for Ghazal and Zarga formation, on other hand, the assumption of the quartz as common mineral in the matrix, displayed with bad correlations as in (Fig.4.13).

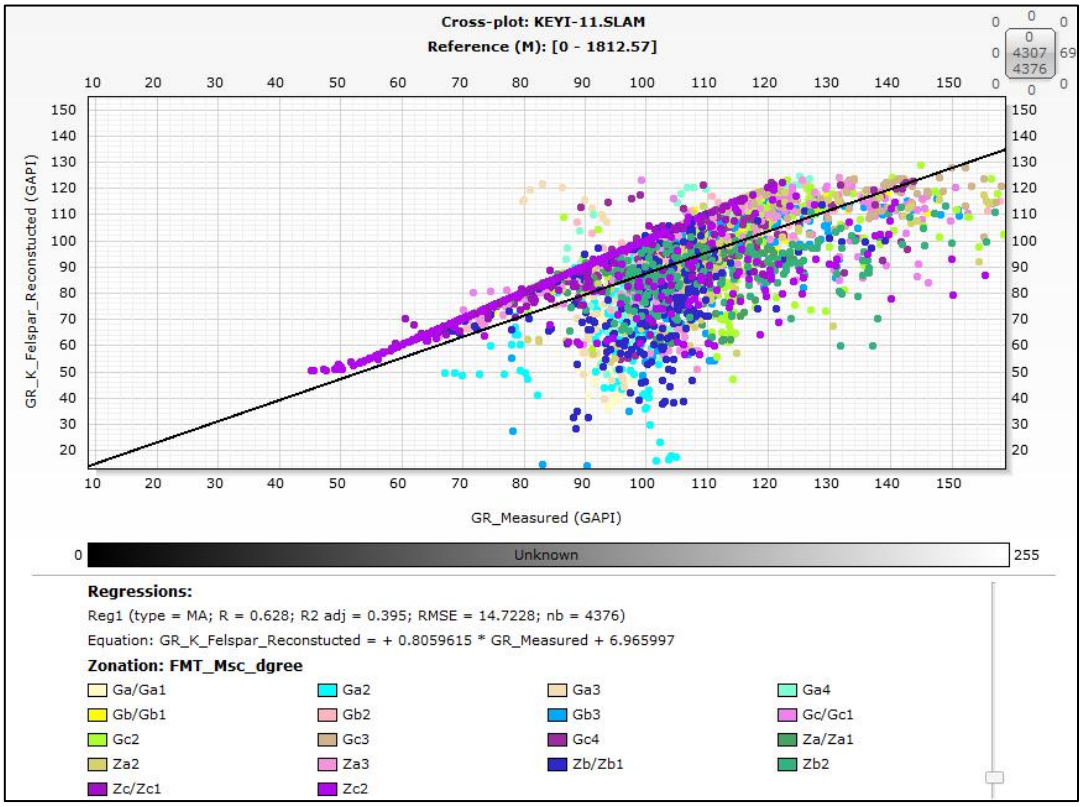

Fig.4-12: The correlation between Gamma ray measurement and reconstructed/model gamma ray, based on K-Feldspar as common mineral in the matrix.

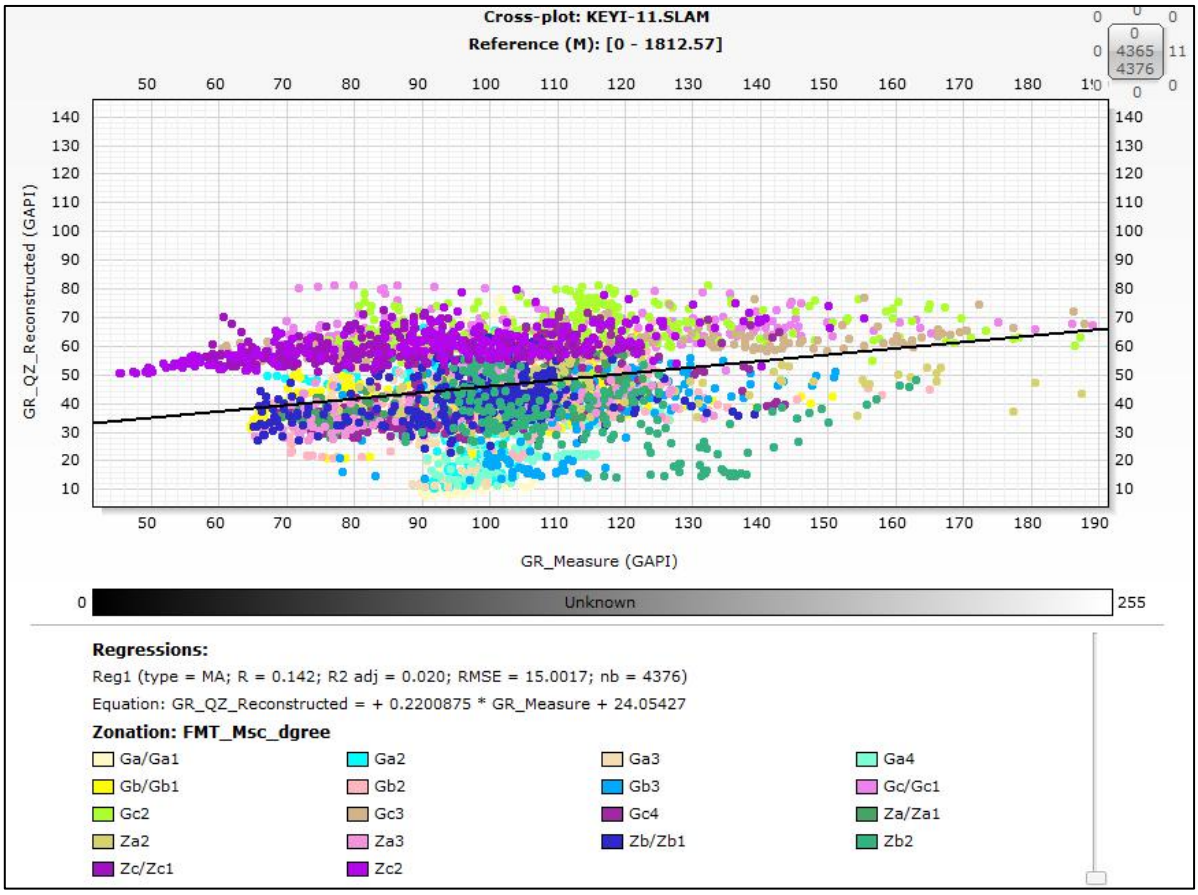

Fig.4-13: The correlation between gamma ray measurement and reconstructed/model gamma ray, based on quartz as common mineral in the matrix.

The interval (1517.0-1538.0m), displayed average effective porosity about 19%, and total porosity about 34% calibrated with core porosity with good matched.

The core water saturation overlay with Dual water saturation log, but the Indonesian water saturation result miss match with the core data, and the average water saturation for oil zones about 0.26% and 0.50% reference to dual water and Indonesian models respectively (Fig.4.14).

The core permeability has some relations with log permeability as displayed in (Fig.4.14).

Three geologic facies identified based on capillary pressure analysis (Fig. 3.31), core porosity and permeability(Fig.4.6),also the permeability decrease with increase of irreducible water saturation (S_{wi}),mainly due to fine grain and poor sorting, regardless of the porosity relation and this supported by (Andrew, 2008) as in (Fig.3.27).

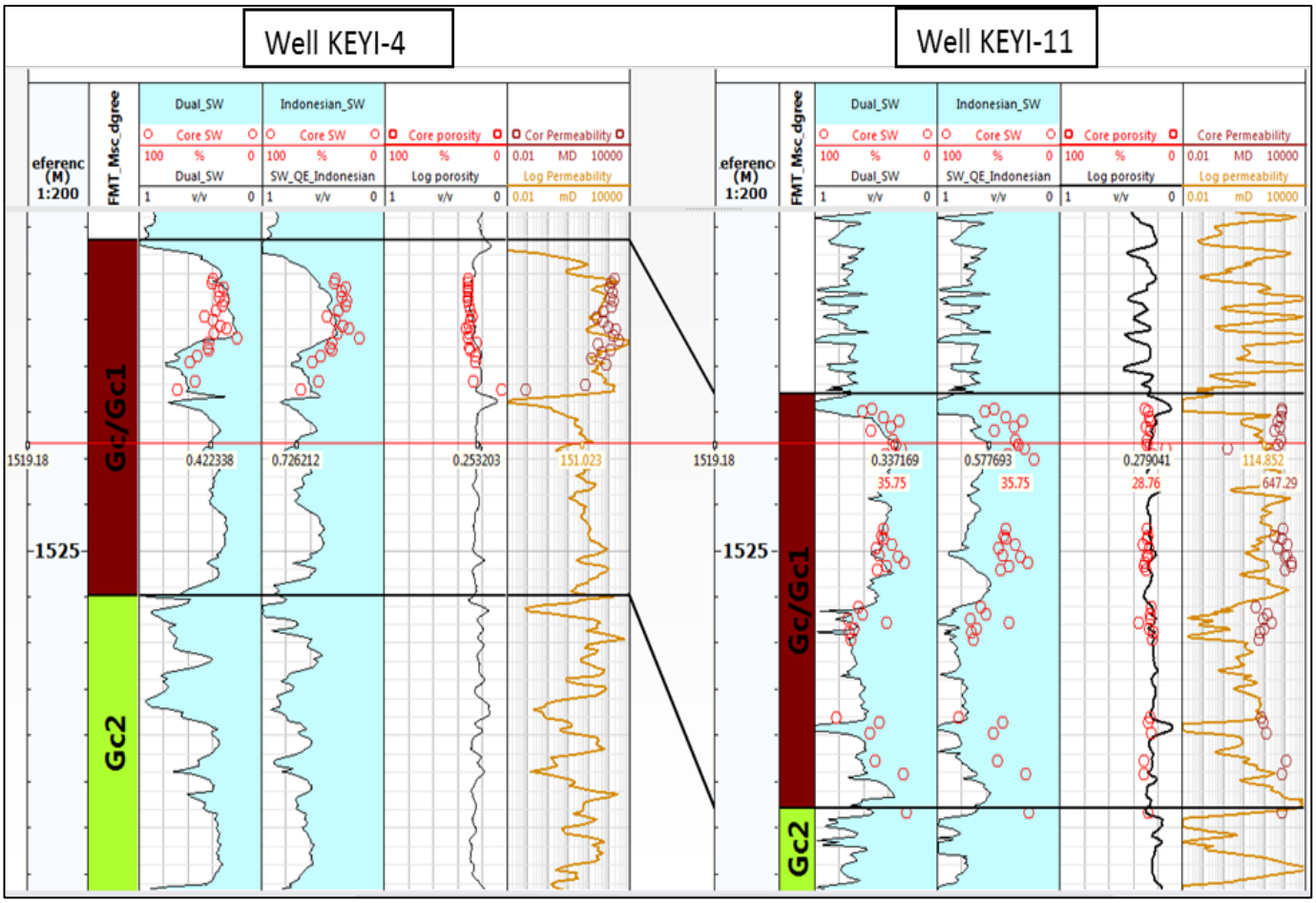

Fig.4-14: Log plot displayed logging interpretation results porosity, water saturation, and permeability calibrated to core data to validate the interpretation results of Ghazal Formation.

4.3.2 Zarga Sub layer Interpretation Results:

The target sub layers (Zc/Zc1 and Zc2) of Zarga formation are characterized by relatively low gamma ray response in clean sand about **69.7** API (Fig.4.15) compare to the Ghazal reservoirs, with average clay volume about 19.2% and 10% of Chlorite and Kaolinite respectively. The dominant mineral in the matrix are k-Feldspar and Quartz with average volume about 27.8% and 16.3% respectively, with considerable amount of Kaolinite (Table.4.3).

Also, there is good correlation between gamma ray measurement and reconstructed or model gamma ray, thus verified the presence of the K-Feldspar as dominant minerals in the matrix for Zarga formation (Fig.4.12), on other hand, the assumption of the quartz as common mineral in the matrix, displayed with bad correlations for both formations (Fig.4.13).

The gamma ray response in clean sand of target layers (Zc1 and Zc2) intervals (1697.0-1700.0m) & (1725.4.0-1728.6m) of Kyi-11 well, is 56-64 API, with average 27% and 17% K-feldspar and quartz respectively (Fig-4.16).

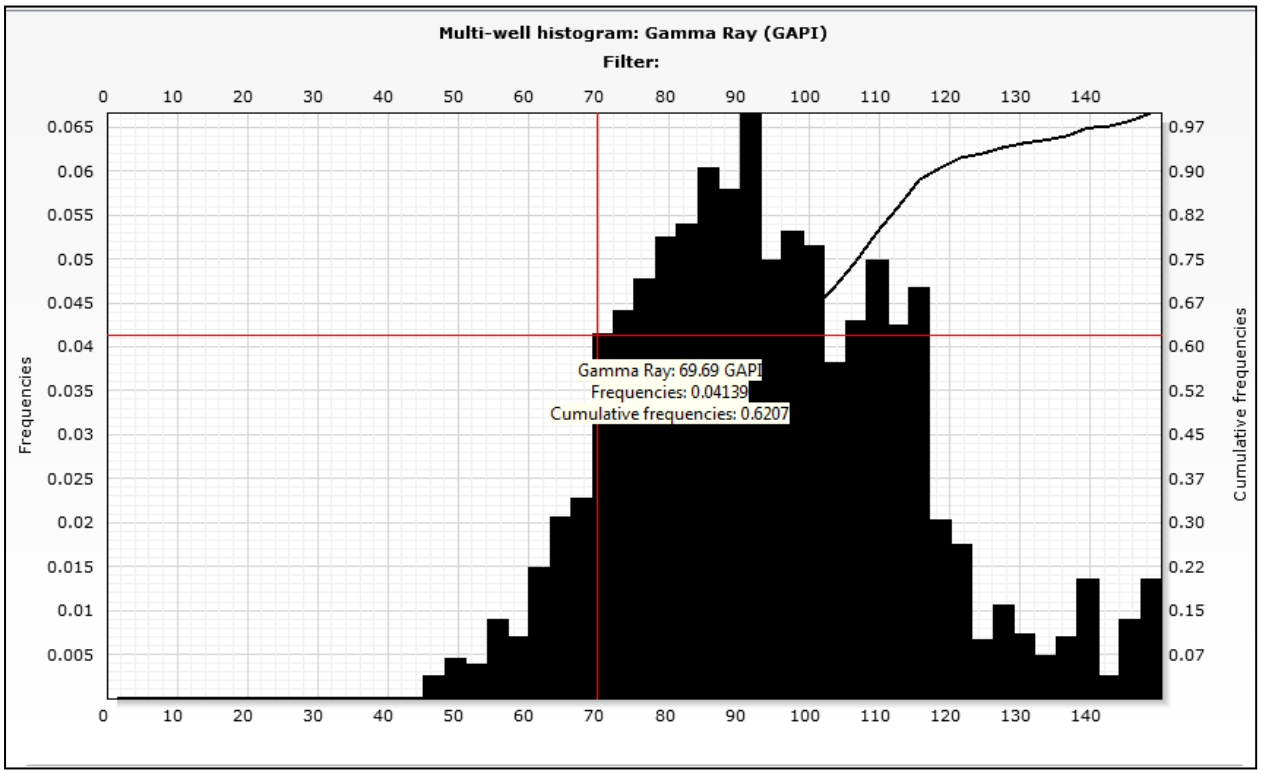

Fig.4-15: Gamma ray multi well histogram in Zarga sub layers, showing minima gamma ray for clean sand with 69.6 API

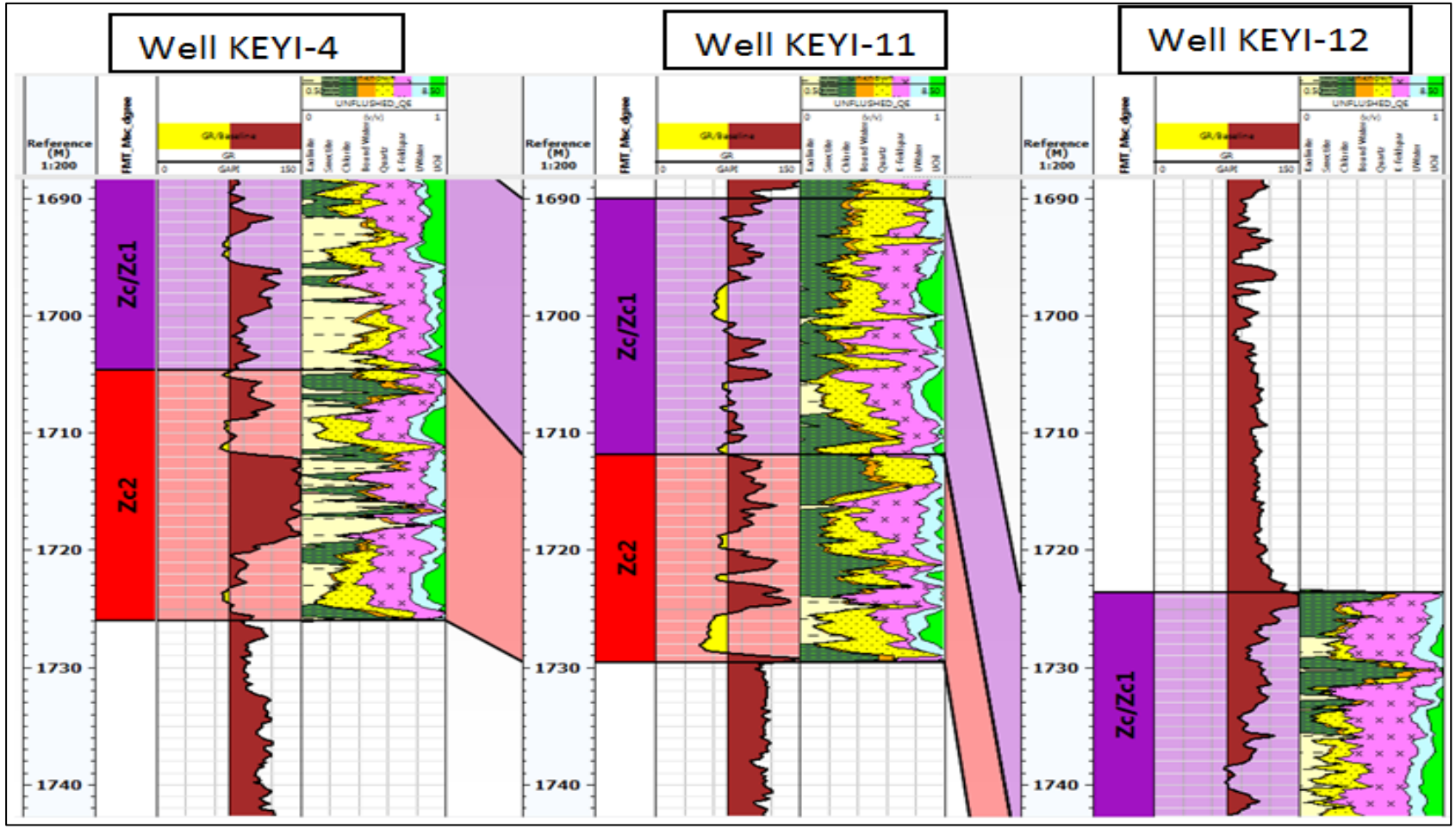

Fig.4-16: Volume fraction of the minerals components in Zarga sub layers, showing relatively high k-feldspar compare to quartz volume, with considerable amount of chlorite.

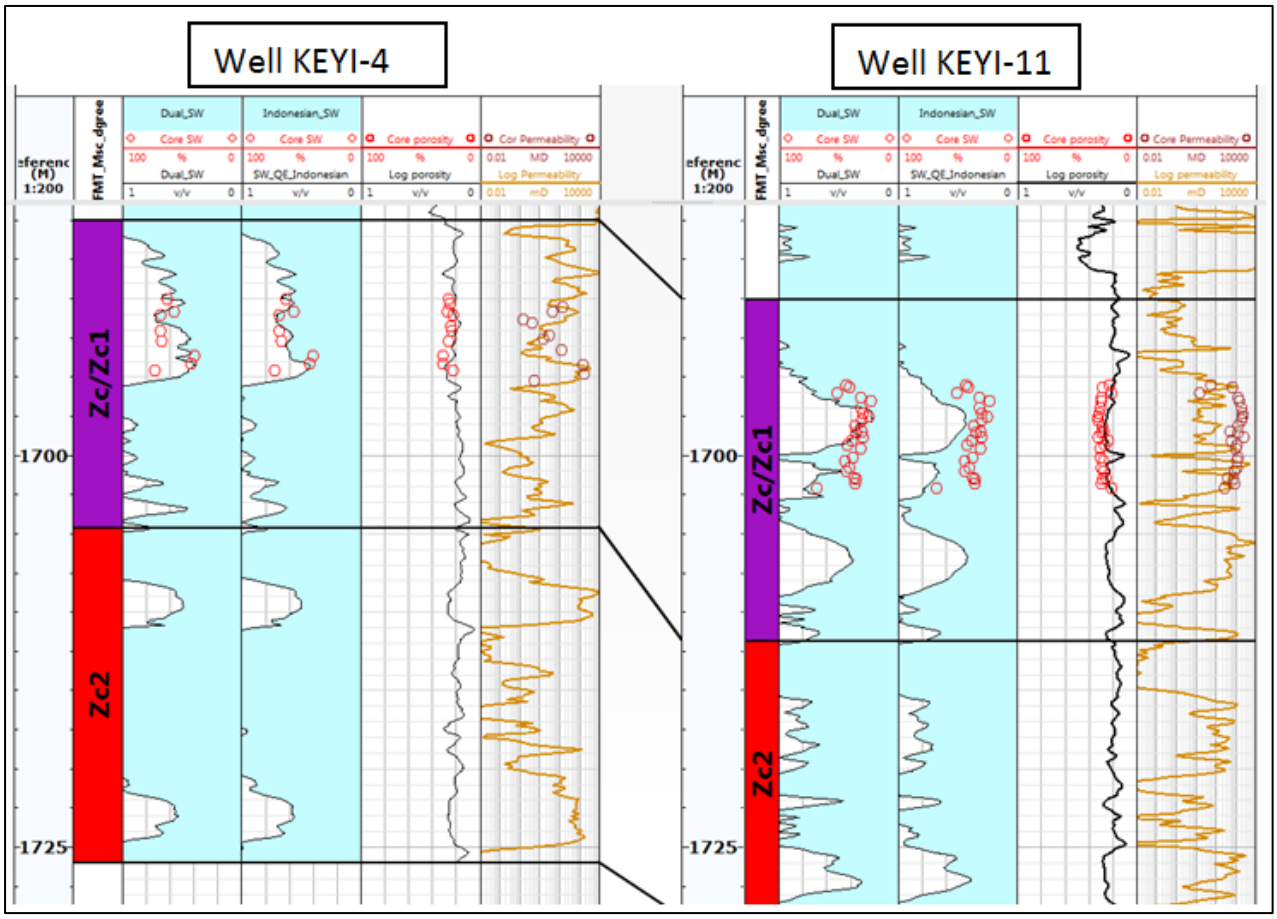

Fig.4-17: Log plot displayed logging interpretation results water saturation, permeability and porosity calibrated with core data to validated the results for Zarga Formation.

The interval (1696.0-1702.0m), displayed with average effective porosity 21%, and total porosity about 25% calibrated to core porosity and overlay with each other very well.

The core water saturation overlay with Dual water saturation log, but the Indonesian water saturation result miss match with the core data, and the average water saturation in range of 0.43% and 0.50% reference to Dual water and Indonesian models respectively (Fig.4.17).

The core permeability didn't match very well with log permeability due to relatively high irreducible water saturation (Fig.4.17).

Three geologic facies identified based on capillary pressure analysis (Fig. 3.32), and core porosity and permeability (Fig.4.7), and the permeability decrease with increase of irreducible water saturation (S_{wi}), mainly due to fine grain and poor sorting, regardless of the porosity relation and this supported by (Andrew, 2008) as in (Fig.3.27) .

4.3.3 Dynamic Elastic Result using to calibrate the Reservoirs Mineralogy.

This method involves there steps:

First, creating synthetic logs from the logging interpretation with different mineral components using log response equations, and the equations needed are (Crain, 2016):

- DENSsyn = Vsh * DENSSH + DENS1 * Vmin1 + DENS2 * Vmin2 + DENS3 * Vmin3 +PHIE*Sw*DENSW+PHI*(1-Sw)*DENSHY …….(4.10)

Where:

DENS syn: is synthetic density.

Vsh: Shale volume.

DENS1, 2, 3: is density parameter for each mineral and fluid.

PHIE: Effective porosity.

Vmin x=volume of each mineral present, normalized so that SUM (V_{minx}) = 1.0

Second, reconstructed dynamic elastic constants computed, by derived with appropriate equations, using sonic log compressional and shear travel time along with synthetic density log data.

Third, reconstructed dynamic elastic result compared to the original dynamic elastic constant models to identify reasonable mineral components results, moreover this results integrated with rock physics results, XRD data and Spectral logs, all these data supported that quartz, kaolinite and K-feldspar existed in the matrix, and original dynamic elastic constant matched with model-1(Table.4.11).

Table. 4-11: Comparisons between initial elastic modules and reconstructed modules

Parameters	Original/initial Elastic Module					Model (1) (Kaolinite_QZ_K_Chlori) Reconstructed Elastic Module					Model (2) (QZ_Kaolinite) Reconstructed Elastic Module					Model (3) (Kaolinite_QZ_K) Reconstructed Elastic Module				
Zones	Gc/Gc1	Gc2	Gc3	Zc/Zc1	Zc2	Gc/Gc1	Gc2	Gc3	Zc/Zc1	Zc2	Gc/Gc1	Gc2	Gc3	Zc/Zc1	Zc2	Gc/Gc1	Gc2	Gc3	Zc/Zc1	Zc2
Top	1518.6	1554.4	1579.9	1723.6	1747.5	1518.6	1554.4	1579.9	1723.6	1747.5	1518.6	1554.4	1579.9	1723.6	1747.5	1518.6	1554.4	1579.9	1723.6	1747.5
Bottom	1554.4	1579.9	1599.4	1747.5	1769.2	1554.4	1579.9	1599.4	1747.5	1769.2	1554.4	1579.9	1599.4	1747.5	1769.2	1554.4	1579.9	1599.4	1747.5	1769.2
Av_Bulk Modulus (Dynamic)	1.97	2	1.8	2.05	2.22	1.42	1.6	1.73	3.18	2.69	2.31	2.25	1.97	2.26	2.43	0.17	0.38	0.62	1.25	1.11
Av_Poisson Ratio (Dynamic)	0.37	0.38	0.36	0.34	0.31	0.37	0.38	0.36	0.34	0.31	0.37	0.38	0.36	0.34	0.31	0.37	0.38	0.36	0.34	0.31
Av_Shear Modulus (Dynamic)	0.55	0.53	0.53	0.74	0.94	0.41	0.42	0.53	1.15	1.15	0.41	0.42	0.53	1.15	1.15	0.06	0.09	0.2	0.46	0.5
Av_Young's Modulus (Dynamic)	1.5	1.45	1.43	1.96	2.45	1.12	1.15	1.42	3.05	2.99	1.75	1.64	1.56	2.17	2.67	0.39	0.53	0.97	1.22	1.3
Av_Bulk Density	2.24	2.25	2.22	2.23	2.26	0.19	0.44	0.86	1.41	1.18	2.62	2.52	2.41	2.46	2.48	1.54	1.55	1.62	2.57	2.48
Av_Shear Slowness	242.45	243.78	243.16	204.16	184.29	242.45	243.78	243.16	204.16	184.29	242.45	243.78	243.16	204.16	184.29	242.45	243.78	243.16	204.16	184.29
Av_Compressional Slowness	106.18	106.1	111.28	100.02	95.29	106.18	106.1	111.28	100.02	95.29	106.18	106.1	111.28	100.02	95.29	106.18	106.1	111.28	100.02	95.29

CONCLUSION AND RECOMMENDATIONS

The challenge facing shaly sand petrophysics have been evaluated, with comprehensive analysis and workflow from data collection ,quality control of well logs, interpretation results and calibrated with conventional (CCA) and special core analysis (SCAL) for reservoir characterizations.

The presence of potassium (K-feldspar) in the matrix is the main challenge to evaluate accurate shale volumes, a combination between photo electrical factor (PEF) and gamma ray measurement consider as apowerful tool, successfully adopted to resolve the Potassium effect, and applied low weight due to high uncertainty.

Another challenge is minerals components and porosity identification; this achieved by using mineral base model integrated with core analysis and dynamic elastic properties results. The uncertainties related to the water saturation evaluation, solved based on dual water model.

The logs analysis was the first method, secondly parameters selection with multi wells cross plots, histogram and core analysis, to identify the lithology, clay type/content, porosity and minerals, thirdly fluid identification base on resistivity, porosity and DST result, finally cut off determination incorporating with DST results to estimate the reservoir properties in summary table results.

Density–neutron cross plot is the best technique for porosity identification, and shale volume estimation, in order to discriminate between shale and sand layers, compare to gamma ray method. The Picket plot method is reliable for formation water salinity identification. The spectral gamma and XRD analysis techniques utilized to verify the presence of the thorium concentration (radioactive minerals) in the matrix.

Probabilistic approach or mineral base model is the best method used in this research to identify the formation components, and Elan Plus software provided with curve SDR (standard deviation of the reconstruction) will point out areas in which log reconstruction is poor. It is then up to you to determine the cause of the inconsistency.

An essential step in the petrophysical evaluation is the determining of the clay type in the reservoirs to calculate accurate effective porosity and fluid saturations, involved with two analytical methods, X-ray diffraction (XRD) and scanning electron microscopy (SEM) base on core data, the studied zones contains of significant amount of kaolinite with trace of Smectite and chlorite of the clay volumes.

The dominate minerals in the matrix composed of K-feldspar with average volume range from 24% to 35%, Kaolinite volume about 10% to 20%, quartz volume about 11% to 16%, and trace of smectite and chlorite for Ghazal and Zarga reservoirs.

Different rocks types have been identified with wide range of irreducible water saturation (19%-32%), (16%-40%) for Ghazal and Zarga Formation respectively.

The average water saturation of the oil zones based on dual water model about 26% and 43% for Gahzal and Zarga reservoirs respectively.

The petrophysical analysis and rock physics modelling of Ghazal and Zarag Formations, confirmed that the minerals composed of feldspar and kaolinite as dominant minerals in the reservirs, with considerable amount of quartz and traces of Smectite and chlorite.

The clay distribution in Ghazal reservoirs is disperse clay and laminar in Zarga reservoirs, based on the difference between total and effective porosity.

The dynamic elastic constant of the formations have been identified through rock physic techniques, and three reconstructed elastic modules have identified, and the K-feldspar, quart, kaolinite and chlorite (model-1), however the original dynamic elastic constant basic model matches closely to that derived with reconstructed dynamic elastic model-1(Table.4.11).

The logging interpretation results indicate the reservoirs of Ghazal and Zarga are rich in feldspar, Kaolinite and quartz.

RECOMMENDATION:

1) It is recommended to use the dynamic elastic constant results of this research, as standard models for Ghazal and Zarga formations.
2) It is recommended to study the mechanical rock properties for hydraulic fractures design, anisotropy analysis, permeability prediction, sand production, and drilling optimization.
3) More core data is required to identify the minerals components and reservoirs properties.

REFERENCES:

Andrew, L. (2008). Capillary Pressure Saturation, Permeability and NMR.Talisman Malaysia Limited.Page-3.

Aaron, D. (2013). Determining Mineralogy from Traditional Well Log Data.Department of Petroleum Engineering Marietta College Marietta, Ohio.

Alian. (2006).Advance formation evaluation course. Egypt.

AlRuwaili,S.(2005). *Frontiers of Formation Evaluation and Petrophysics*. Dhahran. SPE, Page-1.

Che , E. (2011). Integrating petrophysical and elastic rock properties (VP/VS ratio) for log-facies classification in static reservoir modeling.African university of Science and Technology.

Crain,E.(2015).Crain's Petrophysical Handbook[online]https://www.spec2000.net[Acce ssed 21 May. 2015] [Accessed 07 Oct. 2016].

Central Petroleum Laboratories (CPL).(2012).Conventional core analysis report of KYI-4,Sudanese Petroleum Corporation (SPC). Project ID: 00 0010607.pages, 15, 17, 28

Glover, P.(2014).petrophysics MSc Petroleum Geology. University of Aberdeen, page 98, page 150, page 139.

Geophysical Research Institute. (2015). Keyi and Bara Full Field Review (FFR) Study. China.No.03/2014-7810.

Herron, M. (1998).A Robust Permeability Estimator for Siliciclastics.SPE 49301, Annual Technical Conference and Exhibition. New Orleans. Louisiana.

A.Hurst and.J.S. Archer. (1986). some applications of clay mineralogy to reservoir description.page 811.

Mohamed et al.(1999). *Modeling Petroleum Generation in the Southern Muglad Rift Basin AAPG Bulletin*, V. 83, No. 12 (December 1999), P. 1943–1964.

Mohamed eta al. (2008). *STRATIGRAPHY AND TECTONIC EVOLUTION OF THE OIL PRODUCING HORIZONS OF MUGLAD BASIN, SUDAN*,Vol.9, J.Sc. Tech.

Rodolfo, S. B. (2010).`*The Correct Shale-Volume Characterization Increase Hydrocarbon Reserves: Case Study of Cretaceous ormation,Lake Maracaibo*. Venezuela. SPE latin Ammerican and Caribbean Petroleum Engineering Conference SPE 136811.

Sharif, M. (2013).*Rock physics modeling to constrain petrophysical properties of the Marcellus Shale*. University of Texas department of geological Sciences at Austin.

Sharifi G. and etal. (2014). Core Analysis Report of Core Samples from Well: Keyi-11. Petroleum Laboratories, Research and Studies (PLRS).Sudan.pages.21,25,45,61-95

Sclumberger.(2006). Advanced Formation Evaluation course. Abu Dhabi

Schlumberger.(2014).Elan theory, interpretation Models.Version.2014.0.1.chapter2

Javid,S.(2013) Petrography and petrophysical well log interpretation for evaluation of sandstone reservoir quality in the Skalle well. Norwegian University of Science and Technology.P.22-23

Tiab,D and Donaldson,E.(2004).*Petrophysics*.2nd ed. Elsevier: Gulf Professional,page.1